THE UNIVERSITY *of* EDINBURGH

THE ANALYSIS AND DESIGN OF LINEARISED SINGLE-INPUT EXTREMUM CONTROL SYSTEMS

by

George C. Shering

Thesis presented for the degree of Doctor of Philosophy of the University of Edinburgh in the Faculty of Science

September, 1966

Contents

List of Principal Symbols

$q_1, q_2, - - q_n$	plant inputs	input units
c	output from extremum characteristic	output units
z	horizontal disturbance	input units
A	extremum curvature	output units/ input units^2
x	input to extremum characteristic	input units
t	time	sec
$\xi(t)$	white measurement noise	output units
ω	angular frequency	sec^{-1}
$\phi_{zz}(\omega)$	spectral density of z(t)	input units^2.sec
N_z, N_ξ, etc.	spectral density constants	
T, T_1, T_2	time constants	sec
s	Laplace operator	sec^{-1}
α	perturbation frequency	sec^{-1}
a	perturbation amplitude	input units
G(s), $G_2(s)$, H(s)	filter transfer functions	
B	height of extremum	output units
K	controller integrator gain	$\frac{\text{input units}}{\text{output units}^2\text{. time}}$
p(t)	square wave perturbation signal	
Π_e	dimensionless performance criterion	
Π_p, Π_m, Π_c	dimensionless plant parameters	

$\Pi_1, \Pi_2 - - \Pi_j$	dimensionless controller parameters	
$m(t)$	vertical disturbance	output units
Π_α	dimensionless perturbation frequency	
γ	factor relating equivalent circuit estimate of performance to actual performance	
$u'(t)$	equivalent circuit estimate of controller integrator output $u(t)$	input units
$v'(t)$	'useful' low frequency part of multiplier output $v(t)$	output units^2
$z^*(t), x^*(t)$	sampled and held versions of $z(t)$, $x(t)$	input units

CHAPTER 1

A Discussion of Extremum Control

1.1 The extremum control problem

Extremum control is a technique for adjusting the inputs of some controlled object so that its single output will have an extreme value, using only observations of the output to determine the adjustment. Figure 1.1 is a diagrammatic representation of an extremum control system. The plant has n inputs q_1, q_2, - - q_n which must be adjusted by the controller so that the single output c will have a maximum or a minimum value. The only information available to the controller is the measurement of the actual output c. The theory of extremum control systems, to which this thesis is intended to contribute, is concerned with how best to adjust the inputs in order to achieve the required extreme value of the output.

Extremum control has also been called 'optimalising control' (Draper and Li [1]), 'automatic optimisation' (Feldbaum [2]), 'hill climbing' (Jacobs [3]) and 'adaptive control' (Douce [4] and Chang [5]). A considerable amount of work on extremum control systems has been published, but as several review works are available (Tsien [6] and Jacobs [3,7]) no attempt is made here to discuss possible applications of extremum control or to give an exhaustive bibliography.

As with any control system a description of the plant and the definition of a performance criterion for the controller are first essentials. The description of the plant separates extremum

control systems into two main categories, extremum searching systems and extremum regulating systems.

(a) Extremum searching systems. In these systems the values of the inputs which give the output its extreme value are fixed and have only to be found. The criterion of performance of such systems might be the time required, or the amount of computation required, to find the required inputs to some specified accuracy. Examples of such systems are the stochastic approximation systems described by Chang [8] and Kushner [9], and the digital computer function minimisation routine developed by Rosenbrock [10]. This thesis is not concerned with extremum searching systems except that one such system, the digital computer function minimisation routine described in appendix 5, has been designed in order to assist the main work of the thesis.

(b) Extremum regulating systems. In these systems the plant is subject to disturbances which make the best values of the inputs vary with time. The prime requirement of the extremum regulating controller is to continuously adjust the inputs in order to maintain the output as near to its extreme value as possible.

This thesis is concerned with the design of such systems.

1.2 Description of the Plant

Although some work has been done on systems with more than one input, for instance by Feldbaum [2,11] and Douce [4], many problems remain to be solved in connection with the basic single input plant. Only plants with a single input q are considered

in the rest of this thesis.

The extremum characteristic is most simply represented by a parabola when, as in most practical examples, the relationship between the output c and the input q is smooth in the region of the extremum. In the rest of this work the required extremum is assumed to be a minimum as this involves no loss of generality. The change in the value of q which gives minimum output c is most simply represented by the additive disturbance z shown in figure 1.2. The equation of this plant is

$$c = Ax^2 + c_{min} \qquad (1.1)$$

where $$x = z + q \qquad (1.2)$$

Compensation for the changing extremum characteristic represented by figure 1.2 is the fundamental requirement of any extremum regulating controller.

Plants represented by figure 1.2 can be divided into two classes, continuous-time plants and discrete-time plants. In continuous-time plants q, z and c are continuous functions of time whereas in discrete-time plants, such as batch chemical processes, q can be changed and c measured only at fixed points in time. In the rest of this work a continuous-time plant is considered, for the following reasons:

(a) Although some extremum controllers can be used equally well with discrete-time and continuous-time plants, others can only be used with continuous-time plants; so only a continuous plant provides a basis for the comparison of all types of extremum controller.

(b) A discrete-time plant can be considered the sampled version of a continuous-time plant and can be described by the

same parameters with the addition of the sampling frequency.

The criterion of performance

The criterion of performance of any extremum controller used with the plant of figure 1.2 is how well the controller can adjust the input q to compensate for changes in the disturbance z(t) so that the output c(t) will remain as near its minimum value as possible.

The transient response of q(t) has been used [11,12,13,14] as one such criterion of performance. In a practical extremum control system, however, a fast transient response means that the trial adjustment to determine the direction of the extremum must be large. As this trial adjustment itself causes error, engineering insight must be used to obtain a compromise between speed of adjustment, and error due to the perturbation.

An analytic criterion of performance can be defined if some assumptions can be made about the disturbance z(t). As z(t) cannot be measured and may be the result of a number of independent effects a statistical description is appropriate. In this work z(t) is assumed to be an ergodic random process [15] so that an average value of output $\bar{c}$ can be defined. The performance criterion must give information about the difference between the desired value of output c_{min} and the actual average value $\bar{c}$ obtained. This difference is proportional to the 'mean square error' $\overline{x^2(t)}$ at the input to the extremum characteristic. In the rest of this work the smallness of $\overline{x^2(t)}$ is used as the performance criterion.

The problem in terms of stochastic optimal control.

The problem presented in terms of figure 1.2 is trivial as most extremum controllers could be designed to reduce the performance criterion $\overline{x^2(t)}$ to zero. In a practical system this will not be possible because of uncertainty in the measurement of the plant output and because of lags in the plant.

The measurement uncertainty can be represented by adding a white noise $\xi(t)$ at the plant output to give the plant shown in figure 1.3. In the rest of this work it is assumed that $z(t)$ and $\xi(t)$ are uncorrelated, gaussian, ergodic random processes [15] defined by the spectral densities

$$\phi_{zz}(\omega) = \frac{N_z^2}{\omega^2} \quad ; \quad \phi_{\xi\xi}(\omega) = N_\xi^2 \qquad (1.3)$$

The disturbance $z(t)$ is a brownian motion which can be considered the result of integrating a white noise of spectral density N_z^2. The convention used here for defining spectral density is that chosen by Fuller [16] in a paper discussing the various conventions. It is related to the correlation function $\psi(\tau)$ by the formula

$$\phi(\omega) = \int_{-\infty}^{\infty} \psi(\tau) e^{-j\omega\tau} d\tau$$

The plant shown in figure 1.3 presents a problem in stochastic optimal control - how best to adjust the input q, given the measurement $y(t)$ of $c(t)$, in order to minimise the performance criterion $\overline{x^2(t)}$. It may be noted that without any controller $x(t) = z(t)$ and from the definition of $z(t)$ given above $\overline{z^2(t)}$ and hence $\overline{x^2(t)}$ will be infinite. Of particular interest is the value of $\overline{x^2(t)}$ which can be obtained using an optimal controller.

As pointed out by Jacobs [3] lags in the plant are most simply

represented by low pass filters, when the plant shown in figure 1.3 becomes that shown in figure 1.4. The time constants of the input lag and measurement lag are T_1 and T respectively.

The plants considered in the rest of this work are all special cases of that shown in figure 1.4.

1.3 The extremum controller

When a plant and performance criterion have been defined as in section 1.2 the design of the extremum controller is a problem in optimal control. Roberts [17] has developed an approximately optimal controller for a plant similar to that shown in figure 1.4 except that c_{min} is considered to be a brownian motion, possibly correlated with $z(t)$. It is interesting to note that this controller uses sinusoidal perturbation. Florentin [18] has developed an approximately optimal controller for a discrete-time plant which is the sampled equivalent of figure 1.4 but with no measurement lag and with another disturbance added in before the input lag.

Most of the extremum controllers discussed in the literature, however, operate according to certain basic principles developed using engineering insight. These empirical controllers have some advantages, such as a) and b) below, which in some circumstances may outweigh the better performance of the optimal controller.

a) The empirical controllers have general application. The structure of the optimal controller is a function of the plant and performance criterion used, and so may change from plant to plant. Only the parameters in the empirical controller need to be adjusted to suit a particular plant, and it is conceivable that an empirical

controller could be applied to a plant about which little is known and then adjusted for better performance as more is learned about the plant and performance criterion.

b) The empirical controller may be simpler than the optimal controller. The approximately optimal controller described by Roberts is more complicated, and that described by Florentin requires more computation, than most of the empirical controllers.

It is therefore of interest to compare the performances of various types of empirical controller with that of an optimal controller when used with a plant such as that described in section 1.2. A contribution to this comparison is made here by determining the design and performance of one type of empirical controller, and comparing its performance with that of the approximately optimal controller given by Roberts.

The empirical controllers are classified according to their basic principles of operation in the following sub-sections.

1.3.1 Constant speed controllers

a) Continuous-time systems. In these systems the input is adjusted at a constant rate in the direction in which the extremum is estimated to lie. The performance of this type of controller in connection with a plant with lags has been the subject of a number of papers [19,20,21,22]. Katkovnik and Pervozvanskii [23] have considered the effect of measurement noise on this type of system.

b) Discrete-time systems. In these systems the input is adjusted in constant steps in the direction in which the extremum is estimated to lie. Jacobs and Wonham [24] have determined the

performance of such a system in the presence of measurement noise. Xirokostas and Henderson [25] have studied the behaviour of such systems when disturbances, lags and measurement noise are all present.

1.3.2 Extrapolation controllers

These controllers operate by fitting a curve to the extremum characteristic then using this curve to predict the required change in input. Vinograd and Geronimus [26], Perelman [27,28], and Jelonek, Gardiner and Raeside [14], have studied the behaviour of such systems using quadratic prediction in the presence of measurement noise.

1.3.3 Linearised, or Gradient-type, controllers

The rest of the work in this thesis is concerned with this type of controller. The controller operates by making the input adjustment proportional to an estimate of the gradient of the extremum characteristic. If the extremum characteristic is parabolic then the input adjustment will be proportional to the difference between the actual and the desired input, as in a linear control system, so this type of controller has been termed [3,7] 'linearised'.

Most of the linearised controllers considered in the literature derive the estimate of the gradient by adding a sine or square wave perturbation at the plant input and correlating it with its effect on the plant output. Van der Grinten [29], however, has shown how a stochastic perturbation can be used, and Douce and Ng [30] have studied systems using a pseudo-random-binary-sequence. Roberts [17] has shown that under certain circumstances the best method of measuring a gradient is by using a sinusoidal perturbation.

The linearised perturbation systems discussed in the literature can be represented by figure 1.5, and are discussed below in two groups, differentiated by type of controller used.

a) Continuous-time controllers. In these systems the output u(t) of the control unit in figure 1.5 is the continuous output of a linear filter. Such controllers can only be used with a continuous plant.

Continuous perturbation systems with measurement noise have been studied by Nightingale [31] (square wave perturbation), and Jelonek, Gardiner and Paeside [14] (sine wave perturbation). The latter have compared the performance of one such system with that of a discrete-time linearised controller and an extrapolation controller. Eveleigh [32] has considered a sine wave perturbation system with lags and Pervozvanskii [33] a sine wave perturbation system with disturbances and lags. The controllers considered by the above authors incorporate multiplicative demodulation and their analyses assume that the multiplier gives an estimate of the gradient contaminated only by the measurement noise. Douce and Bond [13], however, have shown that the multiplier can give rise to 'large fluctuations' in the control signal u(t) in figure 1.5, so that the performance of the system is degraded.

In this thesis a sine wave perturbation system with disturbances, noise and lags is studied, the fluctuations mentioned by Douce and Bond being taken into account so that a complete design can be obtained.

b) Discrete-time controllers. These controllers use square wave perturbation and the control unit output u(t) in figure 1.5

changes at the same time as the perturbation so that the plant input $q(t)$ is changed only at discrete points in time. These controllers can be used with either discrete-time or continuous-time plants, the input of a continuous plant being held constant over the interval between adjustments.

Feldbaum [11] and Tovstykha [12] have considered the application of this type of controller to a discrete-time plant subject to measurement error and a steadily increasing disturbance. Feldbaum has further considered the application of this type of controller to a continuous plant with measurement noise and a ramp disturbance. Douce and Bond [13] have discussed the steady state performance in the presence of measurement noise.

Chang [5,8] has investigated the design and performance of two types of discrete-time linearised extremum controller, a "derivative sensing" controller and an "alternative biasing" controller. These controllers are studied and compared in connection with a continuous-time plant with a random disturbance and measurement noise. The results obtained for the alternative biasing controller also apply when it is used with a discrete-time plant.

1.4 Aim of Thesis

The rest of this thesis is a study of certain linearised extremum controllers of the empirical type described in the literature. The purpose of the work is to design the controllers to give their best performances in connection with the plant described in section 1.2; then to compare the resulting performances with each other and with that of the approximately optimal controller

described by Roberts. The design procedures and performance results are presented in dimensionless form for simplicity and generality.

A sine wave perturbation continuous-time controller is designed in connection with the plant described in section 1.2, when the random disturbance, the measurement noise, and the lags are all present. The performance of this controller is compared with that of Roberts' approximately optimal controller. The design procedure used and the comparison with the approximately optimal controller are thought to be original.

Three different types of extremum controller are designed, and their performances compared, when the plant has no lags. Sine wave and square wave perturbation continuous-time controllers are designed in this thesis, and Chang's results are used for the discrete-time controller considered by Feldbaum and Douce. The comparison of the performances of the three controllers is thought to be original.

The design procedure used for the continuous-time controllers is partly analytic and partly experimental. The experimental work was carried out on an analogue computer to an accuracy of approximately 5%. The design procedures are verified, and their region of validity determined, by simulating the actual extremum control systems on the analogue computer.

CHAPTER 2

An Introduction to the Work of this Thesis

2.1 Introduction

This chapter lays the foundation for the main work of the thesis. Section 2.2 defines the sine wave perturbation system with lags which is to be designed, and section 2.3 describes the three systems which are to be compared. The non-dimensional representation is introduced in section 2.4. Section 2.5 describes the basic design procedure used, and section 2.6 gives the lay-out of the remainder of the thesis.

2.2 Sine wave perturbation system with lags

Figure 2.1 shows a sine wave perturbation controller of the empirical type described in the literature [6,14,32,33] in connection with the plant described in section 1.2. The plant output is passed through a band-pass filter as suggested by Tsien [6], Nightingale [31] and Eveleigh [32], of transfer function

$$G_2(s) = \frac{2s}{T_2 s^2 + 2s + T_2 \alpha^2} \qquad (2.1)$$

where α is the perturbation frequency. The output of the band-pass filter is demodulated by multiplying it by $a_2 . \cos(\alpha t - \theta_1)$ where

$$\theta_1 = \tan^{-1}\alpha T_1 + \tan^{-1}\alpha T \qquad (2.2)$$

The multiplier output is then modified by the linear filter G(s) and the perturbation $a.\cos\alpha t$ is added to give the plant input q(t).

In chapters 4 and 5 it is shown that the performance of this system is affected by the actual value of c_{min}, being worse for large c_{min}. As has been remarked by Florentin [18] c_{min} can be scaled to take any value, say by adjusting the set point of the measuring device. In figure 2.1 this could be represented by the addition of a constant B_1 to the plant output $y(t)$. Since this work is concerned with the steady state performance it is permissible, and convenient, to combine c_{min} and B_1 and consider the extremum characteristic to be

$$c = Ax^2 + B \qquad (2.3)$$

$$\text{where} \quad B = c_{min} + B_1 \qquad (2.4)$$

and B must be regarded as a controller variable.

For the purposes of analysis and design the system of figure 2.1 can be simplified to that shown in figure 2.2 using equation (2.4) and the substitutions

$$H(s) = \frac{a_2 G(s)}{1 + sT_1} \; ; \; a = a_1(1 + \alpha^2 T_1^2)^{-\frac{1}{2}} \; ; \; \theta = \tan^{-1}\alpha T \qquad (2.5)$$

Any results obtained for the system of figure 2.2 can be modified by equations (2.5) and (2.4) to apply to the system of figure 2.1 provided that H(s) is such that its output can be differentiated so that G(s) can be realised. Figure 2.2 shows the system for which an equivalent circuit is derived in chapter 3.

In chapter 3 reasons are given for choosing the controller transfer function H(s) to be a pure integrator, and for not using the band-pass filter, that is in figure 2.2

$$H(s) = \frac{K}{s} \; ; \; T_2 = 0 \qquad (2.6)$$

Equations (2.6) modify the system of figure 2.2 to give the system shown in figure 2.3, which is the system for which the design procedure is given.

The controller in figure 2.3 has four adjustable parameters; the perturbation amplitude a, the perturbation frequency α, the integrator gain K, and the constant B which affects the mean value of the signal at the multiplier input. The required controller design is the choice of these parameters so that the performance criterion $\overline{x^2(t)}$ will be a minimum. This best choice will depend on the plant, which is described by the spectral densities $\phi_{zz}(\omega)$ and $\phi_{\xi\xi}(\omega)$, the extremum curvature A and the time constant T of the lag.

2.3 The comparison of three controllers

Three different extremum controllers are compared in connection with the same plant, the plant described in section 1.2 but without lags.

The first of these controllers is the sine wave perturbation continuous controller discussed in the previous section. The system considered is a special case of figure 2.3 with T = 0, and is shown in figure 2.4.

The second is similar to that shown in figure 2.4 but uses square wave perturbation as considered by Nightingale [31] and Douce and Bond [13]. The system considered is shown in figure 2.5, the perturbation being $a.p(t)$ where $p(t)$ is a square wave of unit amplitude and a frequency of $\frac{\alpha}{2\pi}$ cycles/sec.

The third is the discrete-time controller considered by Feldbaum [11] and Douce and Bond [13]. The system is shown in

figure 2.6. This is a special case of the derivative sensing system considered by Chang [8], whose results are used to determine its design and performance. The system of figure 2.6 differs from that of figure 2.5 only by the inclusion of a sample and hold device at the integrator output. The sample and hold device is assumed to operate at the end of each perturbation cycle. Feldbaum [11], Grishko [34], and Ng [35] have discussed controllers in which the sample and hold device operates only after some integer number of perturbation cycles. This would be of no advantage in the system of figure 2.6.

The design again consists of the choice of the perturbation amplitude a and frequency α, the integrator gain K and the constant B, in order to minimise $\overline{x^2(t)}$ for a given plant. The value of $\overline{x^2(t)}$ obtained provides a basis for the comparison of the three systems.

It will be shown that the best value of the perturbation frequency α is infinity, when all three controllers achieve the same value of $\overline{x^2(t)}$. This is only of academic interest as all practical plants will have lags which limit the perturbation frequency. What may be of practical interest, however, is how high the perturbation frequency must be to achieve 'adequately good' performance, and also which controller gives the best performance when the perturbation frequency is limited to some finite value. In order to obtain some answers to these questions the perturbation frequency was considered to be a specifiable plant parameter. The design problem is then: given a particular plant and a specified perturbation frequency α, find the values of the controller parameters a, K and B which give the minimum value of $\overline{x^2(t)}$.

Graphs of the variation of this minimum value of $\overline{x^2(t)}$ against the specified perturbation frequency α are obtained for each controller, and are used as a basis for their comparison.

2.4 The dimensionless representation

2.4.1 Some general considerations

The design procedures and performance results for the various systems considered in this work are presented in dimensionless terms. This simplifies the presentation by reducing the number of parameters involved, and makes it more general by eliminating the use of units.

Consider first the use of an optimal controller with a plant described by i parameters. With an optimal controller the performance criterion $\overline{x^2}$ is a minimum for the plant used, and so is determined only by the plant, say by the relation

$$\overline{x^2} = f_{opt} \text{ (i plant parameters)} \qquad (2.7)$$

Let the number of different kinds of unit used in equation (2.7) be k. Then Buckingham's [36] Π-theorem states that equation (2.7) can be re-written using k fewer dimensionless products of the original parameters. Let this new equation be

$$\Pi_e = f'_{opt}(\Pi_{p_1} - - \Pi_{p_{(i-k)}}) \qquad (2.8)$$

where only Π_e involves $\overline{x^2}$ and so can be regarded as a dimensionless performance criterion. Thus when an optimal controller is used the value of Π_e is determined only by the value of the independent dimensionless variables $\Pi_{p_1} - - \Pi_{p_{(i-k)}}$, which

completely define the plant as far as performance is concerned. If $i = k$ then Π_e will be a fixed number, and if $i < k$ the optimal control problem will not exist.

When an empirical controller is used in connection with the plant the performance criterion $\overline{x^2}$ will depend on the j parameters describing the controller as well as the i plant parameters, so that

$$\overline{x^2} = f \text{ (i plant parameters, j controller parameters)} \qquad (2.9)$$

Since this equation has j more parameters than equation (2.7) its dimensionless form must have j more dimensionless parameters, say $\Pi_1 - - \Pi_j$, than equation (2.8) and so can be written

$$\Pi_e = f' \left(\Pi_{p_1} - - \Pi_{p_{(i-k)}} ; \Pi_1 - - \Pi_j \right) \qquad (2.10)$$

$\Pi_1 - - \Pi_j$ must be soluble for the j controller parameters in terms of the i plant parameters.

In dimensionless terms the design procedure for the empirical controller is: given the dimensionless variables $\Pi_{p_1} - - \Pi_{p_{(i-k)}}$ describing the plant, find the values of $\Pi_1 - - \Pi_j$ which minimise Π_e. When $\Pi_1 - - \Pi_j$ take the values given by this design procedure the value of Π_e is again a function of the plant dimensionless parameters only, say

$$\Pi_e = f'_{[\Pi_1 - - \Pi_j]_{opt}} \left(\Pi_{p_1} - - \Pi_{p_{(i-k)}} \right) \qquad (2.11)$$

A comparison between the functions Π_e of $\Pi_{p_1} - - \Pi_{p_{(i-k)}}$ given by the two equations (2.11) and (2.8) gives a comparison of the performance of a properly designed empirical controller with

that of an optimal controller.

2.4.2 System with sine wave perturbation and lags

The dimensionless representation for the system shown in figure 2.3 and discussed in section 2.2 is given here.

The plant is described by four parameters: N_z and N_ξ which specify the disturbance and noise, the measurement lag time constant T, and the extremum curvature A. The units of these parameters are

N_z - input units . time$^{-\frac{1}{2}}$ A - output units/input units^2

N_ξ - output units . time$^{\frac{1}{2}}$ T - time

Equation (2.7) for the performance of the optimal controller for this plant is

$$\overline{x^2} = f_{opt}\,(N_z,\ N_\xi,\ A,\ T) \qquad (2.12)$$

Three kinds of unit - input units, output units, and time, - are used in equation (2.12), so that its dimensionless equivalent corresponding to equation (2.8) is

$$\Pi_e = f'_{opt}\,(\,\Pi_p\,) \qquad (2.13)$$

where Π_e and Π_p can be defined as

$$\Pi_e = \overline{x^2}\left(\frac{A}{N_z N_\xi}\right)^{\frac{2}{3}}\ ;\ \Pi_p = N_z{}^2 T\left(\frac{A}{N_z N_\xi}\right)^{\frac{2}{3}} \qquad (2.14)$$

The variation of the dimensionless performance criterion Π_e with the dimensionless variable Π_p describing the plant defines the performance of any controller used with this plant, the best possible performance being given by the analytic form of equation (2.13).

The controller in the system of figure 2.3 is described by the four parameters a, α, K and B, with units

a - input units K - input units . output units^{-2}. time^{-1}

α - time^{-1} B - output units

Equation (2.9) for the performance of this system becomes

$$\overline{x^2} = f\ (N_z,\ N_\xi,\ A,\ T\ ;\ a,\ \alpha,\ K,\ B) \qquad (2.15)$$

which in dimensionless form is

$$\Pi_e = f'\ (\Pi_p\ ;\ \Pi_1,\ \Pi_2,\ \Pi_3,\ \Pi_4) \qquad (2.16)$$

The design procedure is the choice of $\Pi_1 - - \Pi_4$ for a given Π_p so that Π_e will be a minimum. When the correct design procedure has been used, equation (2.11) for the performance of the empirical controller is

$$\Pi_e = f'_{[\pi_1 - - \pi_4]_{opt}}(\pi_p) \qquad (2.17)$$

A comparison of the functions Π_e of Π_p given by equations (2.17) and (2.13) gives a comparison of the performance of the empirical controller shown in figure 2.3 with the performance of an optimal controller.

The controller dimensionless parameters $\Pi_1 - - \Pi_4$ were chosen to suit the analysis of subsequent chapters, which deal with the development of the analytic form of equation (2.16). The definitions are summarised here:

$$\Pi_1 = \frac{B}{Aa^2} \qquad \Pi_3 = \frac{N_z^{\,2}}{Ka^3A}$$

$$\Pi_2 = \frac{\alpha}{KaA} \qquad \Pi_4 = \frac{KN_\xi^{\,2}}{Aa^3} \qquad (2.18)$$

2.4.3 Plant considered by Roberts [17]

As mentioned in section 1.3 Roberts considers a plant similar to that described in section 1.2 but where c_{min} is a brownian motion m(t) of spectral density

$$\phi_{mm}(\omega) = \frac{N_m^2}{\omega^2} \tag{2.19}$$

Roberts uses two parameters to describe this 'vertical' disturbance m(t): the parameter N_m output units/$\sqrt{\text{time}}$ which describes its magnitude; and a 'coefficient of correlation' which describes how this 'vertical' disturbance m(t) is correlated with the 'horizontal' disturbance z(t) defined in section 1.2. These two parameters, in addition to the parameters N_z, N_ξ, A and T discussed in sub-section 2.4.2 above, describe the plant considered by Roberts. Equation (2.7) for the performance of the optimal controller becomes

$$\overline{x^2} = f_{opt}\ (N_z,\ N_\xi,\ A,\ T, N_m,\ \text{coeff. of correlation}) \tag{2.20}$$

which can be written in dimensionless form as

$$\Pi_e = f'_{opt}\ (\Pi_p,\ \Pi_m,\ \Pi_c) \tag{2.21}$$

Π_e and Π_p are as previously defined by equations (2.14). Π_m can be defined as

$$\Pi_m = T\,\frac{N_m}{N_\xi} \tag{2.22}$$

and gives an indication of the relative importance of the variation m(t) of c_{min}, as compared to the measurement noise $\xi(t)$, in determining the performance of the system. Π_c describes the correlation between m(t) and $\xi(t)$, and can be chosen so that $\Pi_c = 0$ when the correlation is zero.

Roberts gives an approximation to equation (2.21) for the performance of the optimal controller, which is valid in certain circumstances.

The plant considered in the rest of this work is a special case of that considered by Roberts where the vertical disturbance m(t) is zero. With the above definitions of Π_m and Π_c, equation (2.13) for the performance of the special case is obtained from equation (2.21) for the general case by setting $\Pi_m = \Pi_c = 0$.

The performance of a properly designed empirical controller will be compared with the performance of Roberts' approximately optimal controller by comparing an approximation to equation (2.17) obtained in this thesis with Roberts' approximation to equation (2.21) when $\Pi_m = \Pi_c = 0$.

2.4.4 Comparison of three controllers

The three systems shown in figures 2.4, 2.5 and 2.6 are described by exactly the same parameters as the system of figure 2.3 discussed above except that T = 0. Thus each plant is described by the parameters N_z, N_ξ and A, and each controller by a, α, K and B. So equation (2.9) for the performance of the controllers is

$$\overline{x^2} = f\ (N_z,\ N_\xi,\ A\ ;\ a,\ \alpha,\ K,\ B) \qquad (2.23)$$

In dimensionless form this becomes

$$\Pi_e = f\ (\ \Pi_1\ -\ -\ \Pi_4\ ) \qquad (2.24)$$

so that for the best choice of Π_1 - - Π_4, Π_e is a fixed number, which can be compared with that obtained by an optimal controller.

In section 2.3, however, the case where the perturbation frequency α is specifiable is shown to be of interest. Thus in

equation (2.23) α can be grouped with the plant parameters, so that

$$\overline{x^2} = f\ (N_z,\ N_\xi,\ A,\ \alpha\ ;\ a,\ K,\ B) \qquad (2.25)$$

and the design procedure is the choice of a, K and B, given N_z, N_ξ, A and α, so as to minimise $\overline{x^2}$. α can be combined with the plant parameters to give the dimensionless perturbation frequency Π_α, where

$$\Pi_\alpha = \frac{\alpha}{N_z^{\,2}} \left(\frac{N_z N_\xi}{A}\right)^{\frac{2}{3}} \qquad (2.26)$$

and equation (2.24) can be written in the dimensionless form

$$\Pi_e = f\ (\ \Pi_\alpha\ ;\ \Pi_1,\ \Pi_2,\ \Pi_3\ ) \qquad (2.27)$$

where Π_e, Π_1, Π_2 and Π_3 are as defined before by equations (2.14) and (2.18).

The design procedure is: given a dimensionless perturbation frequency Π_α, find the values of Π_1, Π_2 and Π_3 which minimise Π_e. The variation of Π_e with Π_α when Π_1, Π_2 and Π_3 are chosen according to this design procedure is obtained for each of the three systems discussed in section 2.3, and is used as a basis for their comparison.

2.5 The design procedure

The continuous extremum control systems described in sections 2.2 and 2.3 were designed using the procedure outlined in this section.

An analytic form is obtained for equation (2.18) which gives the dependence of the performance criterion Π_e on the dimension-

less controller parameters $\Pi_1 - - \Pi_4$. The values of $\Pi_1 - - \Pi_4$ which minimise Π_e are then found using a digital computer function minimisation routine.

The analytic form of equation (2.16) is obtained partly from theoretical arguments and partly from experimental observations. Analytic techniques are used to develop a linear equivalent circuit for the extremum control system under examination, i.e those shown in figures 2.3, 2.4 and 2.5. This linear equivalent circuit gives an approximation to the output u(t) of the controller integrator for a given disturbance z(t) and measurement noise $\xi(t)$, and so gives an estimate of the transient response of the system. Its main use, however, is to give an estimate of the performance criterion $\overline{x^2(t)}$ as a function of the system parameters.

$$\text{Est}\,[\overline{x^2(t)}] = f_{\text{equiv.cct.}}(\text{system parameters}) \qquad (2.28)$$

This estimate of $\overline{x^2(t)}$ will differ from the true value of $\overline{x^2(t)}$ by some factor γ, defined by the relationship

$$\overline{x^2(t)} = \gamma\ \text{Est}[\overline{x^2(t)}] \qquad (2.29)$$

The factor γ will depend on the particular system and so will be a function $\gamma(\Pi_p ; \Pi_1 - - \Pi_4)$ of the dimensionless variable describing the system. An approximation to $\gamma(\Pi_p ; \Pi_1 - - \Pi_4)$ is obtained experimentally, by simulating the system on an analogue computer. In order to simplify the experimental work the variation of γ was not obtained over the full range of the dimensionless variables $\Pi_p ; \Pi_1 - - \Pi_4$, but only over the part of the range that was thought to be of most interest.

The derivation of the equivalent circuit corresponds to the 'linearisation' suggested by Jacobs [3] and which is the basis of the analyses carried out by Jelonek, Gardiner and Raeside [14], Nightingale [31], Eveleigh [32] and Pervozvanskii [33]. Obtaining the estimate of the validity of the equivalent circuit takes into account the 'large fluctuations' discussed by Douce and Bond [13] and enables a complete design to be obtained. The analytic derivation of the equivalent circuit, the determination of an estimate of its validity, and the design procedure, are thought to be original.

2.6 Layout of thesis

The remainder of the thesis can be divided into two main parts: chapters 3, 4, 5 and 6 which deal with the sine wave perturbation controller when the plant has lags; and chapters 7 and 8 which deal with the comparison of three controllers when the plant has no lags.

In chapter 3 the equivalent circuit for the sine wave perturbation system is derived, and in chapter 4 a quantitative estimate of its validity is made. The results of chapters 3 and 4 are combined in chapter 5 to give the system design and this design is checked experimentally. In chapter 6 the region of usefulness of the design is discussed and the performance of the system is compared with that of Roberts' approximately optimal controller.

In chapter 7 three graphs of the performance criterion Π_e against the dimensionless perturbation frequency Π_α are obtained analytically. In chapter 8 experimental results are discussed and the three controllers are compared. Chapter 9 summarises the results obtained and gives suggestions for future work.

CHAPTER 3

The Equivalent Circuit

3.1 Introduction

In this chapter a linear equivalent circuit is derived for the sine wave perturbation system shown in figure 2.2 and introduced in section 2.2. The purpose of the equivalent circuit is to give an approximation $u'(t)$ to the output $u(t)$ of the controller integrator, for a particular disturbance $z(t)$ and noise $\xi(t)$. This relationship is shown diagrammatically in figure 3.1.

A simple special case of the complete system of figure 2.2 is considered first in order to introduce the equivalent circuit and the assumptions made in its derivation. These assumptions are then used to obtain the equivalent circuit for the complete system.

Some experimental responses of $u(t)$ and $u'(t)$ are presented to show how $u'(t)$ can be used to give the transient response of the extremum control system, and to indicate the nature of the approximation of $u(t)$ by $u'(t)$.

The equivalent circuit is then used to make some observations about the choice of the controller transfer function $H(s)$, and the design of the band-pass filter.

Finally the use of the equivalent circuit to give an estimate of the performance criterion $\overline{x^2}$ is discussed.

3.2 A Simplified system

The derivation of the equivalent circuit is introduced by considering a special case of the system shown in figure 2.2 where the measurement noise, measurement lag and band-pass filter are

neglected and where the controller linear filter is a pure integrator, that is where

$$N_{\zeta} = 0 \; ; \; T = 0 \; ; \; T_2 = 0 \; ; \; H(s) = \frac{K}{s} \tag{3.1}$$

The differential equation of this system is derived by writing an equation for the extremum input,

$$x = z-u + a\cos\alpha t \tag{3.2}$$

Using equation (3.2) in equation (2.3) for the extremum characteristic gives

$$c = A(z-u)^2 + B + 2Aa(z-u)\cos\alpha t + Aa^2\cos^2\alpha t \tag{3.3}$$

Equation (3.3) and standard trigorometric relationships give the multiplier output

$$v = c\cdot\cos\alpha t = Aa(z-u) + [A(z-u)^2 + B + \tfrac{3}{4}Aa^2]\cos\alpha t + Aa(z-u)\cos 2\alpha t + \tfrac{1}{4}Aa^2\cos 3\alpha t \tag{3.4}$$

Equation (3.4) and the integrator differential equation

$$v = \frac{1}{K}\frac{du}{dt} \tag{3.5}$$

combine to give the system differential equation

$$u + \frac{du/dt}{KaA} = z + \{\frac{1}{a}[(z-u)^2 + \frac{B}{A} + \tfrac{3}{4}a^2]\cos\alpha t + (z-u)\cos 2\alpha t + \tfrac{1}{4}a\cos 3\alpha t\} \tag{3.6}$$

If all the terms in brackets { } could be neglected equation (3.6) might be approximated by

$$u' + \frac{du'/dt}{KaA} = z \tag{3.7}$$

Equation (3.7) is the differential equation of the system shown in figure 3.2. Equations (3.6) and (3.7) can be combined to

give the differential equation for difference between u and u' as

$$(u-u') + \frac{1}{KaA}\frac{d(u-u')}{dt} = \{\frac{1}{a}[(z-u)^2 + \frac{B}{A} + \frac{3}{4}a^2]\cos\alpha t + (z-u)\cos 2\alpha t + \frac{1}{4}a\cos 3\alpha t\} \qquad (3.8)$$

If $(u-u')$ as given by equation (3.8) is small then u' will be a good approximation to u and the linear system of figure 3.2 can be used as an equivalent circuit for the extremum control system of figure 2.2 and equations (3.1).

The assumptions used

Equation (3.8) shows that $(u-u')$ is the output of the low pass filter equivalent circuit of bandwidth KaA rads/sec, when the input consists of the terms in brackets { }. $(u-u')$ will be small and the equivalent circuit valid if the terms in brackets { } can be assumed sufficiently high in frequency compared to the bandwidth of the equivalent circuit.

Provided that the perturbation frequency α is high and the disturbance z(t) is band limited then the terms in brackets { } will be in frequency bands around α, 2α and 3α, so $(u-u')$ can be made small if α is large compared to the bandwidth KaA of the equivalent circuit, that is if

$$\frac{\alpha}{KaA} = \Pi_2 >> 1 \qquad (3.9)$$

The dimensionless variable Π_2 is one of those used in section 2.4 to describe the extremum control systems, and for this simple system it is the ratio of the perturbation frequency to the equivalent circuit bandwidth.

The more complicated systems considered in the rest of this

chapter also have equivalent circuits with low pass filtering properties. The main aasumption made in the derivation of these equivalent circuits is the same as that made above for the simple system; that is that terms of frequency around α, 2α and 3α in the differential equation for u(t) can be neglected because of the low pass filtering properties of the equivalent circuit. For the more complicated systems it has proved impossible to derive the complete differential equation for u(t), then group together the terms to be neglected. The equivalent circuit can be derived, however, by neglecting as they arise in the analysis the terms which give rise only to the high frequency 'unwanted' terms in the differential equation for u(t).

A more detailed and quantitative discussion of the validity of the above assumptions, and hence the validity of the equivalent circuit, is given in chapter 4.

3.3 System with measurement lag

The addition of a measurement lag to the basic system considered in the previous section gives a special case of the system shown in figure 2.2 where

$$N_\xi = 0 \; ; \; T_2 = 0 \; ; \; H(s) = \frac{K}{s} \qquad (3.10)$$

The equivalent circuit for this system is derived in a similar way as that for the basic system except that terms giving rise to the high frequency 'unwanted' terms in the differential equation for u(t) are neglected as they arise in the analysis.

The equation for the output of the extremum characteristic is the same as that for the basic system, equation (3.3), and can be written

$$c = 2Aa(z-u)\cos\alpha t + \{A(z-u)^2 + B + Aa^2\cos^2\alpha t\} \qquad (3.11)$$

In equation (3.11) the terms in brackets { } will give rise only to high frequency terms after the multiplier so are 'unwanted' terms as far as the equivalent circuit derivation is concerned. Neglecting the terms in brackets { } equation (3.11) becomes

$$c' = 2Aa(z-u)\cos\alpha t = c''\cos\alpha t \qquad (3.12)$$

where c' can be defined as the 'useful' part of c(t) as it gives rise to the low frequency components of u(t). In appendix 1 it is shown that the relationship between c' and the useful signal v' at the multiplier output can be approximated by the relationship

$$v' = \tfrac{1}{2}(1 + \alpha^2T^2)^{-\frac{1}{2}}c'' \qquad (3.13)$$

provided variations in $c'' = 2Aa(z-u)$ are slow compared to the perturbation frequency α. Combining equations (3.13) and (3.12) gives the useful signal at the multiplier output as

$$v' = \frac{Aa}{(1 + \alpha^2T^2)^{\frac{1}{2}}}(z-u) \qquad (3.14)$$

v' is then filtered by the controller integrator to give the output u' according to the equation

$$v' = \frac{1}{K}\frac{du'}{dt} \qquad (3.15)$$

Assuming u' is a good approximation to u equations (3.14) and (3.15) can be combined to give the differential equation

$$u' + \frac{(1 + \alpha^2T^2)^{\frac{1}{2}}}{KAa}\frac{du'}{dt} = z \qquad (3.16)$$

which is the differential equation of the linear system shown in figure 3.3 which is an equivalent circuit for the system with

measurement lag considered in this section. A comparison of figure 3.3 with figure 3.2 shows that the measurement lag has introduced attenuation into the equivalent circuit and so reduced its bandwidth.

3.4 System with band-pass filter

The addition of a band-pass filter to the basic system discussed in section 3.2 gives a special case of the system shown in figure 2.2 where

$$N_\xi = 0 \; ; \; T = 0 \; ; \; H(s) = \frac{K}{s} \qquad (3.17)$$

The equivalent circuit for this system is derived in exactly the same way as in the previous section, the results for the band-pass filter being substituted for those pertaining to the measurement lag.

The equation for the useful signal at the extremum output is again equation (3.12). In appendix 2 it is shown that the relationship between the useful signal at the extremum output and the low frequency useful signal $v'(t)$ at the multiplier output is approximated by the relationship

$$v' + T_2 \frac{dv'}{dt} = \tfrac{1}{2}c''$$

which from the definition of c" given by equation (3.12) is

$$v' + T_2 \frac{dv'}{dt} = Aa(z-u) \qquad (3.18)$$

Combining equation (3.18) with equation (3.15) for the controller integrator and assuming u' to be a good approximation to u, gives

the differential equation

$$\frac{T_2}{KaA}\frac{d^2u'}{dt^2} + \frac{1}{KaA}\frac{du'}{dt} + u' = z \qquad (3.19)$$

which is the differential equation of the system shown in figure 3.4 which is an equivalent circuit for the system with band-pass filter considered in this section.

A comparison of figure 3.4 with figure 3.2 shows that the use of the band-pass filter introduces a lag into the equivalent circuit.

3.5 Measurement lag and band-pass filter together

The equivalent circuit for systems with measurement lag and band-pass filter operating separately, namely figures 3.3 and 3.4, suggest the system of figure 3.5 as the equivalent circuit when both the measurement lag and the band-pass filter are present, that is for the system of figure 2.2 when

$$N_\xi = 0 \; ; \; H(s) = \frac{K}{s} \qquad (3.20)$$

The measurement lag and band-pass filter are linear filters and operate sequentially on the useful signal at the extremum output so it is reasonable to assume that their equivalent circuit effects act sequentially, as in the system of figure 3.5. Since the band-pass filter attenuates 'unwanted' signals at the output of the measurement lag the presence of the band-pass filter should make the equivalent circuit representation of the measurement lag even more accurate.

3.6 Measurement noise and the complete equivalent circuit

Consider now the complete system of figure 2.2 with the sole restriction that

$$H(s) = \frac{K}{s} \tag{3.21}$$

Since the addition of the measurement noise, band-pass filtering, and multiplication by the common factor $\cos(\alpha t-\theta)$ are linear operations the system of figure 2.2 and equation (3.21) can be redrawn as shown in figure 3.6. There the effect of the measurement noise is represented by the addition of the random signal $\xi''(t)$ at the integrator input.

The measurement noise $\xi(t)$ is the white noise defined in chapter 1, of spectral density

$$\phi_{\xi\xi}(\omega) = N_\xi^2$$

so the spectral density of the random term $r(t)$ after the band-pass filter will be

$$\phi_{rr}(\omega) = N_\xi^2 \left| G_2(j\omega) \right|^2 \tag{3.22}$$

The equivalent random term added in at the input to the controller integrator is given as

$$\xi''(t) = r(t)\cos(\alpha t-\theta)$$

The spectral density of $\xi''(t)$ in terms of the spectral density of $r(t)$ can be shown (Mesch [37]) to be

$$\phi_{\xi''\xi''}(\omega) = \tfrac{1}{4}[\phi_{rr}(\omega+\alpha) + \phi_{rr}(\omega-\alpha)] \tag{3.23}$$

combining equations (3.22) and (3.23) gives

$$\phi_{\xi''\xi''}(\omega) = \tfrac{1}{4}N_\xi^2\{|G_2(j\omega+j\alpha)|^2 + |G_2(j\omega-j\alpha)|^2\} \qquad (3.24)$$

In appendix 2 it is shown that for $\omega<<\alpha$

$$G_2(j\omega+j\alpha) \approx G_2(j\omega-j\alpha) = \frac{1}{1+j\omega T_2} \qquad (3.25)$$

so substituting equation (3.25) in equation (3.24) gives

$$\phi_{\xi''\xi''}(\omega) = \tfrac{1}{2}N_\xi^2\left|\frac{1}{1+j\omega T_2}\right|^2 \qquad (3.26)$$

Thus the effect of the measurement noise can be regarded as being due to an equivalent random term $\xi''(t)$ added to the input $v(t)$ of the controller integrator, so in the equivalent circuit the effect of the measurement noise can be represented by adding $\xi''(t)$ to the low frequency 'useful' signal $v'(t)$ at the input to the controller integrator to give the system shown in figure 3.7. A more convenient representation is shown in figure 3.8 where the white noise $\xi'(t)$ of spectral density

$$\phi_{\xi'\xi'}(\omega) = \tfrac{1}{2}N_\xi^2 \qquad (3.27)$$

is added in before the representation of the band-pass filter.

The system shown in figure 3.8 is an equivalent circuit for the complete system of figure 2.2 and equation (3.21).

3.7 Experimental demonstration of the equivalent circuit

In order to illustrate the physical significance of the approximations made in deriving the equivalent circuit, the extremum control system and its equivalent circuit were simulated on an analogue computer, and the transient response of $u(t)$ and $u'(t)$

from the same initial error was recorded. This also illustrates the use of the equivalent circuit in estimating the transient reponse of the system.

The systems simulated were those for which equivalent circuits are derived in sections 3.2, 3.3, 3.4 and 3.5. In each case the initial error was of magnitude 5a.

In chapter 4 some quantitative conditions for equivalent circuit validity are given. These concern the dimensionless variables $\Pi_1 = \frac{B}{Aa^2}$ and $\Pi_2 = \frac{\alpha}{KaA}$ which partly describe the systems considered in this section. The extremum control systems considered here were simulated with two sets of the dimensionless variables Π_1 and Π_2: with one set, $\Pi_1 = 0$ and $\Pi_2 = 100$, the results of chapter 4 suggest the equivalent circuit to be closely valid; and with the other set, $\Pi_1 = 0$ and $\Pi_2 = 10$, only approximately valid.

The basic system

The results for the basic system considered in section 3.2 are shown in figures 3.9. Figure 3.9a shows the response of the equivalent circuit, 3.9b the response of the actual system with $\Pi_2 = 100$, and 3.9c the response when $\Pi_2 = 10$. Each of these curves starts at -5a and ends near zero, the vertical shift having been introduced for clarity of presentation.

From these curves it is seen that the effect of the equivalent circuit approximation is to neglect the perturbation frequency fluctuation in u(t). This fluctuation is increased when Π_2 is reduced to 10. It can be said that the equivalent circuit gives useful information about the transient response of the actual system.

System with measurement lag

The results for the system with measurement lag discussed in section 3.3 are shown in figures 3.10. The perturbation frequency and measuremcnt lag were such that $\alpha T = 1$.

Figure 3.10c shows that when $\Pi_2 = 10$ there is a substantial difference between the actual response u(t) and the equivalent circuit response u'(t), even when the perturbation frequency terms are neglected. It was found that with lower values of Π_2, or with larger disturbances, the system could become unstable. This instability is discussed further in chapter 4.

System with band-pass filter

The results for the system with band-pass filter discussed in section 3.4 are shown in figures 3.11. The time constant T_2 of the band-pass filter was chosen so that the equivalent circuit predicts a 20% overshoot, that is

$$T_2 = \frac{1}{0.81\ KaA} \tag{3.28}$$

using the equivalent circuit of figure 3.4 and standard relationships for the second order system.

A comparison of the results of figures 3.11 with those of figures 3.9 shows that the band-pass filter effects a considerable reduction in the perturbation frequency oscillations in u(t).

System with measurement lag and band-pass filter

The results for the system with measurement lag and band-pass filter discussed in section 3.5 are shown in figures 3.12. αT was again chosen to be unity and T_2 chosen to give a predicted overshoot of 20%, that is

$$T_2 = \frac{(1+\alpha^2T^2)^{\frac{1}{2}}}{0.81\ KaA} \qquad (3.29)$$

A comparison of figures 3.12 and 3.10 shows again that the difference between u(t) and u'(t) is reduced when the band-pass filter is present.

3.8 Design of the controller filter and of the band-pass filter

The complete equivalent circuit of figure 3.8 can be used to make some observations about the design of the transfer function H(s) and the band-pass filter $G_2(s)$ in the system of figure 2.2.

The equivalent circuit of figure 3.8 is a special case of the system shown in figure 3.13 in which

$$F_1(s) = \frac{KaA}{(1+\alpha^2T^2)^{\frac{1}{2}}} \; ; \; F_2(s) = \frac{K}{s(1+sT_2)} \qquad (3.30)$$

For any specification of $\phi_{zz}(\omega)$, $\phi_{\xi'\xi'}(\omega)$ and $F_1(s)$ the choice of $F_2(s)$ which minimises $\overline{(z-u')^2}$ can be obtained using statistical design techniques. In appendix 3 it is shown that when $F_1(s)$ is a pure gain, as in figure 3.8, and when $\phi_{zz}(\omega)$ and $\phi_{\xi'\xi'}(\omega)$ are as given by equations (1.3) and (3.27), then $F_2(s)$ should represent an integrator, that is

$$F_2(s) = \frac{K}{s} \qquad (3.31)$$

Equation (3.31) is the same as equation (3.30) if $T_2 = 0$, so the equivalent circuit of figure 3.8 suggests that the band-pass filter should not be used, and that the best controller filter is an integrator.

The experimental results of the preceding section indicate

that the band-pass filter makes the equivalent circuit more valid. Thus the band-pass filter may be desirable, for instance to reduce the perturbation frequency fluctuations in u(t) or to reduce interaction in a multivariable system. Also it is shown later that the band-pass filter automatically provides the best mean level at the multiplier input, so eliminating the need to adjust B. Nevertheless the band-pass filter is not considered further in this thesis because the results of the next chapter show that satisfactory results can be obtained, at least in some circumstances without it.

When no band-pass filter is used and the controller filter is an integrator the system of figure 2.2 is simplified by the equations

$$H(s) = \frac{K}{s} \; ; \; T_2 = 0 \qquad (3.32)$$

to give the system shown in figure 2.3, which is the system considered in the rest of this work.

3.9 The use of the equivalent circuit

The main use of the equivalent circuit in this work is to give an estimate $Est[\overline{x^2}]$ of the performance criterion $\overline{x^2(t)}$. From figure 2.3 it can be seen that

$$x(t) = z(t) + q(t) = z(t)-u(t) + a\cos\alpha t \qquad (3.33)$$

so that $$x^2(t) = (z-u)^2 + a^2\cos^2\alpha t + 2a(z-u)\cos\alpha t \qquad (3.34)$$

Assuming that the equivalent circuit signal u'(t) is a good approximation to u(t) then an estimate of $x^2(t)$ can be obtained from equation (3.34) as

$$Est[x^2(t)] = (z-u')^2 + a^2\cos^2\alpha t + 2a(z-u')\cos\alpha t \qquad (3.35)$$

Since the perturbation waveform $\cos\alpha t$ does not appear in the equivalent circuit and since $z(t)$ and $\xi'(t)$ are not correlated with $\cos\alpha t$ then $u'(t)$ is not correlated with $\cos\alpha t$. Thus all three terms in equation (3.34) are uncorrelated and the mean value of $Est[x^2(t)]$ is

$$Est[\overline{x^2}] = \overline{(z-u')^2} + \overline{a^2\cos^2\alpha t} + \overline{2a(z-u')\cos\alpha t} \qquad (3.36)$$

Since $(z-u')$ and $\cos\alpha t$ are uncorrelated the third term in equation (3.36) is zero, and equation (3.36) becomes

$$Est[\overline{x^2}] = \overline{(z-u')^2} + \frac{a}{2}^2 \qquad (3.37)$$

The equivalent circuit of figure 3.8 gives an estimate of $\overline{(z-u')^2}$ as

$$\overline{(z-u')^2} = \frac{1}{2\pi}\int_{-\infty}^{\infty}\left|\frac{j\omega}{j\omega+\frac{KaA}{(1+\alpha^2T^2)^{\frac{1}{2}}}}\right|^2\phi_{zz}(\omega)d\omega + \frac{1}{2\pi}\int_{-\infty}^{\infty}\left|\frac{\frac{1}{2}K}{j\omega+\frac{KaA}{(1+\alpha^2T^2)^{\frac{1}{2}}}}\right|^2\phi_{\xi'\xi'}(\omega)d\omega \qquad (3.38)$$

which, using equation (3.37 and the expressions for $\phi_{zz}(\omega)$ and $\phi_{\xi'\xi'}(\omega)$ given in equations (1.3) and (3.27), gives

$$Est[\overline{x^2}] = [N_z^2 + \tfrac{1}{2}K^2N_\xi^2]\frac{(1+\alpha^2T^2)^{\frac{1}{2}}}{2KaA} + \frac{a}{2}^2 \qquad (3.39)$$

which, in terms of the dimensionless variables defined in section 1.4.2, becomes

$$Est[\Pi_e] = \tfrac{1}{2}\left(\frac{1}{\Pi_3\Pi_4}\right)^{\frac{1}{3}}\left[1 + (\Pi_3+\tfrac{1}{2}\Pi_4)\left\{1 + \Pi_2^2\Pi_p^2\left(\left(\frac{\Pi_4}{\Pi_3^2}\right)^{\frac{2}{3}}\right)\right\}^{\frac{1}{2}}\right] \qquad (3.40)$$

Equation (3.40) gives the equivalent circuit estimate of the dimensionless performance criterion Π_e for any particular plant described by Π_p and a controller described by Π_2, Π_3 and Π_4.

Along with the estimate of its validity given in the next chapter, this equation provides a basis for the best choice of the controller parameters.

CHAPTER 4

The Validity of the Equivalent Circuit

4.1 Introduction

In the previous chapter the equivalent circuit was used to obtain the estimate of the performance given by equation (3.40). Before this equation can be used to design the system some quantitative information about its validity must be obtained. This information is contained in the function $\gamma(\Pi_p , \Pi_1 - - \Pi_4)$ defined in section 2.5 by the relationship

$$\text{Actual } \Pi_e = \gamma(\Pi_p , \Pi_1 - - \Pi_4) \text{ Est}[\Pi_e] \qquad (4.1)$$

If $\gamma(\Pi_p , \Pi_1 - - \Pi_4)$ could be determined exactly then equation (4.1) could be used to find a complete and accurate design.

In this chapter some information about $\gamma(\Pi_p , \Pi_1 - - \Pi_4)$ is obtained experimentally, by simulating the actual system and the equivalent circuit on the analogue computer and taking γ as

$$\gamma = \frac{\text{measured value of } \overline{x^2}}{\text{equivalent circuit estimate of } \overline{x^2}} \qquad (4.2)$$

A complete evaluation of $\gamma(\Pi_p , \Pi_1 - - \Pi_4)$ would involve a 5-dimensional exploration of γ. For reasons of time and complexity this was not done. Instead the experimental work is simplified by heuristic argument to a determination of the variation of γ with the two parameters Π_1 and Π_2, when Π_p, Π_3 and Π_4 take certain specified values. These values of Π_p, Π_3 and Π_4 are chosen so that the resulting function

$\gamma(\Pi_1, \Pi_2)$ can be used as an approximation to $\gamma(\Pi_p, \Pi_1 - - \Pi_4)$ for a range of properly designed systems.

4.2 System with disturbances only

In this section further consideration is given to the basic system with a random disturbance but with no noise or lag, that is the system shown in figure 2.3 with

$$\xi(t) = 0 \; ; \; T = 0 \; ; \; \phi_{zz}(\omega) = \frac{N_z^2}{\omega^2} \tag{4.3}$$

From the definitions of the dimensionless variables given in section 2.4 Π_p and Π_4 are zero for this system, which is therefore described by the dimensionless variables Π_1, Π_2 and Π_3.

A suitable choice of Π_3 is that which gives the best value of perturbation amplitude according to the equivalent circuit. The equivalent circuit estimate of $\overline{x^2}$ for this system is obtained by substituting $N_\xi = 0$ and $T = 0$ in equation (3.39), which then gives

$$\mathrm{Est}[\overline{x^2}] = \frac{N_z^2}{2KaA} + \frac{a^2}{2} \tag{4.4}$$

The value of a which minimises $\mathrm{Est}[\overline{x^2}]$ in equation (4.4) is given when

$$\frac{\delta\, \mathrm{Est}[\overline{x^2}]}{\delta a} = -\frac{N_z^2}{2Ka^2A} + a = 0$$

$$\therefore a^3 = \frac{N_z^2}{2KA} \tag{4.5}$$

so that

$$\Pi_3 = \frac{N_z^2}{Ka^3A} = 2 \tag{4.6}$$

Substituting from equation (4.5) into equation (4.4) gives

$$\text{Est}[\overline{x^2}] = \overline{(z - u')^2} + \frac{a^2}{2} = a^2 + \frac{a^2}{2} \qquad (4.7)$$

If the equivalent circuit is approximately valid so that $\text{Est}[\overline{x^2}]$ is a good approximation to $\overline{x^2}$ then equation (4.7) shows that the contribution of the perturbation to the total error is one half of that due to the imperfect following of the disturbance. This relationship has been noted by Roberts in his approximately optimal controller.

When Π_3 is set according to equation (4.6) γ will be a function only of Π_1 and Π_2. This special case of $\gamma(\Pi_p ; \Pi_1 , \Pi_2 , \Pi_3 , \Pi_4)$ denoted by $\gamma(0 ; \Pi_1 , \Pi_2 , 2 , 0)$ is investigated in the following two sub-sections.

4.2.1 Analytic investigation of $\gamma(0 ; \Pi_1 , \Pi_2 , 2 , 0)$

In this sub-section conditions on Π_1 and Π_2 are determined which will make the difference between the actual signal $u(t)$ and the equivalent circuit signal $u'(t)$ small, that is which will make γ tend to unity.

In section 3.2 an equivalent circuit was obtained for this system and equation (3.8) for the difference between u and u' derived.

In section 3.2 it was argued that $(u - u')$ will be small, and hence γ will be approximately unity, when the following conditions are satisfied:

Condition (i)

The perturbation frequency α is large compared with the

bandwidth KaA of the system, that is

$$\alpha >> KaA \tag{4.8}$$

Condition (ii)

The major frequency components of $(z - u)$ must be at frequencies low compared with $\alpha/2$ so that no appreciable low frequency power is given by the term $(z - u)^2 \cos\alpha t$ in the brackets { } in equation (3.8).

When the above two conditions are satisfied the terms in brackets { } in equation (3.8) will be in narrow frequency bands centred on α, 2α and 3α. These signals make their contribution to $(u - u')$ through the low pass filter represented by equation (3.8). The contributions to $(u - u')$ will therefore be smaller than the actual signals by the factors $\frac{KaA}{\alpha}$, $\frac{KaA}{2\alpha}$ and $\frac{KaA}{3\alpha}$, so that the order of magnitude of the components of $(u - u')$ at frequencies α, 2α and 3α can be listed as expressions (4.9a), (4.9b) and (4.9c)

$$\frac{KaA}{\alpha} \{\text{order of magnitude of } \frac{1}{a}[(z-u)^2 + \frac{B}{A} + \frac{3}{4}a^2]\} \tag{4.9a}$$

$$\frac{KaA}{2\alpha} \{\text{order of magnitude of } (z-u)\} \tag{4.9b}$$

$$\frac{KaA}{3\alpha} \{\text{order of magnitude of } \frac{1}{4}a\} \tag{4.9c}$$

The equivalent circuit will be valid if all the above contributions to $(u - u')$ are small. Since the actual plant input can be considered the sum of u', $(u - u')$ and $a\cos\alpha t$ then $(u - u')$ will be negligible if it is small compared with the perturbation amplitude a. This will be the case if the magnitude of each of the components of $(u - u')$ given by

expressions (4.9a), (4.9b) and (4.9c) are small compared with a, that is when

$$\frac{KaA}{\alpha}\left\{\text{order of magnitude of }\left[\left(\frac{z-u}{a}\right)^2+\frac{B}{Aa^2}+\frac{3}{4}\right]\right\} << 1 \qquad (4.10a)$$

$$\frac{KaA}{2\alpha}\left\{\text{order of magnitude }\frac{z-u}{a}\right\} << 1 \qquad (4.10b)$$

$$\frac{KaA}{3\alpha}\left\{\text{order of magnitude }\frac{1}{4}\right\} << 1 \qquad (4.10c)$$

An estimate of the order of magnitude of $\frac{z-u}{a}$ in inequalities (4.10) can be obtained using equation (4.7), which shows that $\overline{(z-u)^2} = a^2$. If the equivalent circuit is to be approximately valid then $\overline{(z-u')^2} \approx \overline{(z-u)^2}$ so $\frac{\overline{(z-u)^2}}{a^2} \approx 1$, so that a reasonable order of magnitude of $\frac{z-u}{a}$ is unity. Inequalities (4.10) are then satisfied if

$$\Pi_2 = \frac{\alpha}{KaA} >> 1 \qquad (4.11a)$$

$$\Pi_2 >> \left|\frac{B}{Aa^2}\right| = |\Pi_1| \qquad (4.11b)$$

In terms of the (Π_1 , Π_2) plane shown in figure (4.1) conditions (4.11) show that for the equivalent circuit to be valid (Π_1 , Π_2) must lie within the hatched region, and well away from the boundaries.

4.2.2 The experimental determination of $\gamma(0 ; \Pi_1 , \Pi_2 , 2 , 0)$

In this sub-section the actual variation of γ with Π_1 and Π_2 was determined experimentally. The system under discussion, that shown in figure 2.3 with

$$\Pi_p = \Pi_4 = 0 \; ; \; \Pi_3 = 2$$

was simulated on the analogue computer and the actual value of

$\overline{x^2}$ measured. This was compared with the equivalent circuit estimate to give the measured value of γ. The experiment was repeated for various values of Π_1 and Π_2 so that the contours of constant γ in the (Π_1 , Π_2) plane shown in figure 4.2 could be plotted. The accuracy of the results shown in figure 4.2 is of the order of 5%. Details of the experimental work are given in appendix 4.

Figure 4.2 gives a quantitative description of $\gamma(0;\ \Pi_1 , \Pi_2 , 2 , 0)$ and is important to this work because it embodies the approximation to $\gamma(\Pi_p ;\ \Pi_1 , \Pi_2 , \Pi_3 , \Pi_4)$ used in the design procedure. The following observations can be made about figure 4.2.

(a) The experimental results verify the conditions (4.11) derived analytically in the previous section. Figure 4.2 shows that for γ to approach unity then (Π_1 , Π_2) must lie well within the hatched region of figure 4.1 as predicted in the previous section.

(b) There is a value of Π_1 which gives minimum γ for a given value of Π_2. This minimum value of γ is given by the contour which just touches the horizontal line for the given value of Π_2. The value of Π_1 which gives this minimum value of γ is given by the point at which the contour of constant γ touches the line of constant Π_2, that is the minimum on the curve of constant γ. Figure 4.2 shows that the minima of the curves of constant γ satisfy the relationship

$$\Pi_1 = - 1.5\ \gamma \qquad (4.12)$$

that is $$\frac{B}{Aa^2} = -1.5 \frac{\overline{x^2}}{Est[\overline{x^2}]}$$

which becomes, using equation (4.7)

$$B = -A\overline{x^2} \tag{4.13}$$

When equation (4.13) is satisfied, that is Π_1 is set according to equation (4.12), corresponding values of γ and Π_2 can be obtained from figure 4.2. These values of γ and Π_2 are plotted in figure 4.3 which shows how this relationship between γ and Π_2 can be represented by

$$\gamma = 1 + \frac{44}{\Pi_2^3} \tag{4.14}$$

Equation (4.14) shows how the minimum possible value of γ varies with Π_2 and is the equation which is used in the design procedure.

Equation (4.13) which gives the best choice of B for equivalent circuit validity can be explained by reference to equation (3.8) for the difference between u and u'. The only effect B has on (u - u') is due to its effect on components around the perturbation frequency α. These are caused by low frequency signals at the multiplier input. As B is a constant it can reduce the magnitude of these signals only by reducing their mean value $A\overline{x^2} + B$ to zero, which is done when equation (4.13) is satisfied. Because of the above reasoning and experimental results equation (4.13) is used in the rest of this work to choose the value for B. It may be noted that this value of B is obtained automatically if a bandpass or high-pass filter is used before the multiplier.

4.3 System with noise only

In section 4.2.1 the derivation of conditions (4.11) depended on the relationship between terms involving (z - u) and the perturbation amplitude a. There is nothing to suggest a difference when (z - u) is caused by measurement noise rather than by the disturbance. It is therefore reasonable to assume that conditions (4.11) will still apply and the quantitative dependence of γ on $\overline{\Pi}_1$ and $\overline{\Pi}_2$ will be approximately the same as when the system had disturbances only, provided that the relationship of the perturbation amplitude a to the terms in (z - u) is the same.

Consider a special case of figure 2.3 with noise only, that is with

$$z(t) = 0 \; ; \; T = 0 \; ; \; \phi_{\xi\xi}(\omega) = N_\xi^2 \tag{4.15}$$

Thus $\overline{\Pi}_p = \overline{\Pi}_3 = 0$ and the system is described by $\overline{\Pi}_1$, $\overline{\Pi}_2$ and $\overline{\Pi}_4$. $\overline{\Pi}_4$ can be chosen to give, as before for disturbances only, the best perturbation amplitude when the equivalent circuit is valid. Equations (4.15) can be substituted into equation (3.39) to give the equivalent circuit estimate of $\overline{x^2}$ as

$$\text{Est}[\overline{x^2}] = \frac{KN_\xi^2}{4aA} + \frac{a^2}{2} \tag{4.16}$$

When $\text{Est}[\overline{x^2}]$ is a good approximation to $\overline{x^2}$ the best value of the perturbation amplitude is given by setting

$$\frac{\delta \text{Est}[\overline{x^2}]}{\delta a} = -\frac{KN_\xi^2}{4a^2A} + a = 0$$

$$\text{so that} \quad a^3 = \frac{KN_\xi^2}{4A} \tag{4.17}$$

$$\text{and } \overline{\Pi}_4 = \frac{KN_\xi^2}{Aa^3} = 4 \tag{4.18}$$

Substituting from equation (4.17) into (4.16) gives

$$\text{Est}[\overline{x^2}] = \overline{(z-u')^2} + \frac{a^2}{2} = a^2 + \frac{a^2}{2} = 1.5a^2 \qquad (4.19)$$

Equation (4.19) is the same as equation (4.7) so that the error due to the perturbation is again one third of the total. Thus the order of magnitude of terms in $\frac{z-u}{a}$ in the analysis of section 4.2.1 will be the same as for disturbances only, so that conditions (4.11) can be expected to apply.

An experiment similar to that described in section 4.2.2 was carried out with noise only, that is the system of figure 2.3 was simulated on the analogue computer with

$$\Pi_p = \Pi_3 = 0 \ , \ \Pi_4 = 4 \qquad (4.20)$$

and experimental values of γ obtained for various (Π_1 , Π_2). Details of the experimental work are given in appendix 4. The contours of constant γ are shown in figure 4.4 and are, within the limits of experimental error, the same as those shown on figure 4.2. This shows that

$$\gamma(0 ; \Pi_1 , \Pi_2 , 0 , 4) \approx \gamma(0 ; \Pi_1 , \Pi_2 , 2 , 0) \qquad (4.21)$$

The common factor in these two systems is that the perturbation amplitude was chosen to be the best, assuming that the equivalent circuit is approximately valid.

4.4 System with disturbances and noise

Consider a special case of the system shown in figure 2.3 with disturbances and noise, but with no lag, that is T = 0 and hence $\Pi_p = 0$. Equation (3.39) for the equivalent circuit estimate of $\overline{x^2}$ gives

$$\text{Est}[\overline{x^2}] = \frac{N_Z^2 + \frac{1}{2}K^2 N_\xi^2}{2KaA} + \frac{a^2}{2} \qquad (4.22)$$

so that a can be chosen as before by setting

$$\frac{\delta \text{Est}[\overline{x^2}]}{\delta a} = -\frac{N_Z^2 + \frac{1}{2}K^2 N_\xi^2}{2Ka^2A} + a = 0$$

$$\text{so that} \quad a^3 = \frac{N_Z^2 + \frac{1}{2}K^2 N_\xi^2}{2KA} \qquad (4.23)$$

Substituting equation (4.23) in (4.22) gives

$$\text{Est}[\overline{x^2}] = \overline{(z-u')^2} + \frac{a^2}{2} = a^2 + \frac{a^2}{2} = 1.5a^2 \qquad (4.24)$$

Equation (4.24) is the same as equation (4.7) and (4.19) so that again the error due to the perturbation should be one third of the total. It has been shown experimentally that when equation (4.24) holds the variation of γ with Π_1 and Π_2 is the same for systems with noise only and disturbances only. It is therefore reasonable to assume that there will be no difference when there is a combination of disturbances and noise, that is it can be assumed that figure 4.2 gives the variation of γ with Π_1 and Π_2 for a system with disturbances and noise provided that the perturbation amplitude is chosen on the basis of a valid equivalent circuit. The validity of this assumption is verified in part by the success of the design procedure of the next chapter when there is no lag.

4.5 System with disturbances, noise and lag

The presence of the measurement lag can affect the validity of the equivalent circuit in three ways: the representation of the measurement lag by an attenuation factor in the equivalent

circuit must be valid; the measurement lag may cause a change in the 'unwanted' fluctuations (u - u') at the controller integrator output; and the measurement lag may cause the system to be unstable. These three effects are discussed further in the following sub-sections. Some observations are made which suggest that the effect of the lag on the equivalent circuit validity, that is the effect of Π_p on $\gamma(\Pi_p ; \Pi_1 - - \Pi_4)$, can be neglected, at least over some range of values of Π_p.

4.5.1 The effect on (u - u')

Inequalities (4.10) suggest that the main purpose of conditions (4.11) is to ensure that perturbation frequency terms in the integrator output u(t) are kept small. These terms are caused by low frequency signals at the multiplier input. Since the measurement lag is a low-pass filter it will have, to a first approximation, negligible effect on the magnitude of these low frequency signals and hence negligible effect on the magnitude of (u - u').

4.5.2 Validity of representation of lag

From appendix 1 the representation of the measurement lag by the attenuation factor in the equivalent circuit will be valid if variations in the useful signal $c'' = 2Aa(z-u)$ are slow compared with the perturbation frequency α. Variations in c'' are characterised by the bandwidth $KaA(1+\alpha^2T^2)^{-\frac{1}{2}}$ of the equivalent circuit of figure 3.3 Thus the above condition can be written

$$\alpha >> \frac{KaA}{(1+\alpha^2T^2)^{\frac{1}{2}}} \qquad (4.25)$$

Section 4.5.1 shows that conditions (4.11) must be satisfied to make $(u - u')$ small even when the measurement lag is present. Satisfaction of (4.11) however, ensure satisfaction of (4.25) so that when the equivalent circuit is valid as far as $(u - u')$ is concerned, the representation of the lag by the attenuation factor will also be valid.

4.5.3 Stability of system with measurement lag

This can be discussed in terms of the system shown in figure 2.3 with

$$z(t) = \xi(t) = 0 \tag{4.26}$$

The differential equation of this system is

$$\begin{aligned} \dot{y} &= \frac{1}{T}[-y + B + A(a\cos\alpha t - u)^2] \\ \dot{u} &= Ky\cos(\alpha t - \tan^{-1}\alpha T) \end{aligned} \tag{4.27}$$

This is a second-order, non-stationary, non-linear differential equation in u, y and t. In terms of the dimensionless variables $\frac{u}{a}$ and $\frac{y}{Aa^2}$, and the dimensionless time $\tau = \alpha t$, equation (4.27) becomes

$$\begin{aligned} \frac{d}{d\tau}\left(\frac{y(\tau)}{Aa^2}\right) &= \frac{1}{\alpha T}\left[-\left(\frac{y(\tau)}{Aa^2}\right) + \Pi_1 + \left(\cos\tau - \frac{u(\tau)}{a}\right)^2\right] \\ \frac{d}{d\tau}\left(\frac{u(\tau)}{a}\right) &= \frac{1}{\Pi_2}\,\frac{y(\tau)}{Aa^2}\cos(\tau - \tan^{-1}\alpha T) \end{aligned} \tag{4.28}$$

The system is described by the parameters Π_1, Π_2 and αT. Equation (4.28) defines the trajectory from any point in the $\left(\frac{u}{a}, \frac{y}{Aa^2}, \tau\right)$ state-space.

A system described by equation (4.28) was simulated on the

analogue computer with

$$\Pi_1 = 0 \; ; \; \Pi_2 = 5.171 \; ; \; \alpha T = 1.984 \qquad (4.29)$$

and the behaviour of the system from different initial points in the state-space determined. The evolution of $\frac{u}{a}$ and $\frac{y}{Aa^2}$ from the points (16, 0, 0) and (19, 0, 0) is shown in figures 4.5a and 4.5b. It is seen that from the first point the system returns to the expected stable oscillation about the origin of the $\left(\frac{u}{a} , \frac{y}{Aa^2}\right)$ plane, whilst from the second it goes into an oscillation of increasing amplitude. Thus there is a stability boundary in the three-dimensional state-space. Some idea of the shape of this boundary was obtained by taking sections at various values of τ. τ only appears as the argument of a cosine function so only values of τ between 0 and 2π need be considered. The sections were taken at $\tau = 0$, $\frac{\pi}{4}$, $\frac{\pi}{2}$ and $\frac{3\pi}{4}$ (for values of τ given by $\pi + \tau'$ the stability boundary is that for $\tau = \tau'$ rotated about the $\left(\frac{y}{Aa^2}\right)$ axis). For each value of τ points in the $\left(\frac{u}{a} , \frac{y}{Aa^2}\right)$ plane were found experimentally such that the system converged from points nearer the origin but diverged from points farther away. The experimental results are shown in figures 4.6 a-d. These define a region in the state-space within which the system is stable, i.e. will return to stable oscillations about the origin of $\left(\frac{u}{a} , \frac{y}{Aa^2}\right)$ plane. The stability boundary will depend on the dimensionless parameters Π_1 , Π_2 and αT.

Roberts[17] has noted a similar type of instability in his approximately optimal controller. Jelonek, Pomella and Karunaratne[38] have discussed the possibility of instability when the plant has no lags. Although beyond the scope of this work, further

investigation of the stability of such systems would be of interest.

When the system is subjected to the gaussian signals $z(t)$ and $\xi(t)$ there will be a finite probability of the system entering any region in the state space, so if there is a stability boundary then there will be a finite probability of the system becoming unstable. If the stability boundary is sufficiently far away from the region of normal operation, however, this probability may be so small as to be negligible. It is reasonable to expect that the tendency to instability will increase as the effect of the lag becomes more prominent, that is as T_p increases, but will be negligible over some range of values of T_p. This range of values of T_p is determined by the experimental results of the next chapter.

In any practical system the range of the variables will be limited so that not all regions of the phase space will be accessible. This will affect the probability of instability. The analogue computer simulation carried out in the next chapter is an example of such a system. There the accessible region of state-space is limited by the finite dynamic range of the analogue computer.

4.6 Conclusions

In sections 4.2, 4.3 and 4.4 it was shown that for certain well conditioned systems (where the perturbation amplitude is chosen assuming a valid equivalent circuit) the variation of γ is given by figure 4.2. In section 4.5 it was argued that the

effect of Π_p on γ could be neglected, at least over some range of values of Π_p. When Π_p lies in this range and when the equivalent circuit is approximately valid it can be assumed that the variation of γ will still be given by figure 4.2, that is $\gamma(\Pi_p ; \Pi_1 - - \Pi_4)$ can be approximated by $\gamma(\Pi_1 , \Pi_2)$ as given by figure 4.2. This result is used in the design procedure of the next chapter.

CHAPTER 5

The Design and Performance of the Complete System

5.1 Introduction

In this chapter the results of chapters 3 and 4 are combined to yield a complete design procedure for the system shown in figure 2.3. Results for the performance of this system are obtained and expressed in dimensionless form. An investigation is carried out to check that this performance is not critically dependent on accurate knowledge of the plant parameters. The design procedure and performance results are verified experimentally by simulating the system on the analogue computer.

5.2 The design procedure

As explained in chapter 2 the design procedure consists of obtaining an expression for the dimensionless performance criterion Π_e in terms of the plant dimensionless parameter Π_p and the controller parameters $\Pi_1 - - \Pi_4$, then choosing $\Pi_1 - - \Pi_4$ so that Π_e will be a minimum for any given value of Π_p.

The equivalent circuit gives equation (3.40) for the estimate of Π_e and equation (4.1) gives the actual value of Π_e as

$$\Pi_e = \gamma(\Pi_p ; \Pi_1 - - \Pi_4)\, \mathrm{Est}[\Pi_e] \qquad (5.1)$$

The results of chapter 4 suggest that for a range of values of Π_p equation (5.1) can be approximated by

$$\Pi_e \approx \gamma(\Pi_1 , \Pi_2)\, \mathrm{Est}[\Pi_e] \qquad (5.2)$$

where $\gamma(\Pi_1 , \Pi_2)$ is given by figure 4.2. Combining equations (5.2) and (3.40) gives

$$\Pi_e \approx \gamma(\Pi_1,\Pi_2) + \tfrac{1}{2}\left(\frac{1}{\Pi_3\Pi_4}\right)^{\frac{1}{3}}\left[1 + (\Pi_3 + \tfrac{1}{2}\Pi_4)\left\{1 + \Pi_2^2\,\Pi_p^2\left(\frac{\Pi_4}{\Pi_3^2}\right)^{\frac{2}{3}}\right\}^{\frac{1}{2}}\right] \qquad (5.3)$$

In equation (5.3) Π_1 occurs only in the expression for γ so that the value of Π_1 which minimises Π_e in equation (5.3) is that value of Π_1 which minimises $\gamma(\Pi_1, \Pi_2)$. Observation (b) of section 4.1.2 shows that this value of Π_1 is that which allows satisfaction of equation (4.13). When Π_1 takes this value $\gamma(\Pi_1, \Pi_2)$ is given by equation (4.14) so that equation (5.3) becomes

$$\Pi_e \approx \left[1 + \frac{44}{\Pi_2^3}\right] + \tfrac{1}{2}\left(\frac{1}{\Pi_3\Pi_4}\right)^{\frac{1}{3}}\left[1 + (\Pi_3 + \tfrac{1}{2}\Pi_4)\left\{1 + \Pi_2^2\,\Pi_p^2\left(\frac{\Pi_4}{\Pi_3^2}\right)^{\frac{2}{3}}\right\}^{\frac{1}{2}}\right] \qquad (5.4)$$

For any given value of Π_p the choice of Π_2, Π_3 and Π_4 which minimise Π_e is an exercise in function minimisation. No analytic result could be obtained and as no suitable digital computer function minimisation routine was readily available such a routine was developed. Extremum control techniques were used in this routine for the following reasons:

(i) The routine provides an example of an extremum searching system, as discussed in chapter 1.

(ii) The extremum control techniques were thought to be as efficient as any.

The routine is discussed in further detail in appendix 5.

The minimisation was done for values of Π_p in the range 0.01 - 10.0 and the resulting values of Π_e, Π_2, Π_3, Π_4, αT and γ are shown in table 5.1 and are plotted in figures 5.1 a - f.

The values of Π_2, Π_3 and Π_4 obtained from the computer and the value of Π_1 resulting from equation (4.13) constitute the required design. The performance of this type of empirical controller is given by the variation of Π_e with Π_p shown in figure 5.1a. This graph can be used to compare the performance of the controller considered here with the performance of any other controller used with the same plant.

The results shown in figures 5.1 suggest that asymtotic solutions for small and large values of Π_p can be obtained to extend the design procedure over the complete range of Π_p.

(a) $\Pi_p \longrightarrow 0$

This is the asymtotic case where the effect of the lag becomes negligible. Equation (5.4) becomes

$$\Pi_e = \tfrac{1}{2}\left[1 + \frac{44}{\Pi_2^3}\right]\left(\frac{1}{\Pi_3\Pi_4}\right)^{\frac{1}{3}}\left[1 + \Pi_3 + \tfrac{1}{2}\Pi_4\right] \qquad (5.5)$$

From equation (5.5) the best value of Π_2 is infinity so that equation (5.5) becomes

$$\Pi_e = \tfrac{1}{2}\left(\frac{1}{\Pi_3\Pi_4}\right)^{\frac{1}{3}}\left[1 + \Pi_3 + \tfrac{1}{2}\Pi_4\right] \qquad (5.6)$$

The best values of Π_3 and Π_4 are obtained by setting $\frac{\delta\Pi_e}{\delta\Pi_3}$ and $\frac{\delta\Pi_e}{\delta\Pi_4}$, obtained from equation (5.6), equal to zero which gives

$$\Pi_3 = 1 \; ; \; \Pi_4 = 2 \qquad (5.7)$$

Substituting these values in equation (5.6) gives

$$\Pi_e = 1.5\left(\tfrac{1}{2}\right)^{\frac{1}{3}} = 1.191 \qquad (5.8)$$

(b) $\Pi_p \longrightarrow \infty$

This is the case when the effect of the lag becomes predominant. Figures 4.1c, d and f show that as Π_p becomes large

$$\Pi_3 >> 1 + \tfrac{1}{2}\Pi_4 \; ; \; \alpha T = \Pi_2 \Pi_p \left(\frac{\Pi_4}{\Pi_3^2}\right)^{\frac{1}{3}} >> 1 \qquad (5.9)$$

The use of inequalities (5.9) in equation (5.4) gives

$$\Pi_e = \tfrac{1}{2}\left[1 + \frac{44}{\Pi_2^3}\right]\left[\Pi_2 \;\; \Pi_p\right] \qquad (5.10)$$

The best value of Π_2 in equation (5.10) is obtained by putting

$$\frac{\delta \Pi_e}{\delta \Pi_2} = \tfrac{1}{2}\,\Pi_p\left[1 - \frac{88}{\Pi_2^3}\right] = 0 \quad \text{which gives}$$

$$\Pi_2 = 4.45, \text{ when } \gamma = 1.5 \text{ and } \Pi_e = 3.34\,\Pi_p \qquad (5.11)$$

The asymptotes defined by equations (5.8) and (5.11) are shown on figure 5.1a. For $\Pi_p << 0.1$ the error Π_e is approximately constant and the performance of the extremum control system is limited by measurement noise. For $\Pi_p >> 1$ the error Π_e is proportional to Π_p and the performance is determined by the lag.

5.3 Sensitivity of performance to inaccurate knowledge of the plant

The parameters of a practical plant, especially the statistical parameters, may only be known approximately, so it is important that any design procedure should not be critically dependent on accurate knowledge of the plant parameters. A

measure of this dependence is a comparison of the performance of the controller designed using the inaccurate information with the performance which could have been obtained had the plant parameters been known exactly.

The estimated plant parameters N_z, N_ζ, A and T combine to give the estimated plant dimensionless parameter Π_p, and hence the estimated performance Π_e from figure 5.1a. The actual plant parameters N_z', N_ζ', A' and T' combine to give the actual plant parameter Π_p', and hence from figure 4.1a the performance Π_e' which could have been obtained had the plant parameters been known exactly. The controller parameters K, a, α and B given by the design procedure for the estimated plant parameters combine with the actual plant parameters to give the true dimensionless parameters for the system. These can be used in equation (5.4), assuming its validity, to give the actual performance Π_e'' of the system. If the design procedure is valid Π_e'' will always be greater than Π_e' and this difference is the effect of inaccurate knowledge of the plant parameters.

A quantitative indication of the effect of this inaccurate knowledge was obtained by evaluating Π_e''/Π_e' when the estimate of each parameter in turn is assumed to be in error by a factor of 2, the other parameters being assumed known exactly. The results for $\Pi_p = 0.1$ are shown in table 5.2. This value of Π_p was chosen because it lies near the boundary of the region of usefulness of the design procedure, as determined in the next chapter.

From table 5.2 it is seen that inaccurate knowledge of the lag has least effect and that the greatest error is due to under-estimation of the curvature A of the extremum characteristic, when the actual error is 35% greater than that which would have been obtained had the curvature been known exactly. From the values of Π_e''/Π_e' given in table 5.2 it can be concluded that the performance is not unduly sensitive to inaccurate knowledge of the plant parameters.

5.4 Experimental verification of design procedure

In order to verify that the controller given by the design procedure gives the predicted performance and is correctly designed, at least over some range of values of Π_p, the system was simulated on the analogue computer. The performance with the controller parameters given by the design procedure was measured and compared with the predicted performance. The actual control parameters a, K, α and B were then set to values different from those given by the design procedure and the resulting value of Π_e observed. The experimental work was done to an accuracy of the order of 5% and is reported in further detail in appendix 4. The simulation was carried out for plants with Π_p = 0.01, 0.1 and 1.0.

Π_p = 0.01 and 0.1

Table 5.3a and figure 5.1a show how the experimental values of Π_e compare with the predicted values for the systems as designed. It is seen that for both values of Π_p the actual

performance is the same as that predicted, within the limit of experimental error. Tables 5.3b and 5.3c show the performance when each of the controller parameters a, α, K and B take values differing from the designed value. For both values of Π_p it is seen that in every case Π_e is greater than when the designed values are used. This indicates that the designed values of the controllers parameters are in fact the best.

The possibility of instability is discussed in section 4.5.3. In the above mentioned cases no instability was observed over several runs, each of approximately 2,000 perturbation cycles.

The limited dynamic range of the analogue computer was effectively a limitation on the error signal x(t) in figure 2.3 at a value 20 times its mean square value. Even allowing for the non-gaussian distribution of the perturbation component of x(t) this should ensure that the limitation is operative only for a very small fraction (under 0.1%) of the time. The effect of this limitation on the possibility of instability was discussed in section 4.5.3, and the effect on the measurement of $\overline{x^2}$ is evaluated in appendix 4 and shown to be negligible.

$\Pi_p = 1.0$

With this plant and the controller as designed, the system became unstable before the end of each measurement period. It was found that some stable runs could be obtained when the limitation on x(t) was artificially lowered to 15 times $\overline{x^2}$. The measured value of Π_e was then close to the predicted value, as shown on figure 5.1a and in table 5.3a. As shown in table

5.3b other values of the controller parameters could make the system unstable or give a better performance. The controller parameters were varied manually by trial and error and the lowest value of Π_e noted. The results are shown in table 5.3a and this lowest value of Π_e is plotted on figure 5.1a. It is seen that this value of Π_e is approximately 20% lower than that predicted by the design procedure.

The implications of these experimental results are discussed in the next chapter.

Chapter 6

Discussion of Results and Conclusions

6.1 Introduction

This chapter is the last concerning a plant with lags. The experimental results presented in the last chapter are discussed and the region of usefulness of the design procedure determined. The empirical controller considered here is compared with the approximately optimal controller developed by Roberts.[17] Finally this section of the work is concluded with a summary of the major results obtained.

6.2 Region of usefulness of the design procedure

The graph of Π_e against Π_p in figure 5.1a shows that when Π_p is small Π_e tends to the constant value $\Pi_e = \frac{3}{2}(\frac{1}{2})^{\frac{1}{3}} = 1.191$. The performance of the extremum controller in compensating for the disturbance $z(t)$ is then limited by the measurement noise. As the lag increases, however, Π_p increases and Π_e increases. The increase in Π_e is a measure of the effect of the lag on the performance of the system. When $\Pi_p = 0.1$ $\Pi_e = 1.55$ so that the measurement noise is still the main limitation on the performance of the system. When $\Pi_p = 1.0$, $\Pi_e = 4.68$ (from design procedure) or $\Pi_e = 3.14$ (best experimental result from section 5.4), so that the lag is the main limitation on the performance.

The experimental results presented in section 5.4 show that when $\Pi_p = 0.01$ and 0.1 the systems given by the design procedure give

the best performance and are likely to remain stable. The results for $\Pi_p = 1$, however, show that the design procedure breaks down for two reasons:

(a) The design procedure does not give the best controller, shown by the fact that a 20% better performance could be obtained with controller settings different from the designed values. The reason for this is that the assumptions of chapter 4 have become invalid, so it is no longer correct to approximate $\gamma(\Pi_p ; \Pi_1 - - \Pi_4)$ by $\gamma(\Pi_1 , \Pi_2)$.

(b) The system given by the design procedure has a high probability of becoming unstable.

From the above it may be concluded that the design procedure is useful for plants for which Π_p is in the range 0 to 0.1, that is where the performance is limited mainly by the measurement noise.

Extension of region of usefulness

The above conclusion does not mean that the method of extremum control shown in figure 2.3 cannot be used for plants described by $\Pi_p > 0.1$, or that the equivalent circuit design procedure is necessarily inappropriate. The extension of the design procedure would require further work, however, in order to

(i) obtain a more accurate expression for $\gamma(\Pi_p ; \Pi_1 - - \Pi_4)$. This would be done by studying the effect of Π_3, Π_4 and Π_p on γ.

(ii) study further the instability of the system. This could result in some condition $?(\Pi_p ; \Pi_1 - - \Pi_4)$, which if satisfied would ensure stability, or at least a low probability

of instability.

If these results could be obtained it would be possible to use the more accurate equation

$$\Pi_e = \gamma(\Pi_p ; \Pi_1 - - \Pi_4)\ \mathrm{Est}[\Pi_e] \qquad (6.1)$$

to choose $\Pi_1 - - \Pi_4$ subject to the stability condition $?(\Pi_p ; \Pi_1 - - \Pi_4)$, and so obtain the required design.

6.3 Comparison with Roberts'[17] system

The performance of the empirical controller designed here can be compared with the performance of the approximately optimal controller developed by Roberts. The performance of the empirical controller is given by the relationship

$$\Pi_e = f_{[\pi_1 - - \pi_4]_{opt}}(\pi_p) \qquad (6.2)$$

which is given by the graph of figure 5.1a for values of $\Pi_p < 0.1$.

The plant considered by Roberts has the additional vertical disturbance m(t) described in section 2.4.3. As mentioned in that section Roberts gives an approximation, say

$$\Pi_e = f_{\mathrm{Roberts}}(\Pi_p , \Pi_m , \Pi_c) \qquad (6.3)$$

to equation (2.21) which gives the performance of an optimal controller used with the plant considered by Roberts. The dimensionless parameters Π_m and Π_c in equation (6.3) were defined in section 2.4.3 and describe the magnitude of the vertical disturbance and its correlation with the horizontal disturbance z(t). For the special case when this correlation is zero, Roberts' equation (6.3) becomes

$$\Pi_e = \tfrac{3}{2}(\tfrac{1}{2})^{\frac{1}{3}}(1 + 2\Pi_m)^{\frac{1}{3}} \qquad (6.4)$$

and is valid provided that

$$(1 + 2\Pi_m)^{\frac{1}{6}} \frac{\Pi_p}{\Pi_m} << 1 \qquad (6.5)$$

Equation (6.4) suggests that in Roberts' system Π_e is independent of Π_p. This is not true in general but results from the restriction imposed by inequality (6.5) which is that $\Pi_p << \Pi_m$ except for large Π_m, so that effect of Π_p in equation (6.4) is masked by that of Π_m. This restricts the application of Roberts' results to plants with a relatively large vertical disturbance.

The plant considered in this thesis is the special case of that considered by Roberts when there is no vertical disturbance, that is when $\Pi_m = 0$. For finite values of Π_p inequality (6.5) invalidates Roberts' results for such plants. However if Π_p tends to zero as Π_m tends to zero then inequality (6.5) can be satisfied and equation (6.4) gives the performance as

$$\Pi_e = \tfrac{3}{2}(\tfrac{1}{2})^{\frac{1}{3}} \qquad (6.6)$$

which is, from figure 5.1a, the value of Π_e achieved by the empirical controller of figure 2.3 when $\Pi_p = \Pi_m = 0$.

In a discussion on extremum control[39] Roberts has suggested how his controller could be used when $\Pi_m = 0$ for values of $\Pi_p < 0.008$. Figure 5.1a shows that for $\Pi_p < 0.008$ the error in the empirical system is scarcely different from that when $\Pi_p = 0$ so Roberts' controller cannot give a significant improvement in performance.

When $\Pi_p > 0$ the system described by Roberts can become unstable. This instability is of the same nature as that in the empirical controller. Roberts has obtained experimental results which show that with $\Pi_m = 1$ the system is likely to remain stable if $\Pi_p \leq 0.2$. Thus it would appear that the range of values of Π_p over which the system is likely to remain stable is the same for Roberts' controller as for the empirical controller.

From the above it may be concluded that over their common field of application, that is for plants with $\Pi_p < 0.01$ and no vertical disturbance, the performance of the empirical controller is equal to that of the approximately optimal controller. For Π_p in the range 0.01 to approximately 0.1 the empirical controller designed here can be used if there is no vertical disturbance and the controller developed by Roberts can be used if the vertical disturbance is large. For values of $\Pi_p >> 0.1$ the control problem is unsolved.

6.4 Conclusions

The problem of the design and performance of the empirical sine wave perturbation system shown in figure 2.3 has been set up in dimensionless form. A design procedure and performance results have been obtained and shown to be the best when the dimensionless variable describing the plant is in the range $\Pi_p = 0 - 0.1$, that is when the performance of the system is limited mainly by measurement noise. A linear equivalent circuit for the system has been developed and can be used to estimate the transient response of the system.

The performance of this empirical controller has been shown to be as good as that of Roberts' approximately optimal controller over their common field of application, which is when π_p is in the range 0 - 0.01.

Chapter 7

The Performance of Three Types of Controller

7.1 Introduction

The next two chapters consider the performance of three types of controller in connection with a plant with no lags. The three systems are shown in figures 2.4, 2.5 and 2.6 and were introduced in section 2.3. In sections 2.3 and 2.4.4 it was shown that the performance of these three controllers could be compared if the performance criterion Π_e could be obtained as a function of the dimensionless perturbation frequency Π_α.

The value of Π_e used for the comparison must be the lowest possible, that is the value obtained when the system is properly designed. In this chapter design procedures are obtained for each of the three controllers. The first step in the design procedure is to obtain an analytic form for equation (2.27), which is

$$\Pi_e = f(\Pi_\alpha ; \Pi_1 , \Pi_2 , \Pi_3)$$

Π_1, Π_2 and Π_3 can then be chosen to minimise Π_e for a given value of Π_α so that the above equation becomes

$$\Pi_e = f_{[\pi_1, \pi_2, \pi_3]_{opt}}(\Pi_\alpha) \qquad (7.1)$$

Equation (7.1) shows how the best performance varies with the allowable perturbation frequency. An approximation to this variation is obtained analytically in this chapter, for each of the three controllers.

7.2 Sine wave perturbation

The system shown in figure 2.4 is a special case of the system shown in figure 2.3 with

$$T = 0 \quad \text{so} \quad \Pi_p = 0 \tag{7.2}$$

The design procedure of chapter 5 shows that best performance is achieved with

$$\Pi_2 = \infty \; ; \; \Pi_3 = 1 \; ; \; \Pi_4 = 2 \tag{7.3}$$

The definitions of Π_α, Π_2, Π_3 and Π_4 given by equations (2.18) and (2.26) show that

$$\Pi_\alpha = \frac{\alpha}{N_Z^2}\left(\frac{N_Z N_\xi}{A}\right)^{\frac{2}{3}} = \Pi_2\left(\frac{\Pi_4}{\Pi_3^2}\right)^{\frac{1}{3}} \tag{7.4}$$

Equations (7.3) and (7.4) show that the best value of the perturbation frequency is infinity.

When $\Pi_p = 0$ and Π_1 is correctly chosen the design procedure of chapter 5 gives equation (5.5) for the performance of the system. Substituting from equation (7.4) into equation (5.5) gives the performance in terms of Π_α, Π_2 and Π_3 as

$$\Pi_e = \tfrac{1}{2}\left(1 + \frac{44}{\Pi_2^3}\right)\left(\frac{\Pi_2}{\Pi_3 \Pi_\alpha}\right)\left(\Pi_3 + \tfrac{1}{2}\Pi_3^2\left(\frac{\Pi_\alpha}{\Pi_2}\right)^3 + 1\right) \tag{7.5}$$

The digital computer routine (appendix 5) was used to determine the values of Π_2 and Π_3 which minimise Π_e according to equation (7.5) for certain specified values of Π_α. The results are shown in table 7.1 and the graph of Π_e against Π_α is shown in figure 7.1. This variation of performance with perturbation frequency is used in the comparison of the three systems.

The computer results can be extended by considering the two asymtotic cases for $\Pi_\alpha >> 10$ and $\Pi_\alpha << 1$, that is for high and low perturbation frequencies.

(a) $\Pi_\alpha >> 10$

Figure 7.1 suggests that increasing the perturbation frequency Π_α much above 10 has little effect on Π_e. As $\Pi_\alpha \longrightarrow \infty$ then $\Pi_2 \longrightarrow \infty$ and $\gamma \longrightarrow 1$ so that equation (7.5) becomes

$$\Pi_e = \tfrac{1}{2}\left[\frac{\Pi_2}{\Pi_\alpha} + \tfrac{1}{2}\,\Pi_3 \left(\frac{\Pi_\alpha}{\Pi_2}\right)^2 + \frac{\Pi_2}{\Pi_3 \Pi_\alpha} \right] \qquad (7.6)$$

Minimum Π_e is obtained when $\frac{\delta \Pi_e}{\delta \Pi_2} = \frac{\delta \Pi_e}{\delta \Pi_3} = 0$ which gives

$$\Pi_e = \tfrac{3}{2}(\tfrac{1}{2})^{\frac{1}{3}} = 1.191 \; ; \text{ with } \Pi_3 = 1 \text{ and } \Pi_2 = (\tfrac{1}{2})^{\frac{1}{3}} \Pi_\alpha \qquad (7.7)$$

An observation can be made about the relative magnitudes of the contributions of the disturbance, noise and perturbation to the total error Π_e. These three contributions are proportional to the three terms Π_3, $\frac{1}{2}\,\Pi_3^2 \left(\frac{\Pi_\alpha}{\Pi_2}\right)^3$ and 1 in equation (7.5). The value of $\frac{1}{2}\,\Pi_3^2 \left(\frac{\Pi_\alpha}{\Pi_2}\right)^3$ was computed for each value of Π_α and it was found that

$$\tfrac{1}{2}\,\Pi_3^2 \left(\frac{\Pi_\alpha}{\Pi_2}\right)^3 \equiv 1 \qquad (7.8)$$

Since $\Pi_3 = 1$ for this asymtotic case all three contributions are equal, in particular the 'intentional' error due to the perturbation is one half of the 'unintentional' error. This observation is made because the above relationship between the intentional and unintentional errors is suggested by Roberts[17] to be optimal.

(b) $\Pi_\alpha << 1$

Table 7.1 shows that as Π_α becomes small Π_3 becomes large so that using relationship (7.8)

$$\Pi_3 >> 1 + \tfrac{1}{2}\Pi_3^2\left(\frac{\Pi_\alpha}{\Pi_2}\right)^3 \qquad (7.9)$$

Using inequality (7.9) in equation (7.5) gives

$$\Pi_e = \frac{1}{2\Pi_\alpha}\left[\Pi_2 + \frac{44}{\Pi_2^2}\right] \qquad (7.10)$$

Π_e is a minimum when

$$\frac{\delta\Pi_e}{\delta\Pi_2} = \frac{1}{2\Pi_\alpha}\left[1 - \frac{88}{\Pi_2^3}\right] = 0 \quad \text{which is when}$$

$$\Pi_2 = 4.45 \; ; \; \gamma = 1 + \frac{44}{\Pi_2^3} = 1.5 \; ; \; \Pi_e = \frac{3.34}{\Pi_\alpha} \qquad (7.11)$$

The asymtotes corresponding to equations (7.7) and (7.11) are shown on figure 7.1.

7.3 Square wave perturbation

7.3.1 Introduction

In this section the graph of Π_e versus Π_α is obtained for the square wave perturbation system shown in figure 2.5. The design procedure used for this system is exactly the same as that developed in chapters 3, 4 and 5 for the sine wave system: an equivalent circuit is derived, experimental results for its validity are obtained, then these are combined to give an equation for the performance, which provides a basis for the choice of the controller parameters. As the reasoning is

exactly the same as in the sine wave case the heuristic arguments, justifications and explanations are not given and only the analytic and numerical work is presented.

7.3.2 The equivalent circuit

The equivalent circuit is obtained by considering only the 'useful' signals.

From figure 2.5 the signal at the extremum output is

$$c = A\,[z-u + ap(t)]^2 + B$$
$$= 2Aa\,(z-u)\,p(t) + A(z-u)^2 + Aa^2 + B \qquad (7.12)$$

and the useful signal is

$$c' = 2Aa(z-u)p(t) \qquad (7.13)$$

This gives the useful signal $v'(t)$ at the multiplier output

$$v' = 2aA(z-u)p(t)^2 + \xi(t)\,p(t)$$
$$= 2aA(z-u) + \xi'(t) \qquad (7.14)$$

where $\xi'(t) = +\xi(t)$ for the first half of each perturbation cycle

$= -\xi(t)$ for the second half of each perturbation cycle

Since $\xi(t)$ is a white noise $\xi'(t)$ will also be a white noise with the same spectral density N_ξ^2.

Equation (7.14) combines with the integrator differential equation

$$v' = \frac{1}{K}\frac{du'}{dt}$$

to give, assuming u' is a good approximation to u

$$\frac{1}{K}\frac{du'}{dt} = 2aA(z-u') + \xi'(t) \qquad (7.15)$$

Equation (7.15) is the differential equation of the system shown in figure 7.2.

The equivalent circuit of figure 7.2 gives

$$\overline{(z-u')^2} = \frac{N_z^2}{4KaA} + \frac{KN_\xi^2}{4aA} \qquad (7.16)$$

which gives an estimate of the error as

$$\text{Est}[\overline{x^2}] = \overline{(z-u')^2} + \text{mean square perturbation}$$

$$= \frac{N_z^2}{4KaA} + \frac{KN_\xi^2}{4aA} + a^2 \qquad (7.17)$$

In terms of the dimensionless variables Π_2, Π_3 and Π_α equation (7.17) is

$$\text{Est}[\,\Pi_e\,] = \frac{1}{4}\left[\frac{\Pi_2}{\Pi_3\Pi_\alpha}\right]\left[\,\Pi_3 + \Pi_3^2\left(\frac{\Pi_\alpha}{\Pi_2}\right)^3 + 4\,\right] \qquad (7.18)$$

7.3.3 Validity of the equivalent circuit

The actual error can again be given as

$$\text{actual } \Pi_e = \gamma(\,\Pi_\alpha\,;\,\Pi_1\,,\,\Pi_2\,,\,\Pi_3\,)\,\text{Est}[\,\Pi_e\,] \qquad (7.19)$$

where γ gives a quantitative estimate of the validity of the equivalent circuit. As in the sine wave case the function $\gamma(\,\Pi_1\,,\,\Pi_2\,)$ obtained by considering a system with disturbances only, is used as an approximation to $\gamma(\,\Pi_\alpha\,;\,\Pi_1\,,\,\Pi_2\,,\,\Pi_3\,)$.

An experimental investigation of a system with disturbances only was carried out. As in section 4.2.2 for the sine wave system the perturbation amplitude was chosen to give the minimum value of $\text{Est}[\overline{x^2}]$. Equation (7.17) gives the estimate of $\overline{x^2}$ for disturbances only as

$$\text{Est}[\overline{x^2}] = \frac{N_z^2}{4KaA} + a^2 \qquad (7.20)$$

The best value of a is given by

$$\frac{\delta(\mathrm{Est}[\overline{x^2}])}{\delta a} = -\frac{N_z^2}{4a^2AK} + 2a = 0$$

$$\text{which gives } a^3 = \frac{N_z^2}{8KA} \text{ or } \Pi_3 = \frac{N_z^2}{Ka^3A} = 8 \tag{7.21}$$

$$\text{when } \mathrm{Est}[\overline{x^2}] = 3a^2 \tag{7.22}$$

This system, that is figure 2.5 with no noise and $\Pi_3 = 8$, was simulated on the analogue computer and γ measured for various values of Π_1 and Π_2. Contours of constant γ were plotted on the (Π_1 , Π_2) plane and are shown in figure 7.3. This figure is similar to the corresponding figure 4.2 for sine wave systems. In particular there is a value of Π_1 which gives minimum γ for any given Π_2. From figure 7.3 this value is given by the relationship

$$\Pi_1 = -3\gamma \tag{7.23}$$

$$\text{or } \frac{B}{Aa^2} = -3\frac{\overline{x^2}}{\mathrm{Est}[\overline{x^2}]}$$

which when combined with equation (7.22) gives

$$B = -A\overline{x^2} \tag{7.24}$$

which is the same as equation (4.13) obtained for the sine wave system. When Π_1 is chosen so that B satisfies equation (7.24) corresponding values of Π_2 and γ can be obtained from figure 7.3. These are shown plotted in figure 7.4 which also shows how these corresponding values can be approximated by the relationship

$$\gamma = 1 + \frac{230}{\Pi_2^3} \tag{7.25}$$

which is similar in form to equation (4.14) for the sine wave

system.

7.3.4 System design

As in the sine wave case $\gamma(\Pi_1, \Pi_2)$ given by figure 7.3 is used as an approximation to $\gamma(\Pi_\alpha ; \Pi_1, \Pi_2, \Pi_3)$ so that equation (7.19) is approximated by

$$\Pi_e = \gamma(\Pi_1, \Pi_2) \frac{1}{4} \left[\frac{\Pi_2}{\Pi_3 \Pi_\alpha} \right] \left[\Pi_3 + \Pi_3^2 \left(\frac{\Pi_\alpha}{\Pi_2} \right)^3 + 4 \right] \quad (7.26)$$

Π_1 occurs only in $\gamma(\Pi_1, \Pi_2)$ so that Π_e is minimised when Π_1 is chosen so that B satisfies equation (7.24). $\gamma(\Pi_1, \Pi_2)$ is then given by equation (7.25) so that equation (7.26) becomes

$$\Pi_e = \frac{1}{4} \left(1 + \frac{230}{\Pi_2^3} \right) \left(\frac{\Pi_2}{\Pi_3 \Pi_\alpha} \right) \left(\Pi_3 + \Pi_3^2 \left(\frac{\Pi_\alpha}{\Pi_2} \right)^3 + 4 \right) \quad (7.27)$$

Equation (7.27) is the equivalent of equation (7.5) for the sine wave case and has the same form, the numerical differences being due to the different perturbation wave-form and the different experimental results.

The digital computer function minimisation routine was used to determine the values of Π_2 and Π_3 in equation (7.27) which minimise Π_e for a range of values of Π_α. The results are shown in table 7.2 and the required variation of Π_e with Π_α is plotted in figure 7.5.

The graph of figure 7.5 can be extended by considering the asymtotic cases of high and low perturbation frequencies.

(a) $\Pi_\alpha >> 10$

The computer results show that as $\Pi_\alpha \longrightarrow \infty$, $\Pi_2 \longrightarrow \infty$

so that equation (7.27) becomes

$$\Pi_e = \frac{1}{4}\left[\frac{\Pi_2}{\Pi_\alpha} + \Pi_3\left(\frac{\Pi_\alpha}{\Pi_2}\right)^2 + \frac{4\Pi_2}{\Pi_3\Pi_\alpha}\right] \qquad (7.28)$$

Minimum Π_e is obtained by setting $\frac{\delta\Pi_e}{\delta\Pi_2} = \frac{\delta\Pi_e}{\delta\Pi_3} = 0$ which gives

$$\Pi_e = \frac{3}{2}(\tfrac{1}{2})^{\frac{1}{3}} \text{ ; when } \Pi_3 = 4 \text{ and } \Pi_2 = 2(\tfrac{1}{2})^{\frac{1}{3}}\Pi_\alpha \qquad (7.29)$$

The relative contributions of the disturbance, noise and perturbation to Π_e are given by the terms Π_3, $\Pi_3^2\left(\frac{\Pi_\alpha}{\Pi_2}\right)^3$ and 4 in equation (7.27). $\Pi_3^2\left(\frac{\Pi_\alpha}{\Pi_2}\right)^3$ was calculated for each value of Π_α and it was found that

$$\Pi_3^2\left(\frac{\Pi_\alpha}{\Pi_2}\right)^3 \equiv 4 \qquad (7.30)$$

Equations (7.30) and (7.29) show that the three contributions to Π_e are equal so that as in the sine wave case the 'intentional' error is one half of the 'unintentional' error.

(b) $\Pi_\alpha << 1$

Table 7.2 shows that as Π_α becomes small Π_3 becomes large so that using relationship (7.30)

$$\Pi_3 >> 4 + \Pi_3^2\left(\frac{\Pi_\alpha}{\Pi_2}\right)^3 \qquad (7.31)$$

so that equation (7.27) becomes

$$\Pi_e = \frac{1}{4}\frac{\Pi_2}{\Pi_\alpha}\left[1 + \frac{230}{\Pi_2^3}\right] \qquad (7.32)$$

Minimum Π_e is obtained when

$$\frac{\delta\Pi_e}{\delta\Pi_2} = \frac{1}{4\Pi_\alpha}\left[1 - \frac{460}{\Pi_2^3}\right] = 0$$

that is when

$$\Pi_2 = 7.72 \; ; \; \gamma = 1.5 \; ; \; \Pi_e = \frac{2.9}{\Pi_\alpha} \qquad (7.33)$$

The asymtotes corresponding to equations (7.29) and (7.33) are shown on figure 7.5.

7.4 Square wave perturbation with sample and hold

7.4.1 Introduction

The discrete-time controller in the system of figure 2.6 is that considered by Douce and Bond[13] and Feldbaum[12]. Douce and Bond have studied the performance of a system when the plant has measurement noise, and Feldbaum has shown that, with a ramp disturbance in the presence of measurement noise, zero error can be achieved with infinite perturbation frequency and infinitesimal perturbation amplitude. This controller is a special case of the 'derivative sensing' controller studied by Chang[8] when the plant is subject to a random disturbance and measurement noise. Chang's results are used here to provide a design and performance results for the system shown in figure 2.6.

The sample and hold unit was used by Douce and Bond in order to reduce 'large fluctuations' in the 'parameter setting' u(t). This reduction is achieved partly by the elimination of the effect of the mean value of the plant output. Figure 2.6 shows that this mean value is applied to the controller integrator in a positive sense for the first perturbation cycle then in a negative sense for the remaining half cycle, so that the net effect when

the sampler operates is zero. The sample and hold unit thus eliminates the need to adjust B.

Since B, and hence Π_1, has no effect on the performance of the system the design problem is the choice of Π_2 and Π_3 to minimise Π_e for a given Π_α. The resulting variation of Π_e with Π_α is the required performance result.

7.4.2 The system design

In figure 2.6 the sampler operates at times $i\tau$ [$i = 0, 1, 2$ ---] where

$$\tau = \frac{2\pi}{\alpha} \tag{7.34}$$

and α rads/sec is the angular perturbation frequency. The perturbation waveform ap(t) is such that

$$\begin{aligned} p(t) &= +1 \quad [i\tau \leqq t < (i + \tfrac{1}{2})\,\tau] \\ &= -1 \quad [(i + \tfrac{1}{2})\,\tau \leqq t < (i + 1)\,\tau] \end{aligned} \tag{7.35}$$

Thus, writing u_i for $u(i\tau)$ etc., the equation of motion of u(t) in figure 2.7 can be written

$$u_{i+1} = u_i + K\int_{i\tau}^{(i+\frac{1}{2})\tau} [A(z-u_i+a)^2 + B + \xi]\,dt - K\int_{(i+\frac{1}{2})\tau}^{(i+1)\tau} [A(z-u_i-a)^2 + B + \xi]\,dt \tag{7.36}$$

The assumption made by Chang is that z(t) is varying slowly compared with the perturbation so that z(t) can be considered a constant z_i over the period of one perturbation cycle. This assumption is discussed further in the next section. When this assumption is made equation (7.36) can be written

$$u_{i+1} = u_i + 2K\tau Aa(z_i - u_i) + K\int_{i\tau}^{(i+1)\tau} \xi'(t)dt \qquad (7.37)$$

where $\xi'(t) = \xi(t)\ [i\tau \leq t < (i + \frac{1}{2})\tau]$

$= -\xi(t)\ [(i + \frac{1}{2})\tau \leq t < (i + 1)\tau]$

Since $\xi(t)$ is a white noise $\xi'(t)$ will be a white noise with the same spectral density N_ξ^2.

$$\therefore \qquad u_{i+1} = u_i + 2K\tau Aa(z_i - u_i) + V \qquad (7.38)$$

where V is an independent random variable of variance[40] $K^2 N_\xi^2 \tau$.

In section 11.12 of his book[8] Chang gives equations (11.82) and (11.83) as the equations of motion of his derivative sensing system. Combining these equations and expressiong the results in terms of the nomenclature used in figure 2.6 gives

$$u_{i+1} = u_i + \sum_{j=0}^{i} w_{i-j}[4aA(z_i - u_i) + v] \qquad (7.39)$$

where v is an independent random variable. For the case where z_i has the same sampled spectral density as z(t), given by

$$\Phi_{zz}(z) = \frac{N_z^2 \tau}{(1-z^{-1})(1-z)} \qquad (7.40)$$

Chang shows that the minimum value of $\overline{[z_i - u_i]^2}$ is obtained when

$w_{i-j} = 0$ for $j < i$; w_{i-j} = constant = W for $j = i$

so that equation (7.39) becomes

$$u_{i+1} = u_i + 4WAa[z_i - u_i] + Wv \qquad (7.41)$$

Equation (7.41) is the same as equation (7.38) if

$$W = \frac{K\tau}{2} \tag{7.42}$$

and the variance of v is

$$\sigma_v^2 = \frac{K^2 N_\xi^2 \tau}{W^2} = \frac{4 N_\xi^2}{\tau} \tag{7.43}$$

Using equations (7.42) and (7.43) and the nomenclature of figure 2.6, Chang's results give the following equations for the best design and performance of the system:

$$\frac{\overline{x^2}}{N_z^2 \tau} = \frac{1+2b}{1-b^2} \; ; \; K = \frac{1-b}{2aA\tau} \; ; \; a^2 = N_z^2 \tau \frac{b}{1-b^2} \tag{7.44a}$$

where the parameter b is given by the relationship

$$\frac{4b^2}{(1-b)^3(1+b)} = \frac{N_\xi^2}{A^2 N_z^4 \tau^3} \tag{7.44b}$$

In terms of the dimensionless parameters equations (7.44) become

$$\Pi_e = \frac{1+2b}{[2b(1-b^2)]^{\frac{2}{3}}} \text{ when } \Pi_2 = \frac{4\pi}{1-b} \text{ and } \Pi_3 = \frac{2(1+b)}{b} \tag{7.45a}$$

where b is given by

$$\frac{4b^2}{(1-b)^3(1+b)} = \left(\frac{\Pi_\alpha}{2\pi}\right)^3 \tag{7.45b}$$

For any given value of perturbation frequency Π_α equation (7.45b) can be solved (numerically) for b so that equations (7.45a) give the best design parameters Π_1 and Π_3, and the resulting performance Π_e.

The required graph of Π_e versus Π_α is shown in figure 7.6. This graph can be extended using the asymptotes derived from equations (7.45)

As $\Pi_\alpha \longrightarrow \infty$, $b \longrightarrow 1$ and $\Pi_e \longrightarrow \frac{3}{2}(\frac{1}{2})^{\frac{1}{3}} = 1.191$ (7.46)

$$\text{As } \Pi_\alpha \longrightarrow 0 \ , \ b \longrightarrow 0 \text{ and } \Pi_e \longrightarrow \frac{2\pi}{\Pi_\alpha} \qquad (7.47)$$

The asymtotes corresponding to equations (7.47) are shown on figure 7.6.

7.4.3 The assumption used

The assumption used in the previous section was that z(t) is constant over the perturbation cycle yet has the sampled spectral density given by equation (7.40). This is effectively approximating z(t) by its sampled and held version z*(t). A diagrammatic representation of this approximation is shown in figure 7.7.

This approximation affects the results obtained in two ways:

(a) the estimate of the performance $\overline{x^{*2}}$ in figure 7.7 will differ from the actual performance $\overline{x^2}$ for any given q(t).

(b) The variation of z(t) over one perturbation, as compared with the assumed constancy of z*(t), will give increased uncertainty in the measurement of y(t), so that the performance with the actual disturbance z(t) will be worse than that predicted.

The effect of these errors will decrease as the perturbation frequency increases, and the experimental results of the next chapter indicate the region over which the assumption is valid. Although beyond the scope of this work, compensation for the above errors, particularly (b), might be made to increase the region of validity of the results.

It is interesting to note that z*(t) has the same continuous spectral density as z(t), that is sampling and holding a brownian

motion does not affect its continuous spectral density. This result is shown as follows: the brownian motion z(t) can be considered the result of integrating a white noise n(t) of spectral density N_z^2, as shown in figure 7.7.

Hence $$z^*[i\tau] = \int_0^{i\tau} n(t)dt \text{ and } z^*[(i+1)\tau] = \int_0^{(i+1)\tau} n(t)dt$$

so $$z^*[(i+1)\tau] - z^*[i\tau] = \int_{i\tau}^{(i+1)\tau} n(t)dt = \lambda_i \qquad (7.48)$$

where λ_i is an independent random variable of variance $N_z^2\tau$. Thus

$$z^*[m\tau] = \sum_{i=0}^{n} \lambda_i \qquad (7.49)$$

Thus $z^*(t)$ consists of the sum of independent random quantities λ_i, when the spectral density of $z^*(t)$ is shown by Chang on pages 51 - 56 of his book to be

$$\phi_{z^*z^*}(\omega) = \frac{\text{Variance of } \lambda_i}{\omega^2 \tau} = \frac{N_z^2}{\omega^2} \qquad (7.50)$$

which is the same as the spectral density of z(t).

Chapter 8

A Comparison of Three Controllers

8.1 Introduction

In the previous chapter graphs of the performance Π_e for each of the three systems against the allowable perturbation frequency Π_α, were obtained analytically. As the derivation of these graphs involved certain approximations, some experiments were carried out in order to:

(a) verify that for some range of values of Π_α the design procedures give the best systems,

(b) to determine this range of usefulness of the design procedures.

In this chapter the experimental work is described and the results discussed, then the experimental results and the graphs of Π_e against Π_α obtained in the previous chapter, are together used to compare the three controllers.

8.2 The experimental investigation

The three systems shown in figures 2.4, 2.5 and 2.6 were simulated on the analogue computer. To facilitate comparison the three systems were simulated simultaneously and subjected to the same disturbance and noise.

For each system the value of Π_e was measured for various values of Π_α, the controller parameters Π_1, Π_2 and Π_3 being as given by the design procedures. The results are shown in table 8.1 and are plotted on the same graphs as the analytic

results obtained in the previous chapter, figures 7.1, 7.5 and 7.6. From these graphs it is seen that in each case for $\Pi_\alpha > 10$ there is good agreement between the predicted and experimental values of Π_e, the experimental accuracy being of the order of 5%. As Π_α is reduced below 10 the experimental values of Π_e become increasingly greater than the predicted values. This error in the analytic results can be explained as follows:

(a) For the continuous systems, tables 7.1 and 7.2 show that when Π_α becomes less than 10, then γ becomes significantly different from unity. Thus the error can be attributed to the invalidity of the assumption in chapter 4, that the perturbation amplitude would be chosen according to an approximately valid equivalent circuit.

(b) For the system with the sample and hold unit it was assumed that the disturbance $z(t)$ could be approximated by its sampled and held equivalent $z^*(t)$. This approximation becomes increasingly inaccurate as the sampling frequency, that is as Π_α, becomes lower. In order to check that this approximation was the only cause of the error the system was simulated with the disturbance actually being the sampled and held signal $z^*(t)$. The results are shown in table 8.2 and are plotted on the theoretical curve of figure 7.6. It is seen that the experimental values of Π_e are close to the theoretical ones for all values of Π_α. This indicates that apart from this approximation the theoretical and experimental work is accurate.

In order to check that the designed values of the controller

parameters are the best when $\Pi_\alpha = 10$ the three systems were simulated with the actual controller parameters a and K each altered in turn by a factor of two from the designed settings. The value of B in the continuous systems was also varied from its designed setting of $-A\overline{x^2}$ to $-5A\overline{x^2}$ and $+3A\overline{x^2}$. The resulting values of Π_e are shown in table 8.3. It is seen that in each case Π_e is greater than that obtained with the design values of the parameters, which indicates that the design values are the best for $\Pi_\alpha = 10$. As the experimental values of Π_e become closer to the predicted values as Π_α is increased above 10 it is reasonable to suppose that the design procedure becomes more accurate, so that it can be concluded that for values of $\Pi_\alpha \geq 10$ the design procedures give the best settings of the controller parameters.

8.3 The comparison

In order to facilitate the comparison the three theoretical graphs of Π_e versus Π_α are plotted together in figure 8.1 and the three sets of experimental results are plotted together in figure 8.2.

The comparison can be made in terms of performance and in terms of practical considerations.

Performance

(1) From figure 8.1 it is seen that the best value of perturbation frequency is infinity, when all three controllers give equally good performance, a value of $\Pi_e = 1.5(\frac{1}{2})^{\frac{1}{3}} = 1.191$. The experimental results of figure 8.2 substantiate this result.

(2) For any given finite value of perturbation frequency, figure 8.1 indicates that the continuous controllers give a better performance than the controller with the sample and hold unit. This result is again substantiated by the experimental results, at least for values of Π_α down to 10. Figure 8.1 also suggests that the square wave perturbation continuous controller is better than the sine wave controller at low values of perturbation frequency. As the low frequency asymtotes for these two controllers depend largely on the experimental results for γ, this small difference in performance could be the result of experimental error. It may be noted, however, that for 4 out of the 5 values of Π_α in figure 8.2 the experimental results for the square wave controller are better than those for the sine wave controller.

(3) As mentioned in section 2.3 no practical plant will be without lags so the perturbation frequency will be limited. Figures 8.1 and 8.2, however, show that as Π_α is increased Π_e approaches its lowest value asymtotically; so that there is a wide range of perturbation frequencies, say $\Pi_\alpha > 10$, over which the performance is nearly as good as the best obtainable. In some plants it may be possible to choose a perturbation frequency so that $\Pi_\alpha > 10$ but at which the effect of any lags is negligible. For these plants the controller design given here will give nearly the best performance as little could be gained by raising the perturbation frequency.

When this design approach is used a basis of comparison is the perturbation frequency required to bring Π_e to within some

fraction, say 10%, of its smallest value 1.191. From the theoretical results of figure 8.1 this value of Π_α is approximately 8 for the continuous systems and 30 for the system with sample and hold; from the experimental results of figure 8.2 these values are 13 and 30 respectively. Since the perturbation frequency required by this design procedure is higher for the system with sample and hold the range of plants in which the effect of the lags can be neglected is smaller.

Douce and Bond[13] have shown that in some circumstances the sample and hold unit can improve the performance. The results given here show that when disturbances and noise are present a properly designed continuous controller can perform as well or better than a controller with a sample and hold unit.

Practical considerations

The controller with the sample and hold unit has the advantage of eliminating the need to adjust B. The sample and hold unit, however, might increase the complexity of the practical controller and could be difficult to manufacture for high perturbation frequencies. This controller would, however, be the simplest to implement using a digital computer.

The relative merits of the square wave and sine wave perturbation continuous controllers may depend on the frequency of the perturbation. At sub-audio frequencies the square wave perturbation controller would be the simplest as the multiplier could be a simple switch. At audio or radio frequencies the sine wave perturbation may be easier to generate and apply and a continuous multiplier would have to be used for both controllers.

Conclusion

From the above it can be concluded that whilst all three controllers give equal performance for the ideal case of infinite perturbation frequency, in practical systems where the perturbation frequency is limited the continuous controllers give better performance than the controller with a sample and hold unit, at the expense of requiring the adjustment of the additional controller parameter B. The balance of practical advantage will be determined by the particular application.

Chapter 9

Conclusions

9.1 Summary

Certain single input, linearised extremum controllers of the empirical type described in the literature have been designed, and their performances have been compared with that of an approximately optimal controller.

The plant is subject to disturbances, lags and measurement noise. A dimensionless performance criterion and description of the plant have been used to present the results.

A design procedure for a sinusoidal perturbation controller in connection with the above plant has been obtained, using a linear equivalent circuit for the system together with an experimentally obtained estimate of the equivalent circuit validity. Experimental results have shown that the resulting design is the best, and that the system is likely to remain stable, when the performance of the system is limited mainly by the measurement noise. This empirical controller has been compared with Roberts[17] approximately optimal controller and has been shown to perform equally well if the effect of the lag is small.

The performances of three different types of extremum controller have been compared when the plant lags can be neglected. The three controllers use sine wave perturbation, square wave perturbation, and square wave perturbation with a sample and hold unit in the controller. It has been shown that all three

controllers give a performance equal to that of the approximately optimal controller when the perturbation frequency is infinite. When the perturbation frequency is limited, as in a practical system, the controllers without the sample and hold unit give better performance, at the expense of requiring the adjustment of an additional controller parameter.

9.2 Further work

Theoretical work on extremum control can proceed in two ways:

(a) The determination of optimal controllers for various plants and performance criteria.

(b) The design of empirical controllers for use with these plants, and a comparison of the empirical controllers with each other and with the optimal controller.

The contribution of this thesis to (b) above has been limited by the instability of the perturbation system with lags, and by the inaccuracy of the determination of γ. Further investigation of these factors would be of interest.

The plant without lags used in the comparison of the three systems is the simplest continuous-time stochastic plant for which the optimal control problem exists, and the addition of the measurement lag gives the simplest plant with a lag. It would be interesting to determine the performance of other empirical controllers, for instance the stepping controller considered by Jacobs and Wonham[24], the pseudo-random-binary-sequence controller considered by Douce and Ng[30] and the alternative-biasing controller considered by Chang[8], when used with these plants.

ACKNOWLEDGEMENTS

This research was carried out under the supervision of Dr. O.L.R. Jacobs, whose advice and assistance are gratefully acknowledged.

Thanks are accorded to Professor W.E.J. Farvis for the opportunity to do this work, and to the S.R.C. (formerly D.S.I.R.) for the provision of the analogue computing facilities.

Appendix 1

An Equivalent Circuit for the Demodulation of a Low Pass Filtered Signal

The relationship between the 'useful' signal $c''(t)\cos\alpha t$ and its effect on the multiplier output is shown diagrammatically in figure A1.1. This appendix shows that the 'useful' low frequency part, $v'(t)$, of the multiplier output is approximated by the relationship

$$v'(t) = \tfrac{1}{2}(1+\alpha^2T^2)^{-\frac{1}{2}}\, c''(t)$$

provided that variations in $c''(t)$ are slow compared with the perturbation frequency α. This relationship describes the attenuation factor shown in figure A1.2, which can therefore be regarded as an equivalent circuit for figure A1.1.

The analysis presented in this appendix was contributed by Dr. O.L.R. Jacobs.

Using the notation of figure A1.1, the filter differential equation is

$$y + T\frac{dy}{dt} = c''\cos\alpha t$$

But
$$y + T\frac{dy}{dt} = T\, e^{-\frac{t}{T}}\frac{d}{dt}\left(y\, e^{\frac{t}{T}}\right)$$

So
$$y = \frac{1}{T}\, e^{-\frac{t}{T}} \int_{t_1}^{t} c''\; e^{\frac{t}{T}} \cos\alpha t\, dt$$

where t_1 is some zero initial condition time. Using the relation

$$\int e^{\frac{t}{T}} \cos\alpha t\, dt = \frac{Te^{\frac{t}{T}}}{(1+\alpha^2T^2)^{\frac{1}{2}}} \cos(\alpha t-\theta)$$

where $\theta = \tan^{-1}\alpha T$, to integrate by parts for y; forming the product

$$v = y \cos(\alpha t - \theta)$$

and rearranging the resulting expression gives

$$v = \left\{ \frac{c''}{2(1+\alpha^2T^2)^{\frac{1}{2}}} - \frac{T\cos\theta}{2(1+\alpha^2T^2)} \frac{dc''}{dt} + \frac{1}{2T} \sum_{n=2}^{\infty} (-1)^n \left(\frac{T}{(1+\alpha^2T^2)^{\frac{1}{2}}} \right)^{n+1} \cos n\theta \frac{d^n c''}{dt^n} \right\}$$

$$+ \left\{ \frac{1}{2T} \sum_{n=0}^{\infty} (-1)^n \left(\frac{T}{(1+\alpha^2T^2)^{\frac{1}{2}}} \right)^{n+1} \cos(2\alpha t - (n+2)\theta) \frac{d^n c''}{dt^n} \right\}$$

$$- \left\{ e^{\frac{t_i - t}{T}} \cos(\alpha t - \theta) \frac{1}{T} \sum_{n=0}^{\infty} (-1)^n \left(\frac{T}{(1+\alpha^2T^2)^{\frac{1}{2}}} \right)^{n+1} \cos(\alpha t_i - (n+1)\theta) \frac{d^n c''}{dt^n}(t_i) \right\}$$

The last term in brackets { } depends on the initial conditions and will be negligible if $t - t_i >> T$. The second term consists of components at frequency 2α and can be neglected, according to the assumptions of section 3.2, because of the low pass filtering properties of the equivalent circuit. Thus an equivalent circuit relating v to c'' need only approximate the first term in brackets { }. The complexity of the equivalent circuit is determined by the number of terms in the first set of brackets { } which are considered. The simplest equivalent circuit is the gain $\frac{1}{2}(1+\alpha^2T^2)^{-\frac{1}{2}}$, obtained by considering only the first term. The simplest indication of the dynamic effects of the system is obtained by considering the first two terms. These can be approximated, as suggested by Eveleigh[32], by a low pass filter of gain K' and time constant T'. It is shown here that

the criterion for this equivalent circuit to be valid is such that it can be replaced by the simple gain

$$K' = \tfrac{1}{2}(1+\alpha^2T^2)^{-\frac{1}{2}}$$

which is the simplest possible equivalent circuit.

The differential equation of the equivalent circuit is

$$v' + T' \frac{dv'}{dt} = K'c'' ,$$

which gives, by a procedure similar to that used above for the original system,

$$v' = K'c'' - K'T' \frac{dc''}{dt} + K' \sum_{n=2}^{\infty} (-1)^n (T')^n \frac{d^n c''}{dt^n}$$

$$- \frac{K'}{T'} e^{\frac{(t_1 - t)}{T'}} \sum_{n=0}^{\infty} (-1)^n (T')^{n+1} \frac{d^n c''}{dt^n} (t_1).$$

The equivalent circuit parameters K' and T' are determined by equating the first two terms in the expressions for v and v'; they are

$$K' = \tfrac{1}{2}(1+\alpha^2T^2)^{-\frac{1}{2}} \text{ and } T' = \frac{T}{1+\alpha^2T^2}$$

Using these values an expression for the error in approximating v by v' is given by

$$v-v' = \left\{ \frac{1}{2T} \sum_{n=2}^{\infty} (-1)^n \left(\frac{T}{(1+\alpha^2T^2)^{\frac{1}{2}}} \right)^{n+1} (\cos n\theta - (\cos\theta)^n) \frac{d^n c''}{dt^n} \right\}$$

$$+ \left\{ \frac{1}{2T} \sum_{n=0}^{\infty} (-1)^n \left(\frac{T}{(1+\alpha^2T^2)^{\frac{1}{2}}} \right)^{n+1} \cos(2\alpha t - (n+2)\theta) \frac{d^n c''}{dt^n} \right\}$$

$$+ \left\{ \frac{K'}{T'} e^{\frac{t_1-t}{T'}} \sum_{n=0}^{\infty} (-1)^n (T')^{n+1} \frac{d^n c''}{dt^n}(t_1) - \right.$$

$$\left. - \frac{1}{T} e^{\frac{t_1-t}{T}} \cos(\alpha t - \theta) \sum_{n=0}^{\infty} (-1)^n \left(\frac{T}{(1+\alpha^2T^2)^{\frac{1}{2}}} \right)^{n+1} \cos(\alpha t_1 - (n+1)\theta) \frac{d^n c''}{dt^n}(t_1) \right\}$$

Considering the above three terms in brackets { } for v-v':-

The third term, due to initial conditions, can be neglected if $t-t_1 >> T$, which can always be satisfied. The second term consists of components at frequency 2α and can be neglected, as before, because of the low pass filtering properties of the equivalent circuit.

Thus if the equivalent circuit is to be valid the first term, due to second and higher derivatives of c" must be small compared to v'. Neglecting initial condition effects this condition can, after some algebra, be written

$$\sum_{n=2}^{\infty} \left(\frac{-1}{\alpha} \right)^n (\sin\theta)^n (\cos n\theta - 2(\cos\theta)^n) \frac{d^n c''}{dt^n} << c'' - T' \frac{dc''}{dt}$$

In order to see how the frequency range of variations in

c'' is limited by the above condition substitute

$$c'' = e^{j\Omega t}$$

Assuming that $\Omega << \alpha$, which is necessary if the sum is to converge and which, from the results given in chapter 3, must always be so in the extremum control system, the condition becomes, after some algebra

$$\Omega << \left(\alpha^2 + \frac{1}{T^2}\right)^{\frac{1}{2}}$$

But $\left(\alpha^2 + \frac{1}{T^2}\right)^{\frac{1}{2}} > \alpha$ and it has already been assumed that $\Omega << \alpha$ so that $\Omega << \alpha$ is a sufficient condition for the equivalent circuit to be valid.

$$\text{Now } \left(\alpha^2 + \frac{1}{T^2}\right)^{\frac{1}{2}} < \frac{1+\alpha^2T^2}{T} = \frac{1}{T'}$$

So when the equivalent circuit is valid, variations in c'' are slow compared with the equivalent low pass filter bandwidth $1/T'$. Then the effect of the low pass filter can be approximated by the gain K'.

Thus provided $\Omega << \alpha$ the equivalent circuit can be assumed to be the gain K' so that

$$v' = \tfrac{1}{2}(1+\alpha^2T^2)^{-\frac{1}{2}}\, c''.$$

Appendix 2

An Equivalent Circuit for the Demodulation of a Band-pass Filtered Signal

In this appendix it is shown that the relationship between the useful signal $c'(t) = c''(t)\cos\alpha t$ and its effect on the multiplier output $v(t)$, shown diagrammatically in figure A2.1, can be approximated by the low pass filter equivalent circuit shown in figure A2.2, of differential equation

$$v' + T_2 \frac{dv'}{dt} = \tfrac{1}{2} c'' .$$

Assume $c'(t)$ has a Fourier transform[41] given by

$$C'(j\omega) = \int_{-\infty}^{\infty} c'(t)\, e^{-j\omega t}\, dt$$

Now $$c'(t) = c''(t)\cos\alpha t = \tfrac{1}{2}\left(c''(t)\, e^{j\alpha t} + c''(t)\, e^{-j\alpha t}\right)$$

combining the above two equations gives

$$C'(j\omega) = \tfrac{1}{2}\left(C''(j\omega - j\alpha) + C''(j\omega + j\alpha)\right)$$

Now $$Y(j\omega) = C'(j\omega).G_2(j\omega) \text{ and } y(t) = \frac{1}{2\pi}\int_{-\infty}^{\infty} Y(j\omega)\, e^{j\omega t}\, dt$$

and $v(t) = y(t)\cos\alpha t$, so after some algebra

$$v(t) = \frac{1}{8\pi}\int_{-\infty}^{\infty} C''(j\omega)\Big(G_2(j\omega+j\alpha) + G_2(j\omega-j\alpha)\Big)\, e^{j\omega t}\, d\omega$$

$$+ \frac{1}{8\pi}\Big(\int_{-\infty}^{\infty} C''(j\omega)\, G_2(j\omega+j\alpha)\, e^{j\omega t}\, d\omega\Big)\, e^{j2\alpha t}$$

$$+ \frac{1}{8\pi}\Big(\int_{-\infty}^{\infty} C''(j\omega)\, G_2(j\omega-j\alpha)\, e^{j\omega t}\, d\omega\Big)\, e^{-j2\alpha t}$$

Now let the transfer function of the equivalent filter relating $v'(t)$ to $c''(t)$ be $\frac{1}{2}\, G_2'(j\omega)$

$$\therefore\quad v'(t) = \frac{1}{4\pi}\int_{-\infty}^{\infty} C''(j\omega) G_2'(j\omega)\, e^{j\omega t}\, d\omega$$

so that $v(t)$ can be written

$$v(t) = v'(t) + \left\{\frac{1}{8\pi}\int_{-\infty}^{\infty} C''(j\omega)\Big(G_2(j\omega+j\alpha) + G_2(j\omega-j\alpha) - 2\, G_2'(j\omega)\Big)e^{j\omega t}\, d\omega\right\}$$

$$+ \left\{\frac{1}{8\pi}\Big(\int_{-\infty}^{\infty} C''(j\omega)\, G_2(j\omega+j\alpha)\, e^{j\omega t}\, d\omega\Big)\, e^{j2\alpha t} +\right.$$

$$\left. + \frac{1}{8\pi}\Big(\int_{-\infty}^{\infty} C''(j\omega)\, G_2(j\omega-j\alpha)\, e^{j\omega t}\, d\omega\Big)\, e^{-j2\alpha t}\right\}$$

If $v'(t)$ is to be a good approximation to $v(t)$ then the two terms in brackets { } must be negligible. The second term consists of components at frequency 2α which can be neglected,

according to the assumptions in section 3.2, because of the low pass filtering properties of the equivalent circuit. The first term can be neglected if it is small compared with $v'(t)$. This will be the case if

$$[G_2(j\omega+j\alpha) + G_2(j\omega-j\alpha) - 2\,G_2'(j\omega)] \ll 2\,G_2'(j\omega)$$

$$\text{Now} \quad G_2(j\omega) = \frac{\frac{2}{T_2}\,j\omega}{(j\omega)^2 + \frac{2}{T_2}\,j\omega + \alpha^2} = \frac{1}{1 + j\,\frac{T_2}{2}\left(\omega - \frac{\alpha^2}{\omega}\right)}$$

$$\text{so} \qquad G_2(j\omega+j\alpha) = \frac{1}{1 + j\omega T_2\left(1 - \frac{\omega}{2\alpha} + \frac{1}{12}\,\frac{\omega^3}{\alpha^3} - \text{---}\right)}$$

$$\text{and} \qquad G_2(j\omega-j\alpha) = \frac{1}{1 + j\omega T_2\left(1 + \frac{\omega}{2\alpha} - \frac{1}{12}\,\frac{\omega^3}{\alpha^3} + \text{---}\right)}$$

so if $\omega \ll \alpha$, $G_2(j\omega+j\alpha) \approx G_2(j\omega-j\alpha) \approx \frac{1}{1 + j\omega T_2}$

If $\omega < \alpha$ so that $\frac{1}{12}\,\frac{\omega^3}{\alpha^3}$ can be neglected then

$$G_2(j\omega+j\alpha) + G_2(j\omega-j\alpha) = \frac{2(1 + j\omega T_2)}{1 + 2j\omega T_2 + (j\omega T_2)^2\left(1 - \frac{\omega^2}{4\alpha^2}\right)}$$

$$= \frac{2}{1 + j\omega T_2} \quad \text{if} \quad \frac{\omega^2}{4\alpha^2} \ll 1$$

So $G_2'(j\omega) = \frac{1}{1 + j\omega T_2}$ and if no significant variations in c'' occur at frequencies above a value ω such that $\frac{\omega^2}{4\alpha^2} \ll 1$ then $v'(t)$ will be a good approximation to $v(t)$.

Appendix 3

The Design of the Best Linear Filter

In the system shown in figure 3.13 the transfer function $F_1(s)$ and the spectral densities of $z(t)$ and $\xi'(t)$ are fixed. This appendix gives a procedure for choosing $F_2(s)$ so that the 'mean square error' $\overline{x'^2}(t)$ will be a minimum. In particular it is shown that when

$$\phi_{zz}(\omega) = \frac{N_z^2}{\omega^2} \; ; \; \phi_{\xi'\xi'}(\omega) = \tfrac{1}{2} N_\xi^2 \qquad (A3.1)$$

and when $F_1(s)$ is a pure gain then $F_2(s)$ should represent an integrator.

The notation and procedure used in this appendix are based on those used by Brown[42].

Figure 3.13 gives the Laplace transform of $x'(t)$ as

$$X'(s) = Z(s) - F_2(s)\xi'(s) - F_1(s)\,F_2(s)\,X'(s)$$

$$= \frac{1}{1 + F_1(s)F_2(s)}\,Z(s) - \frac{F_2(s)}{1 + F_1(s)F_2(s)}\,\xi'(s) \qquad (A3.2)$$

and as $z(t)$ and $\xi(t)$ are assumed to be uncorrelated

$$\phi_{x'x'}(\omega) = \left| \frac{1}{1+F_1(j\omega)F_2(j\omega)} \right|^2 \phi_{zz}(\omega) + \left| \frac{F_2(j\omega)}{1+F_1(j\omega)F_2(j\omega)} \right|^2 \phi_{\xi'\xi'}(\omega) \qquad (A3.3)$$

Let $F_1 \equiv F_1(j\omega)$ and $\overline{F}_1 \equiv F_1(-j\omega)$ etc. and put

$$F = \frac{F_2}{1+F_1F_2} \quad \text{so that} \quad F_2 = \frac{F}{1 - FF_1} \qquad (A3.4)$$

If F can be found then F_2 is obtained using equation (A3.4).

Substituting from equations (A3.4) in equation (A3.3) gives

$$\phi_{x'x'} = \left| F_1 F - 1 \right|^2 \phi_{zz} + \left| F \right|^2 \phi_{\xi'\xi'}$$

$$= [F_1 F - 1][\overline{F}_1 \overline{F} - 1]\, \phi_{zz} + F\overline{F}\, \phi_{\xi'\xi'}$$

$$= F\overline{F}[F_1 \overline{F}_1 \phi_{zz} + \phi_{\xi'\xi'}] - [F_1 F + \overline{F}_1 \overline{F}]\, \phi_{zz} + \phi_{zz} \qquad \text{(A3.5)}$$

Now put

$$\phi_{uu} = F_1 \overline{F}_1 \phi_{zz} + \phi_{\xi'\xi'} \qquad \text{(A3.6)}$$

Substituting equation (A3.6) in (A3.5) gives

$$\phi_{x'x'} = \phi_{uu}\left(F\overline{F} - (FF_1 + \overline{F}_1 \overline{F})\, \frac{\phi_{zz}}{\phi_{uu}}\right) + \phi_{zz}$$

$$= \phi_{uu}\left(F - \overline{F}_1\, \frac{\phi_{zz}}{\phi_{uu}}\right)\left(\overline{F} - F_1\, \frac{\phi_{zz}}{\phi_{uu}}\right) - F_1 \overline{F}_1\, \frac{\phi_{zz}^2}{\phi_{uu}} + \phi_{zz}$$

$$= \phi_{uu} \left| F - \overline{F}_1\, \frac{\phi_{zz}}{\phi_{uu}} \right|^2 + \frac{\phi_{zz}\phi_{uu} - F_1 \overline{F}_1\, \phi_{zz}^2}{\phi_{uu}} \qquad \text{(A3.7)}$$

$$\therefore \overline{x'^2(t)} = \frac{1}{2\pi} \int_{-\infty}^{\infty} \phi_{uu} \left| F - \overline{F}_1 \frac{\phi_{zz}}{\phi_{uu}} \right|^2 d\omega + \frac{1}{2\pi} \int_{-\infty}^{\infty} \frac{\phi_{zz}\phi_{uu} - F_1 \overline{F}_1 \phi_{zz}^2}{\phi_{uu}}\, d\omega \qquad \text{(A3.8)}$$

$$= \qquad I_1 \qquad + \qquad I_2$$

Since I_2 is independent of F the problem is the choice of F in order to minimise I_1. An absolute minimum is obtained when

$$F = \overline{F}_1\, \frac{\phi_{zz}}{\phi_{uu}} \qquad \text{(A3.9)}$$

but F will have poles with +ve real parts, due to $\overline{F}_1$, ϕ_{zz} and ϕ_{uu}, and will therefore be unrealisable.

The realisability restriction on F is introduced using the standard techniques of Wiener optimisation. If ϕ_{uu} is rational it can, since it must be even, be expressed as $\psi(s)\,\psi(-s)$ where $\psi(s)$ has no poles or zeros with +ve real parts, so

$$\phi_{uu} = \psi(s)\,\psi(-s) = |\,\psi\,|^2 \tag{A3.10}$$

and

$$I_1 = \frac{1}{2\pi}\int_{-\infty}^{\infty} \left|\, \psi F - \overline{F}_1\,\frac{\phi_{zz}}{\overline{\psi}} \,\right|^2 d\omega \tag{A3.11}$$

Now let

$$\psi F - \overline{F}_1\,\frac{\phi_{zz}}{\overline{\psi}} = F_3 \tag{A3.12}$$

and let the inverse transform of $F_3(s)$ be

$$f_3(t) = \frac{1}{2\pi j}\int_{-j\infty}^{j\infty} F_3(s)\, e^{st}\, ds \tag{A3.13}$$

Let $f_3(t) = f_{3-}(t) + f_{3+}(t)$

where $f_{3-}(t) = f_3(t)$ for $-\infty \leq t \leq 0$

$= 0$ for $t > 0$

$f_{3+}(t) = 0$ for $-\infty \leq t \leq 0$

$= f_3(t)$ for $t > 0$ (A3.14)

Now $F_3(s) = \int_{-\infty}^{\infty} f_3(t)e^{-st}dt = \int_{-\infty}^{0} f_3(t)e^{-st}dt + \int_{0}^{\infty} f_3(t)e^{-st}dt$

$$= \int_{-\infty}^{\infty} f_{3-}(t)e^{-st}dt + \int_{-\infty}^{\infty} f_{3+}(t)e^{-st}dt$$

$$= F_{3-}(s) + F_{3+}(s) \tag{A3.15}$$

All poles of $F_{3-}(s)$ have +ve real parts and no poles of $F_{3+}(s)$ have +ve real parts.

The procedure used above for F_3 can be used to separate $\left(\overline{F}_1 \frac{\phi_{zz}}{\overline{\psi}}\right)$ into $\left(\overline{F}_1 \frac{\phi_{zz}}{\overline{\psi}}\right)_-$ and $\left(\overline{F}_1 \frac{\phi_{zz}}{\overline{\psi}}\right)_+$ so from equation (A3.12)

$$\psi F - \left(\overline{F}_1 \frac{\phi_{zz}}{\overline{\psi}}\right)_+ - \left(\overline{F}_1 \frac{\phi_{zz}}{\overline{\psi}}\right)_- = F_{3-} + F_{3+} \qquad \text{(A3.16)}$$

Since ψ and F have no poles with +ve real parts then

$$\psi F - \left(\overline{F}_1 \frac{\phi_{zz}}{\overline{\psi}}\right)_+ = F_{3+}(s)$$

$$\text{and} \qquad -\left(\overline{F}_1 \frac{\phi_{zz}}{\overline{\psi}}\right)_- = F_{3-}(s) \qquad \text{(A3.17)}$$

$$\text{Now} \quad I_1 = \frac{1}{2\pi}\int_{-\infty}^{\infty} \left| F_3(j\omega) \right|^2 d\omega$$

$$= \int_{-\infty}^{\infty} [f_3(t)]^2 \, dt \quad \text{[Parseval's theorem]}$$

$$= \int_{-\infty}^{\infty} [f_{3-}(t)]^2 \, dt + \int_{-\infty}^{\infty} [f_{3+}(t)]^2 \, dt$$

$$= \frac{1}{2\pi}\int_{-\infty}^{\infty} \left| F_{3-}(j\omega) \right|^2 d\omega + \frac{1}{2\pi}\int_{-\infty}^{\infty} \left| F_{3+}(j\omega) \right|^2 d\omega$$

$$\therefore I_1 = \frac{1}{2\pi}\int_{-\infty}^{\infty} \left| \psi F - \left(\overline{F}_1 \frac{\phi_{zz}}{\overline{\psi}}\right)_+ \right|^2 d\omega + \frac{1}{2\pi}\int_{-\infty}^{\infty} \left| \left(\overline{F}_1 \frac{\phi_{zz}}{\overline{\psi}}\right)_- \right|^2 d\omega \qquad \text{(A3.18)}$$

The second integral in equation (A3.18) gives the error due to $f_{3-}(t)$ which is independent of F since F must be realisable. The first integral can be made zero if

$$F = \frac{1}{\bar{\psi}} \left(\bar{F}_1 \frac{\phi_{zz}}{\bar{\psi}} \right)_+ \qquad \text{(A3.19)}$$

when $\overline{x'^2(t)}$ takes its minimum value

$$\overline{x'^2(t)} = \frac{1}{2\pi} \int_{-\infty}^{\infty} \left| \left(\bar{F}_1 \frac{\phi_{zz}}{\bar{\psi}} \right)_- \right|^2 d\omega + \frac{1}{2\pi} \int_{-\infty}^{\infty} \frac{\phi_{zz}\phi_{uu} - F_1 \bar{F}_1 \phi_{zz}^2}{\phi_{uu}} d\omega \qquad \text{(A3.20)}$$

For the particular case when $\phi_{zz}(\omega)$ and $\phi_{\xi'\xi'}(\omega)$ are given by equation (A3.1) then

$$\phi_{zz}(s) = -\frac{N_z^2}{s^2} \quad ; \quad \phi_{\xi'\xi'}(s) = \tfrac{1}{2} N_\xi^2 \qquad \text{(A3.21)}$$

and when $F_1(s)$ is a pure gain, say K_1

$$F_1(s) = F_1(-s) = K_1 \qquad \text{(A3.22)}$$

Equations (A3.6), (A3.21) and (A3.22) give

$$\phi_{uu}(s) = -\frac{K_1^2 N_z^2}{s^2} + \tfrac{1}{2} N_\xi^2 \qquad \text{(A3.23)}$$

$$\phi_{uu}(s) = \frac{K_1^2 N_z^2 - \tfrac{1}{2} N_\xi^2 s^2}{-s^2}$$

$$= \frac{\left(K_1 N_z + \frac{1}{\sqrt{2}} N_\xi s \right)\left(K_1 N_z - \frac{1}{\sqrt{2}} N_\xi s \right)}{(s)(-s)} = \psi(s)\,\psi(-s)$$

$$\therefore \psi = \frac{K_1 N_z + \frac{1}{\sqrt{2}} N_\xi s}{s} \quad ; \quad \bar{\psi} = \frac{K_1 N_z - \frac{1}{\sqrt{2}} N_\xi s}{-s} \qquad \text{(A3.24)}$$

$$\overline{F}_1 \frac{\phi_{zz}}{\overline{\psi}} = \frac{K_1 N_z^2}{-s^2} \cdot \frac{-s}{K_1 N_z - \frac{1}{\sqrt{2}} N_\xi s} = \frac{K_1 N_z^2}{s(K_1 N_z - \frac{1}{\sqrt{2}} N_\xi s)}$$

$$= \frac{N_z}{s} + \frac{\frac{1}{\sqrt{2}} N_z N_\xi}{K_1 N_z - \frac{1}{\sqrt{2}} N_\xi s}$$

$$= \left(\overline{F}_1 \frac{\phi_{zz}}{\overline{\psi}}\right)_+ + \left(\overline{F}_1 \frac{\phi_{zz}}{\overline{\psi}}\right)_- \qquad \text{(A3.25)}$$

Substituting from equations (A3.25) and (A3.24) into equation (A3.19) gives the best F(s) as

$$F(s) = \frac{s}{K_1 N_z + \frac{1}{\sqrt{2}} N_\xi s} \cdot \frac{N_z}{s}$$

$$= \frac{N_z}{K_1 N_z + \frac{1}{\sqrt{2}} N_\xi s} \qquad \text{(A3.26)}$$

substituting equation (A3.26) in (A3.4) to get the best $F_2(s)$ gives

$$F_2(s) = \frac{N_z}{K_1 N_z + \frac{1}{\sqrt{2}} N_\xi s - K_1 N_z}$$

$$= \frac{\sqrt{2}\, N_z}{N_\xi s} \qquad \text{(A3.27)}$$

Equation (A3.27) shows that the best $F_2(s)$ represents an integrator.

Appendix 4

Details of Experimental Work

A4.1 Introduction

This appendix gives details of the analogue computer simulations described in the main text. The analogue computers used were Solartron types 247 and SC30. Figure A4.1 is a photograph of these computers.

The systems examined experimentally are described in the main text by the non-dimensional parameters defined in Chapter 2. The number of actual system parameters is greater than the number of non-dimensional parameters by three, the number of different types of unit used; so an arbitrary choice of three actual system parameters, involving the three different types of unit, can be made. This choice must be made so as to ensure an accurate simulation. The considerations governing this choice are discussed in sections 2-7 in this appendix and in sections 8-10 the actual simulation details are given.

A4.2 Magnitude scaling

In the analogue computer all variables are measured in machine units, where the machine unit is the full scale range of the computer, in this case 100 Volts. The scaling requirement is two-fold: no variable should exceed unity, in order to prevent overloading; and all variables should range over an appreciable fraction of unity, in order to achieve good accuracy.

The curvature A of the extremum characteristic, which relates the input unit scaling to the output unit scaling, was chosen to

be

$$A = 1 \qquad (A4.1)$$

so that the limitation to unity would have the same effect on both the input unit and the output unit scaling.

In Chapter 1 it was assumed that $z(t)$ and $\xi(t)$ were gaussian so some of the signals in the simulation will have a finite probability of exceeding unity. Overloading was avoided by limiting $x(t)$ to unity using a diode limiter. This limiter causes error in the simulation so the scaling involves a compromise between the requirements that $x(t)$ should be small, so that the limiter will introduce negligible error, and large so that the errors due to computer inaccuracies will be minimised. This compromise was effected by choosing a scaling which makes $\overline{x^2(t)}$ of the order of 0·1. The way in which this effects the required compromise is discussed below.

A measure of the normal range of $x(t)$ is its root mean square value $(\overline{x^2(t)})^{\frac{1}{2}}$. When $\overline{x^2(t)}$ is 0·1 this is approximately 0·3, which was considered large enough for reasonable accuracy.

An estimate of the effect of the limitation on $x(t)$ can be made by assuming that $x(t)$ is the sum of the perturbation, of amplitude a, and the gaussian equivalent circuit signal $x'(t)$. The effect of the limitation on $x(t)$ at unity is then similar to that of a limitation on $x'(t)$ at $(1 - a)$.

Consider the effect of a limiter on $x'(t)$. Let

$$r = \frac{x'(t)}{(x'^2(t))^{\frac{1}{2}}}$$

where $x'^2(t)$ is the variance of $x'(t)$ since ergodicity is assumed.

The probability density of $x'(t)$ can then be written

$$p(x') = \frac{1}{\sqrt{2\pi}} e^{-\frac{1}{2}r^2}$$

The fraction of time the limiter operates on $x'(t)$ is given by

$$\sqrt{\frac{2}{\pi}} \int_b^\infty e^{-\frac{1}{2}r^2} dr \qquad \text{(A4.2)}$$

where b is the value of r at which limitation occurs. A typical value of the perturbation amplitude a is 0·1, so a value of $\overline{x^2(t)}$ of 0·1 will make $\overline{x'^2(t)} < 0{\cdot}1$ and $b > 3$. When $b = 3$ in equation (A4.2) the limiter is in operation for only 0·27% of the time so its effect was assumed negligible.

One specific error introduced by the limiter is a reduction in the observed value of $\overline{x'^2(t)}$. The observed value of $\overline{x'^2(t)}$ is given, as a fraction of the value without the limiter, by the expression

$$\sqrt{\frac{2}{\pi}} \int_0^b r^2 e^{-\frac{1}{2}r^2} dr + b^2 \sqrt{\frac{2}{\pi}} \int_b^\infty e^{-\frac{1}{2}r} dr$$

which, using the relation

$$\int r e^{-\frac{1}{2}r^2} dr = - e^{-\frac{1}{2}r^2}$$

to integrate by parts, becomes

$$1 + (b^2-1) \sqrt{\frac{2}{\pi}} \int_b^\infty e^{-\frac{1}{2}r^2} dr - b\sqrt{\frac{2}{\pi}} e^{-\frac{1}{2}b^2} \qquad \text{(A4.3)}$$

When $b = 3$ expression (A4.3) gives the observed value of $\overline{x'^2(t)}$ as 0.51% below the value without limitation. This error was

considered negligible.

A4.3 Accuracy of simulation

The main accuracy specifications for the analogue computer are ± 0.2% of reading for the linear units and ± 0.2% of full scale for the multipliers. The zero setting accuracy of the multipliers is ± 0.1% of full scale and the potentiometers can be set to 0.03% of full scale.

The overall accuracy of a simulation is difficult to estimate theoretically and is normally obtained by observing the performance of a system whose response can be calculated. The experimental results shown in figures A4.6, A4.8 and A4.9 for the variation of γ with Π_2 indicate that γ will be within 5% of unity when it is expected to be unity from theoretical considerations. This suggests that the simulation accuracy is better than 5%. The possibility that larger simulation errors are compensating for equal and opposite errors in the theoretical results was discounted, as an accuracy of better than 5% is not untypical for a simulation of the size used in this work.

A4.4 Statistical accuracy

A statistical error in the measurement of $\overline{x^2(t)}$ results from the use of a finite measuring time. An estimate of this error can be made by assuming that the stochastic part of $x(t)$ is characterised by the equivalent circuit signal $x'(t)$. In all of the equivalent circuits $x'(t)$ is a gaussian ergodic

random process of spectral density

$$\phi_{x'x'}(\omega) = \frac{\text{constant}}{\Omega^2 + \omega^2}$$

where Ω is the bandwidth of the equivalent circuit. Jacobs[40] has shown that the normalised variance of the estimate of $\overline{x'^2(t)}$ obtained by integrating is given by the relation normalised variance $\approx \frac{2}{\Omega t_i}$ where t_i is the integration time, provided that $\Omega t_i >> 1$. In practice there are limitations on Ω and t_i so that some finite variance must be accepted. The limitation on Ω was determined by the characteristics of the analogue computer and one of the random signal generators. A number of factors limit the maximum possible value of t_i; these are

(i) The disturbance $z(t)$ is the brownian motion defined in chapter 1 and will have a variance[40] $N_z{}^2 t_i$ at time t_i, assuming zero initial conditions. The fact that the probability of $z(t)$ exceeding unity must be small limits this variance and hence t_i.

(ii) Drift in the computer integrators will cause error in the generation of $z(t)$ and the measurement of $\overline{x^2(t)}$. This error is proportional to t_i.

(iii) The time required to carry out the experiments is limited.

In most cases it was found possible to satisfy the relationship

$$t_i = \frac{800}{\Omega}$$

which makes the normalised standard deviation of the results to be 5%.

A4.5 Random signal sources

The disturbance and noise signals were derived from two separate 'white' noise sources.

(a) Disturbance z(t)

The brownian motion z(t) defined in chapter 1 can be obtained by integrating a gaussian white noise of spectral density $\phi(\omega) = N_z^2$. The output of the random signal generator type R.G. 77 made by Servomex Ltd. was used as an approximation to this white noise. Figure A4.2 is a photograph of this instrument. The spectral density of the output is specified to be constant up to 10 cycles/sec. In each experiment z(t) was fed into a simulation of the equivalent circuit and the resulting value of $\overline{x'^2(t)}$ measured. This indicated that in the flat region the spectral density was 0.16 V^2/rad per sec.

(b) Noise $\xi(t)$

This noise was generated by the 'home-made' random signal generator shown in figure A4.3. The output was $\pm$ V volts with a probability of changeover of 0.5 every 1/1500 sec. The spectral density of the output is given by Chang[8] as

$$\phi(\omega) = \frac{V^2}{1500}\left(\frac{\sin\frac{\omega}{3000}}{\frac{\omega}{3000}}\right)^2 .$$

In the analogue computer the output of the random signal generator was modified by the system shown in figure A4.4. In this system the output of the random signal generator is limited to $\pm$ 0.2 machine units in order to stabilise the signal levels, then multiplied by 5 so that the spectral density becomes

$$\phi(\omega) = \frac{1}{1500}\left(\frac{\sin\frac{\omega}{3000}}{\frac{\omega}{3000}}\right)^2 \text{ (machine units)}^2\text{/rad per sec.}$$

In order to produce an approximately gaussian signal the second order filter is used after the limiter. The transfer function of this filter is

$$G(s) = \frac{1}{1 + 2\times10^{-3}s + 2\times10^{-6}\ s^2}$$

giving a damping ratio of $1/\sqrt{2}$ and a natural frequency of 112.5 cycles/sec. A measure of how gaussian the signal has become is the peak to r.m.s. ratio, which for the above system is approximately 3. This was considered to be adequate.

The resulting signal has a spectral density of 1/1500 (machine units)^2/rad per sec within 2% up to 40 cycles/sec.

A4.6 Time scaling

The time scale of the simulation was determined by assigning a value to the equivalent circuit bandwidth Ω or to the perturbation frequency α.

The frequency range of the simulation should be as high as possible to reduce the measuring times, but is limited by the frequency response of the analogue computer multipliers which give a phase-shift of 10^0 at 100 cycles/sec, and by the output of the Servomex random signal generator whose output is flat only up to 10 cycles/sec. A time scale which made the perturbation frequency of the order of 10 cycles/sec was used.

A4.7 Some practical scaling considerations

Each simulation was built up, as far as possible, by a piece-wise simulation of each part of the system so that signals in the simulation could be readily identified with those in the actual system. Some exceptions had to be made in the interests of accuracy. These were:

(a) the disturbance z(t) was not simulated explicitly. At the end of the measuring time t_i the disturbance z(t) will have a variance $N_z^2 t_i$, assuming zero initial conditions. The probability of z(t) exceeding unity must be small so $N_z^2 t_i$ must be of the order of 0.1. This proved a more serious restriction on t_i than was tolerable, so instead of z(t) the signal $\frac{1}{c} z(t)$ was simulated where c is some constant so that the relationship

$$\left(\frac{N_z}{c}\right)^2 t_i \sim 0.1$$

allowed a reasonable value of t_i. This signal was then added to $\frac{1}{c}q(t)$ and x(t) obtained as

$$x(t) = c\left(\frac{1}{c}z(t) + \frac{1}{c}q(t)\right)$$

(b) the plant output y(t) was not simulated explicitly, in order to avoid the possibility of overloading the computer.

Now $y(t) = \{Ax^2 + B\} * \{\text{output lag}\} + \xi(t)$

where $\{P\} * \{Q\}$ is the output of Q when the input is the signal P. In the steady state

$$y(t) = \{Ax^2\} * \{\text{output lag}\} + B + \xi(t)$$

and the multiplier output is $v(t) = y(t)\cos(\alpha t - \theta)$

$\therefore v(t) = [\{Ax^2\} * \{\text{output lag}\}]\cos(\alpha t - \theta) + B\cos(\alpha t - \theta) + \xi(t)\cos(\alpha t - \theta)$

and $v(t)$ is the input to the controller integrator. Each of the three terms in the above expression for $v(t)$ was simulated separately then added together at the input to the controller integrator.

Experiments

A4.8 Variation of γ with Π_1 and Π_2

In this section the experiments described in sections 4.2.2, 4.3 and 7.3.3 are discussed in detail.

In each of the three experiments the magnitude scaling was fixed by choosing A = 1 and the perturbation amplitude a = 0.1, in order to comply with the accuracy considerations given in the preceding sections. The time scale was fixed by choosing a value for the equivalent circuit bandwidth Ω. The remaining system parameters are then uniquely defined by the non-dimensional parameters.

The value of γ, where

$$\gamma = \frac{\overline{x^2(t)}}{\overline{x'^2(t)} + \text{mean square value of perturbation}},$$

was obtained by comparing the measured value of $\overline{x^2(t)}$ with a measured value of $\overline{x'^2(t)}$ rather than the calculated value of $\overline{x'^2(t)}$. This measured value of $\overline{x'^2(t)}$ was obtained by subjecting a simulation of the equivalent circuit to the actual disturbance $z(t)$ or noise $\xi(t)\cos\alpha t$. This eliminates the first order effects of any errors in the generation of $z(t)$ or $\xi(t)$ and so improves the accuracy of the experiments.

(a) Sine wave perturbation - disturbances only.

This experiment was discussed in non-dimensional terms in section 4.2.2, where it is specified that

$$\Pi_3 = \frac{N_z^2}{Ka^3A} = 2.$$

The time scale of the simulation was chosen so that the equivalent circuit bandwidth Ω was

$$\Omega = KaA = 1 \text{ rad/sec.}$$

The value of $\overline{x^2(t)}$ was measured by integrating for 250 secs, which from section A4.4 gives an approximate standard deviation of the results of $\sqrt{\frac{2}{250}} \approx 9\%$.

The analogue computer diagram is shown in figure A4.5. The experimental procedure was as follows: $\Pi_1 = B/Aa^2$ was set to some fixed value by adjusting B, then γ was measured for a range of values of $\Pi_2 = \alpha/KaA$ sufficient to make γ vary from approximately 2 to under 1.05. This was repeated for a range of values of Π_1. The results are shown in table A4.1. Graphs of the variation of γ with Π_2 were drawn for each value of Π_1 and are shown in figures A4.6a and A4.6b. From these graphs the data was obtained to build up figure 4.2.

(b) Sine wave perturbation - noise only.

This experiment is discussed in non-dimensional terms in section 4.3 where it is specified that

$$\Pi_4 = \frac{KN_c^2}{Aa^3} = 4.$$

In this case Ω was chosen so that

$$\Omega = KaA = 2.5 \text{ rad/sec.}$$

The measurement time was again 250 secs so that the approximate standard deviation of the results is $\sqrt{2/625} \approx 6\%$.

The experimental procedure was the same as that described above for the system with disturbances only. The analogue computer diagram is shown in figure A4.7, the results in table A4.2 and the graphs of γ versus Π_2 in figure A4.8.

(c) Square wave perturbation - disturbances only.

This experiment is discussed in non-dimensional terms in section 7.3.3 where it is specified that

$$\Pi_3 = \frac{N_z^2}{Ka^3A} = 8.$$

In this case Ω was chosen so that

$$\Omega = 2KaA = \Pi \text{ rad/sec.}$$

The measurement time was again 250 secs so that the approximate standard deviation of the results is $\sqrt{2/250\pi} \approx 5\%$.

The experimental procedure was the same as that described in (a) above. The analogue computer diagram is the same as that shown in figure A4.5 for sine wave perturbation. The results are given in table A4.3, and the graphs of γ versus Π_2 in figure A4.9.

A4.9 Simulation of complete system

This is the experiment described in non-dimensional terms in section 5.4. The scaling for this simulation was determined by choosing $A = 1$, $\alpha = 100$ rad/sec, and the value of $\overline{x^2(t)}$ predicted by the design procedure to be 0.05. The remaining system parameters were then given by the dimensionless variables

specified by the design procedure. The analogue computer diagram is shown in figure A4.10.

A4.10 Comparison of three systems

This experiment is described in dimensionless terms in section 8.2. The scaling for the simulation was determined by choosing A = 1, α = 63 rad/sec, and by choosing $\overline{x^2(t)}$ theoretical to be 0.1 for the systems with Π_α = 40, 20 and 10, $\overline{x^2(t)}$ theoretical = 0.05 for Π_α = 8, and $\overline{x^2(t)}$ theoretical = 0.025 for Π_α = 4.

The three systems were simulated together, their separate disturbance and noise signals differing only by a multiplying factor. The analogue computer diagram is shown in figure A4.11.

Appendix 5

The Function Minimisation Routine

A5.1 Introduction

This appendix describes the digital computer function minimisation routine used in the design procedures.

The routine is based on a procedure suggested by Powell[43], which Fletcher[44] has shown to be relatively efficient. In this work a simplification of Powell's procedure was used in order to reduce program development time.

The thirteen 3-dimensional function minimisations discussed in Chapter 5 took less than one minute on an English Electric KDF 9 computer and involved approximately 100 function evaluations per minimisation.

The underlying principles of the routine are discussed in sections A5.2, A5.3 and A5.4, and the actual program used for the three dimensional minimisation is given in section A5.5. This program is written in Atlas Autocode[45].

A5.2 General procedure

The purpose of the routine is to find the coordinates x(1), x(2) -- x(j) written x(1:j) of the point $\underline{x}$ which minimises w in the relation

$$w = f(\underline{x}) \qquad \text{A5.1}$$

The evaluation of w from equation (A5.1) is carried out in a separate routine called PERFCRIT, which will depend on the particular function to be minimised.

The values of w for various trial values of x(1:j) is the only information used. The partial derivatives of w with respect to x(1:j) could have been obtained for the particular cases of f($\underline{x}$) considered in this work, but were not employed in the routine, as this would mean considerable complication without, it is thought, any significant increase in the speed of minimisation.

The procedure used is basically changing one variable at a time, that is minimising w along lines parallel to the x(1:j) coordinate axes. In addition a new direction in the j-dimensional space is defined and w minimised in this new direction. The routine stops when the above cycle fails to produce an improvement in x(1:j) greater than some specified quantities R(1:j).

The organisation of the routine is discussed in more detail in the next section.

A5.3 Organisation of routine

The main function minimisation routine, called 'fumin', calls on two sub-routines, 'minline' and 'evaluate'.

The routine minline finds the minimum value of w along a line in the j-dimensional x(1:j) space. The line is specified by a point $\underline{p}$ whose coordinates are p(1:j), and a direction $\underline{\ell}$ specified by the components ℓ(1:j) of a unit length along the line. This minline sub-routine is discussed in further detail in the next section.

The routine evaluate obtains the coordinates x(1:j) of a point at distance s(n) [n = 1, 2 or 3] along the line $\underline{\ell}$ from $\underline{p}$ as

$$\underline{x} = \underline{p} + s(n)\,\underline{\ell}$$

so that the routine PERFCRIT can obtain the value of w corresponding to s(n).

An iteration of the basic procedure is as follows:

(i) From a starting point $\underline{p}_o$ find the minimum with respect to the first variable x(1), that is along the line $\underline{\ell}$ = (1, 0 -- 0). Let the resulting point $\underline{p}_1$ be the starting point for the next line minimisation.

(ii) Repeat the line minimisation for each of the j parameters to find the point $\underline{p}_j$.

(iii) Define a new direction as that of the line joining $\underline{p}_o$ and $\underline{p}_j$ and find the minimum along this line. Call this point $\underline{p}_f$.

(iv) Compare $\underline{p}_f$ with $\underline{p}_o$. If the differences between the coordinates of $\underline{p}_f$ and $\underline{p}_o$ are less than the quantities specified as R(1:j) then accept $\underline{p}_f$ as the required minimum. Otherwise $\underline{p}_f$ becomes the starting point $\underline{p}_o$ of the next iteration cycle.

A5.4 Minimisation along a line

Minimisation along a line requires the following information:

(i) The coordinates p(1:j) of a point $\underline{p}$ on the line.

(ii) The direction $\underline{\ell}$ of the line, specified by the components ℓ(1:j) of a unit length along the line.

(iii) The accuracy r to which the minimum along the line is to be found.

(iv) The maximum step m which should be taken along the line. This was taken as m = 1000 r.

The extrapolation extremum control technique discussed in Chapter 1 was employed, using a quadratic defined by three points to predict the position of the minimum. The three points are specified

by their distances s(1), s(2) and s(3) along the line $\underline{\ell}$ from $\underline{p}$ and the corresponding function values are f(1), f(2) and f(3). The distance d of a turning point in w in the direction $\underline{\ell}$ from $\underline{p}$ is then given by the relation

$$d = \tfrac{1}{2} \cdot \frac{[s(2)^2-s(3)^2]f(1)+[s(3)^2-s(1)^2]f(2)+[s(1)^2-s(2)^2]f(3)}{[s(2)-s(3)]f(1)+[s(3)-s(1)]f(2)+[s(1)-s(2)]f(3)} \qquad (A5.2)$$

This turning point is a minimum if ft < 0 where

$$ft = \frac{[s(2)-s(3)]f(1)+[s(3)-s(1)]f(2)+[s(1)-s(2)]f(3)}{[s(1)-s(2)][s(2)-s(3)][s(3)-s(1)]} \qquad (A5.3)$$

If the turning point is predicted to be a maximum or if the value of d is such that to calculate $f(\underline{p} + d\underline{\ell})$ a step greater than m must be taken, the maximum allowable step m is taken in the direction of decreasing w to give a new prediction point to replace the most distant of the original points.

Otherwise d is used to provide a new prediction point, replacing the most distant of the original three. When d is within the required accuracy r of one of the three points used to calculate d then this value of d is accepted as giving the minimum along the line.

To avoid division by zero the denominator of equation A5.2 was evaluated separately and checked. If this denominator is zero the three points indicate a linear variation of w along the direction of minimisation. If w is constant the centre point is taken as the minimum. If not, a step of ten times the distance between the two outermost points is taken in the direction of decreasing w, in order to provide a new prediction point.

A5.5 The computer program

```
***A
JOB
UEDIN, LP/1816   0000 SHERING ELE, GENMIN RESULTS
COMPUTING 5000 INSTRUCTIONS
OUTPUT
0 LINE PRINTER 300 LINES
STORE 30 BLOCKS
EXECUTION 1 MINUTES
COMPILER AA

begin
real v,w
array x,R(1:3)
integer i,j,n
routine spec fumin
routine spec PERFCRIT

j=3
R(1)=0.001; R(2)=0.0002; R(3)=0.001
x(1)=1;x(2)=2;x(3)=10
n=0
cycle i=1,1,13
read(v)
fumin
newline
print(v,3,3);print(x(1),3,3);print(x(2),3,3);print(x(3),3,3);print(w,3,3)
print(n,4,0)
repeat
stop


routine PERFCRIT
real b,c
n=n+1
b=1/exp(log(x(1))/3)
c=exp(log(x(2))/3)
w=½*(1+44/x(3)↑3)*(b/c)*(1+(x(1)+½x(2))*sqrt(1+v↑2*x(3)↑2*c↑2*b↑4))
end
```

```
routine fumin; comment finds x(1:j) to accuracy R(1:j) to give minimum w
real m,r,r',w1,h,h2
integer T,N,i,k
array s,f(1:3),p,l,Q,X(1:j)
routine spec minline
routine spec evaluate(integer n)

N=0
cycle i=1,1,j; Q(i)=100R(i);p(i)=x(i); repeat
s(1)=0;evaluate(1)
1:N=N+1
->3 unless N>30; caption stopped at Nmax; newline; return
3:cycle i=1,1,j; X(i)=x(i); repeat; w1=w
cycle i=1,1,j
r=R(i); m=1000r
cycle k=1,1,j; p(k)=x(k); l(k)=0; repeat
l(i)=1
s(1)=0; f(1)=w
s(2)=Q(i); evaluate(2)
s(3)=2Q(i); s(3)=-Q(i) if f(2)≥f(1); evaluate(3)
minline
repeat

cycle i=1,1,j
Q(i)=½*|x(i)-X(i)|; Q(i)=R(i) if Q(i)<R(i); Q(i)=100R(i) if Q(i)>100R(i)
repeat
->1 if N<2
h2=0; cycle i=1,1,j; h2=h2+(x(i)-X(i))²; repeat; h=sqrt(h2)
cycle i=1,1,j
l(i)=(x(i)-X(i))/h
r'=|R(i)/(l(i)+1α-7)|
if i=1 then r=r'
if i>1 and r'<r then r=r'
repeat
m=1000r
cycle i=1,1,j; p(i)=X(i); repeat
s(1)=0; f(1)=w1
->4 if h>½r; s(2)=½r; evaluate(2); s(3)=-½r; evaluate(3); ->5
4:s(2)=h; f(2)=w; s(3)=½h; evaluate(3)
5:minline
cycle i=1,1,j; ->1 if |x(i)-X(i)|>R(i); repeat
return
```

```
routine minline
comment minimisation along l from p
integer i,imax, imin,C
real a,d,e,max,min,ft
T=0
C=0
6:T=T+1; return if T>5
  a=(s(2)-s(3))*f(1)+(s(3)-s(1))*f(2)+(s(1)-s(2))*f(3)
  ->15 unless a=0
  if f(1)=f(2) or f(1)=f(3) or f(2)=f(3) then return
  if f(1)>f(2) and f(1)>f(3) then imax=1; if f(1)<f(2) and f(1)<f(3) then imin=1
  if f(2)>f(3) and f(2)>f(1) then imax=2; if f(2)<f(3) and f(2)<f(1) then imin=2
  if f(3)>f(1) and f(3)>f(2) then imax=3; if f(3)<f(1) and f(3)<f(2) then imin=3
  s(imax)=s(imin)+10*(s(imin)-s(imax));evaluate(imax)
  ->6
15:d=½*((s(2)²-s(3)²)*f(1)+(s(3)²-s(1)²)*f(2)+(s(1)²-s(2)²)*f(3))/a
  ft=a/((s(1)-s(2))*(s(2)-s(3))*(s(3)-s(1)))
max=0
cycle i=1,1,3
e=|d-s(i)|
->1 if e<r
10: ->2 if max>e
max=e; imax=i
2: repeat
C=0
->3 if ft<0 and max<m
->4  if ft<0  and max>m
->5
3:s(imax)=d; evaluate(imax); ->6
4:cycle i=1,1,3
  e=|d-s(i)|
  ->12 if i>1
  min=e; imin=1
  12: ->7 if min<e
  min=e; imin=i
  7: repeat
  ->13 if min>m
  s(imax)=d; evaluate(imax)
  ->6
  13: s(imax)=s(imin)+m
  s(imax)=s(imin)-m if (d-s(imin))<0; evaluate(imax)
  ->6
5:d=s(imax)+m if (d-s(imax))<0
  d=s(imax)-m if (d-s(imax))>0
  max=0
  cycle i=1,1,3
  e=|d-s(i)|
  ->8 if max>e
  max=e; imax=i
  8: repeat
  s(imax)=d; evaluate(imax)
  ->6
1: ->10 if ft>0
s(1)=d; evaluate(1)
end; comment end of line minimisation
```

```
routine evaluate(integer n)
integer i
cycle i=1,1,j; x(i)=p(i)+s(n)*l(i); repeat
PERFCRIT
f(n)=w
end

end; comment end of fumin

end of program

0.01  0.02  0.04  0.08  0.1  0.2  0.4  0.8  1.0  2.0  4.0  8.0  10.0

***Z
```

References

(1) Draper, C. S. and Li, Y. T: 'Principles of Optimalising Control Systems and an Application to the Internal Combustion Engine', American Society of Mechanical Engineers, 1951.

(2) Feldbaum, A. A: 'The statistical theory of gradient systems of automatic optimisation for an object with a quadratic characteristic', Automation and Remote Control Vol. 21, No. 2, 1960.

(3) Jacobs, O. L. R: 'Hill Climbing', Control Feb., 1962.

(4) Douce, J. L: 'The Behaviour of Adaptive Controllers', Proceedings I.F.A.C. 1963.

(5) Chang, S. S. L: 'Optimisation of the Adaptive Function by z-transform Method', Transactions A.I.E.E. part II, July, 1960.

(6) Tsien, H.S: 'Engineering Cybernetics', (McGraw-Hill Book Company, Inc. 1954) Chapter 15.

(7) Grensted, P. E. W. and Jacobs, O. L. R: 'Automatic Optimisation', Transactions of the Society of Instrument Technology Vol. 13, No. 3, 1961.

(8) Chang, S. S. L: 'Synthesis of Optimal Control Systems', (McGraw-Hill Book Company, Inc. 1961).

(9) Kushner, H. J: 'Hill-climbing methods for the optimisation of multiparameter noise disturbed systems', Transactions American Society of Mechanical Engineers June, 1963.

(10) Rosenbrock, H. H: 'An automatic method for finding the greatest or least value of a function', Computer Journal No. 8, 1961.

(11) Feldbaum, A. A: 'Problems in the Statistical Theory of Systems of Automatic Optimisation', Proceedings I.F.A.C. 1960.

(12) Tovstykha, T. I: 'On the Question of Choice of Parameters in the Control Part of a Gradient-Type Automatic Optimisation System', Automation and Remote Control Vol. 22, No. 8, 1961.

(13) Douce, J. L. and Bond, A. D: 'The Development and performance of a self-optimising system', Proceedings I.E.E. March, 1963.

(14) Jelonek, Z. J., Gardiner, A. B. and Raeside, D: 'A theoretical comparison of three types of self-optimising control systems', Paper 12, U.K.A.C. Conference, Nottingham 1965.

(15) Jacobs, O. L. R: 'Some properties of random processes', Transactions of the Society of Instrument Technology Dec., 1964.

(16) Fuller, A. T: 'Notes on the random telegraph signal as an approximation to white noise', Journal of Electronics and Control No. 6, 1963.

(17) Roberts, J. D: 'Extremum or hill-climbing regulation: a statistical theory involving lags, disturbances and noise', Proceedings I.E.E. January, 1965.

(18) Florentin, J. J: 'An Approximately Optimal Extremal Regulator', Journal of Electronics and Control August, 1964.

(19) Morosonov, I. S: 'Methods of Extremum Control', Automation and Remote Control Vol. 18, No. 11, Nov., 1957.

(20) Perret, R. and Rouxel, R: 'Principle and Application of an Extremal Computer', Proceedings I.F.A.C. 1963.

(21) Eveleigh, V. W: 'Limit cycle conditions in optimalising controllers', I.F.A.C. (Teddington) Symposium 1965.

(22) Brobov, Y. I., Kornkov, R. V. and Putsillo, V. P: 'Relay hill climber with lag', Automation and Remote Control Vol. 24, No. 2, Feb., 1963.

(23) Katkovnik and Pervozvanskii: 'Dynamics of relay self-oscillating extremum control systems', Automation and Remote Control Vol. 22, No. 12.

(24) Jacobs, O. L. R. and Wonham, W. M: 'Extremum Control in the Presence of Noise', Journal of Electronics and Control Vol. 11, No. 3, Sept., 1961.

(25) Xirokostas, D. A. and Henderson, J. G: 'Extremum control of dynamic systems in the presence of random disturbances and noise' Proceedings I.F.A.C. 1966.

(26) Vinograd,and Geronimus: 'The extrapolation method of searching for the minimum of a quadratic function', Automation and Remote Control Vol. 22, No. 6.

(27) Perelman, I. I: 'The statistical investigation of extrapolation extremal control systems for an object with a parabolic characteristic', Automation and Remote Control Vol. 22, No. 11.

(28) Perelman, I. I: 'A comparison of the simplest gradient and extrapolation systems'. Automation and Remote Control Vol. 24, No. 4.

(29) Van der Grinten, P.M.E.M: 'The Application of Random Test Signals in Process Optimisation', Proceedings I.F.A.C. 1963.

(30) Douce, J. L. and Ng, K. C: 'The use of pseudo-random signals in adaptive control', I.F.A.C. (Teddington) Symposium 1965.

(31) Nightingale, J. M: 'Parameter perturbation adaptive control systems with imposed constraints', Proceedings I.E.E. Part C, Monograph No. 518, May, 1962.

(32) Eveleigh, V. W: 'General Stability Analysis of Sinusoidal Perturbation Extrema Searching Adaptive Systems', Proceedings I.F.A.C. 1963.

(33) Pervozvanskii, A. A: 'Continuous extremum control systems in the presence of random noise', Automation and Remote Control Vol. 21, No. 7.

(34) Grishko, N. V: 'The determination of optimal characteristics for an extremal system with random disturbance', Automation and Remote Control Vol. 22, No. 8.

(35) Ng, K. C: 'High-frequency perturbation in hill-climbing systems', Proceedings I.E.E. November, 1964.

(36) Buckingham, E: 'Model experiments and the forms of empirical equations', Article No. 1487, Transactions of the American Society of Mechanical Engineers, 1915.

(37) Mesch, F: 'A Comparison of the Measuring Time in Self-Adjusting Control Systems', Proceedings I.F.A.C. 1963.

(38) Jelonek, Z. J., Pomella, P. L. V. and Karunaratne, N. S: 'Oscillations in feedback systems subjected to periodic interference, and stability of a self-optimising control system', Proceedings I.E.E. Nov., 1964.

(39) Roberts, J. D: in discussion with Shering, G. C. on 'Performance of hill-climbing systems - the gradient estimation problem', Proceedings I.E.E. August, 1965.

(40) Jacobs, O. L. R: 'The Measurement of the Mean Square Value of Certain Random Signals', Journal of Electronics and Control August, 1960.

(41) Papoulis, A: 'The Fourier Integral and its Applications', McGraw-Hill Book Company, Inc. 1962, Chapter 7.

(42) Brown, B. M: 'The Mathematical Theory of Linear Systems', Chapman and Hall Ltd., 1961.

(43) Powell, M. J. D: 'An efficient method of finding the minimum of a function of several variables without calculating derivatives', The Computer Journal July, 1964

(44) Fletcher, R: 'Function minimisation without evaluating derivatives - a review', The Computer Journal April, 1965.

(45) Schofield, P. D. and Osborne, M. R: 'Programming in Atlas Autocode' Edinburgh University Computer Unit Report No. 1 1965.

Table 5.1 - Computer results for design

Π_p	Π_e	Π_2	Π_3	Π_4	αT	γ
0·01	1·22	16·94	1·06	1·96	0·204	1·01
0·02	1·25	13·15	1·13	1·92	0·301	1·02
0·04	1·33	10·42	1·27	1·83	0·436	1·04
0·08	1·48	8·47	1·50	1·70	0·617	1·07
0·1	1·55	7·97	1·60	1·65	0·688	1·09
0·2	1·92	6·75	2·04	1·45	0·951	1·14
0·4	2·62	5·89	2·68	1·22	1·30	1·22
0·8	4·00	5·31	3·61	0·98	1·79	1·29
1·0	4·68	5·17	4·00	0·90	1·98	1·32
2·0	8·04	4·85	5·50	0·685	2·75	1·39
4·0	14·74	4·67	7·66	0·506	3·83	1·43
8·0	28·1	4·56	10·74	0·367	5·37	1·46
10·0	34·8	4·54	11·98	0·329	5·99	1·47

Table 5.2 - Sensitivity of Performance to inaccurate plant knowledge

$\Pi_p = 0·1$ $\Pi_e = 1·55$

	$N_z' = 2N_z$	$N_z' = \frac{1}{2}N_z$	$N_\xi' = 2N_\xi$	$N_\xi' = \frac{1}{2}N_\xi$	$A' = 2A$	$A' = \frac{1}{2}A$	$T' = 2T$	$T' = \frac{1}{2}T$
Π_p'	0·252	0·0397	0·063	0·159	0·159	0·063	0·2	0·05
Π_e'	2·1	1·326	1·42	1·78	1·78	1·42	1·92	1·365
Π_e''	2·41	1·54	1·715	2·0	2·4	1·58	2·02	1·4
$\frac{\Pi_e''}{\Pi_e'}$	1·15	1·16	1·21	1·125	1·35	1·11	1·05	1·03

Table 5.3 - Results from simulation of complete system

Table 5.3a

Π_p	0·01	0·1	1·0
Π_e from theory	1·22	1·55	4·68
Π_e experimental	1·24	1·52	4·55
$\Pi_{e_{min}}$ experimental	"	"	3·14

Note 1) Limiter on x set to $20\overline{x^2}$ for $\Pi_p = 0{\cdot}01$ and $0{\cdot}1$

$15\overline{x^2}$ for $\Pi_p = 1{\cdot}0$

2) $\Pi_{e_{min}}$ experimental for $\Pi_p = 1{\cdot}0$ was obtained with 1·5a, 1·5K, 1·5f and $B = -A\overline{x^2}$ i.e with $\Pi_2 = 3{\cdot}44$, $\Pi_3 = 0{\cdot}79$ and $\Pi_4 = 0{\cdot}4$

Table 5.3b

Π_p	0·01	0·1	1·0
Π_e with twice designed perturbation amplitude a	2·02	2·18	3·7
" " half " " "	1·73	1·9	5·5
Π_e with twice designed gain K	1·49	2·08	unstable
" " half " " "	1·4	1·93	4·55
Π_e with twice designed perturbation frequency α	1·27	1·9	4·55
" " half " " " α	1·28	1·84	unstable

Table 5.3c

$B/A\overline{x^2}$	-10	+10	-5	+3	0	-2	+1
$\Pi_p = 0{\cdot}01$	1·54	1·7					
$\Pi_p = 0{\cdot}1$			2·2	1·85			
$\Pi_p = 1{\cdot}0$					3·9	6·75	unstable

Table 7.1

sine wave perturbation

Π_α	Π_2	Π_3	Π_e	γ
100·0	79·41	1·001	1·191	1·00
80·0	63·56	1·002	1·191	1·00
40·0	32·01	1·012	1·192	1·00
20·0	16·77	1·085	1·203	1·01
10·0	10·06	1·426	1·260	1·04
8·0	8·866	1·650	1·303	1·06
4·0	6·594	2·993	1·586	1·15
2·0	5·450	6·361	2·278	1·27
1·0	4·875	15·22	3·805	1·38
0·8	4·766	20·56	4·597	1·41
0·4	4·569	54·60	8·652	1·45
0·2	4·492	150·5	16·90	1·48
0·1	4·464	421·8	33·52	1·50

Note $\frac{1}{2}\Pi_3^2\left(\frac{\Pi_\alpha}{\Pi_2}\right)^3 \equiv 1$

Table 7.2

square wave perturbation

Π_α	Π_2	Π_3	Π_e	γ
100·0	158·8	4·002	1·191	1·00
80·0	127·1	4·004	1·191	1·00
40·0	63·83	4·031	1·192	1·00
20·0	32·98	4·234	1·199	1·01
10·0	19·09	5·275	1·241	1·03
8·0	16·64	5·997	1·274	1·05
4·0	12·04	10·44	1·504	1·13
2·0	9·765	21·58	2·086	1·25
1·0	8·609	50·52	3·392	1·36
0·8	8·385	67·87	4·072	1·39
0·4	7·977	178·1	7·570	1·45
0·2	7·814	488·4	14·71	1·48
0·1	7·753	1365	29·12	1·49

Note $\Pi_3^2\left(\frac{\Pi_\alpha}{\Pi_2}\right)^3 \equiv 4$

Table 7.3

System with sample and hold

b	Π_α	Π_2	Π_3	Π_e
·923	98·75	163·2	4·167	1·223
·905	79·24	132·3	4·210	1·231
·820	39·76	69·81	4·439	1·274
·676	19·96	38·79	4·959	1·363
·469	9·974	23·67	6·264	1·565
·397	7·992	20·84	7·038	1·674
·199	3·995	15·69	12·05	2·289
·082	1·998	13·69	26·39	3·686
·030	0·9830	12·96	68·67	6·781
·022	0·795	12·85	92·91	8·256
·007	0·367	12·66	287·7	17·38
·002	0·1585	12·59	1002	39·79
·001	0·0998	12·58	2002	63·08

Table 8.1

Π_α	40	20	10	8	4
Π_e for sine wave perturbation system	1·24	1·2	1·42	1·39	2·16
Π_e for square wave perturbation system	1·21	1·28	1·35	1·35	1·87
Π_e for system with sample and hold	1·22	1·48	1·7	1·79	2·95

Table 8.2

Π_α	40	8	4	2	1
Π_e for sampled system, disturbance z*(t)	1·4	1·66	2·2	3·47	7·1

Table 8.3

System	as designed	2a	½a	2K	½K	$\frac{B}{\overline{Ax}^2}=5$	$\frac{B}{\overline{Ax}^2}=3$
$\frac{\Pi_e \text{ measured}}{\Pi_e \text{ theory}}$ - sine	1·08	1·5	1·72	1·4	1·22	1·2	1·21
$\frac{\Pi_e \text{ measured}}{\Pi_e \text{ theory}}$ - square	1·00	1·47	1·44	1·17	1·19	1·15	1·07
$\frac{\Pi_e \text{ measured}}{\Pi_e \text{ theory}}$ sampled	1·03	1·47	1·34	1·34	1·19	—	—

Table A4.1 Sine wave perturbation, disturbances only.

Π_1	Π_2	γ
0	3·0	2·36
	5·5	1·51
	7·55	1·08
	9·45	1·10
	11·0	1·04
3	4·5	2·32
	6·3	1·35
	8·2	1·17
	11	1·09
	15·1	1·05
6	5·5	2·26
	7·55	1·42
	11	1·19
	15·1	1·10
	20·1	1·03
9	6·9	1·98
	11	1·40
	15·1	1·18
	20·1	1·08
	25·1	1·05
12	8·2	2·1
	12·6	1·46
	17·6	1·19
	25·1	1·09
	31·4	1·04
15	9·45	2·24
	15·1	1·41
	20·1	1·22
	25·1	1·13
	31·4	1·07
	37·7	1·04
18	11	2·32
	17·6	1·43
	25·1	1·20
	31·4	1·12
	37·7	1·08
	44	1·05

Π_1	Π_2	γ
-3	3·14	2·12
	4·5	1·31
	6·3	1·12
	8·2	1·05
-6	3·46	2·6
	4·1	1·55
	4·5	1·71
	5·5	1·48
	7·55	1·14
	11	1·10
	15·1	1·04
-9	4·1	2·53
	5·5	1·69
	6·3	1·51
	8·2	1·38
	11	1·17
	15·1	1·08
	18·9	1·06
-12	6·3	1·85
	11	1·32
	15·1	1·16
	20·1	1·09
	25·1	1·06
-15	7·55	1·94
	12·6	1·40
	18·9	1·16
	25·1	1·10
	31·4	1·06
-18	8·2	2·21
	12·5	1·56
	18·9	1·26
	25·1	1·14
	31·4	1·09
	37·7	1·06
-21	11	1·96
	17·6	1·39
	25·1	1·19
	31·4	1·12
	37·7	1·09
	44	1·07

Table A4.2 Sine wave perturbation, noise only

Π_1	Π_2	γ
0	3·14	1·8
	3·77	1·61
	5·02	1·22
	6·9	1·21
	8·8	1·10
	10·7	1·05
	12·5	1·03
3	3·77	2·54
	5·02	1·59
	6·9	1·25
	8·8	1·15
	10·7	1·12
	12·5	1·07
	15·1	1·05
6	5·02	2·26
	7·55	1·53
	11·3	1·19
	15·1	1·12
	18·8	1·07
9	7·55	1·93
	10	1·48
	13·8	1·23
	17·6	1·15
	21·4	1·10
	25·1	1·07
12	7·55	2·47
	11·3	1·57
	15·1	1·28
	20·1	1·17
	25·1	1·11
	30·2	1·06
15	10	2·11
	15·1	1·44
	21·4	1·21
	27·6	1·11
	33·8	1·07
	40·1	1·05

Π_1	Π_2	γ
-3	3·14	1·92
	4·4	1·18
	6·3	1·13
	8·2	1·06
	10	1·06
-6	3·77	1·6
	5·02	1·27
	7·55	1·17
	10	1·07
	12·5	1·04
-9	5·02	1·66
	7·55	1·33
	11·3	1·14
	15·1	1·08
	18·8	1·06
-12	5·02	2·06
	7·55	1·57
	11·3	1·29
	15·1	1·14
	18·8	1·11
	21·4	1·08
	25·1	1·06
-15	7·55	1·85
	11·3	1·42
	15·1	1·27
	20·1	1·16
	25·1	1·10
	30·2	1·07
-18	7·55	2·35
	10	1·75
	15·1	1·37
	21·4	1·20
	27·6	1·12
	33·8	1·08
	40·1	1·07

Table A4.3 Square wave perturbation, disturbances only

Π_1	Π_2	γ
0	7	1·92
	8	1·56
	9	1·37
	10	1·26
	12	1·14
	14	1·09
	16	1·11
	18	1·08
	20	1·05
6	8	1·8
	8	2·01
	9	1·91
	10	1·63
	11	1·41
	12	1·31
	13	1·27
	15	1·17
	17	1·18
	20	1·11
	24	1·07
	30	1·04
12	10	2·21
	12	1·71
	14	1·46
	16	1·34
	18	1·24
	20	1·21
	24	1·12
	30	1·07
	40	1·04
18	12	2·38
	13	2·01
	14	1·86
	16	1·63
	20	1·34
	26	1·20
	32	1·13
	40	1·08
	46	1·06

Π_1	Π_2	γ
-3	5	2·26
	6	1·73
	7	1·74
	8	1·46
	9	1·26
	10	1·31
	11	1·15
	12	1·16
	13	1·11
	14	1·09
	15	1·11
	16	1·07
	17	1·05
	18	1·08
	20	1·05
-6	6	1·83
	7	1·67
	8	1·39
	9	1·50
	10	1·21
	11	1·23
	12	1·19
	14	1·13
	16	1·08
	18	1·06
	20	1·05
-12	7	1·92
	8	1·56
	10	1·46
	11	1·33
	12	1·31
	14	1·21
	16	1·12
	18	1·11
	20	1·08
	22	1·08
	25	1·05

Table A4.3 continued

Π_1	Π_2	γ
24	16	1·98
	20	1·59
	24	1·37
	30	1·22
	40	1·12
	50	1·06
	60	1·05
30	18	2·04
	20	1·80
	24	1·55
	30	1·31
	35	1·24
	40	1·16
	50	1·12
	60	1·08
	70	1·05

Π_1	Π_2	γ
-18	9	2·14
	10	1·68
	12	1·42
	14	1·39
	16	1·29
	20	1·20
	25	1·17
	30	1·11
	36	1·06
	40	1·06
-24	11	2·08
	13	1·74
	16	1·51
	20	1·35
	25	1·22
	32	1·13
	40	1·09
	50	1·04
-30	13	2·09
	14	1·84
	16	1·73
	20	1·53
	25	1·33
	30	1·26
	40	1·14
	50	1·08
	60	1·06

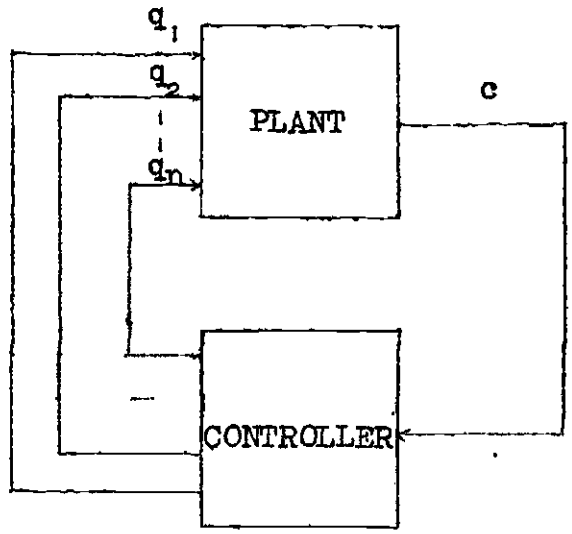

Fig. 1.1 Diagrammatic representation of extremum control system

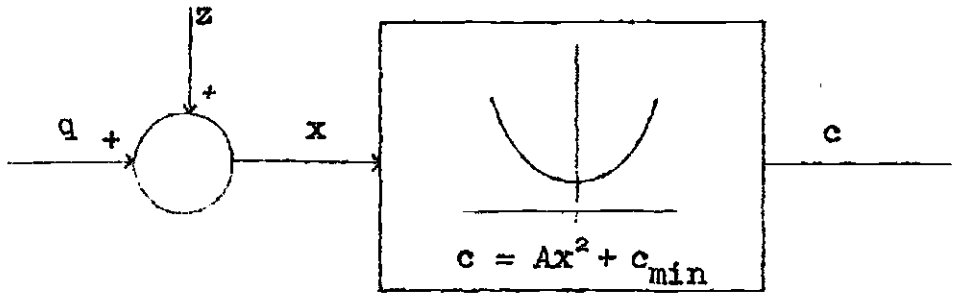

Fig. 1.2 Simplest plant requiring extremum regulation

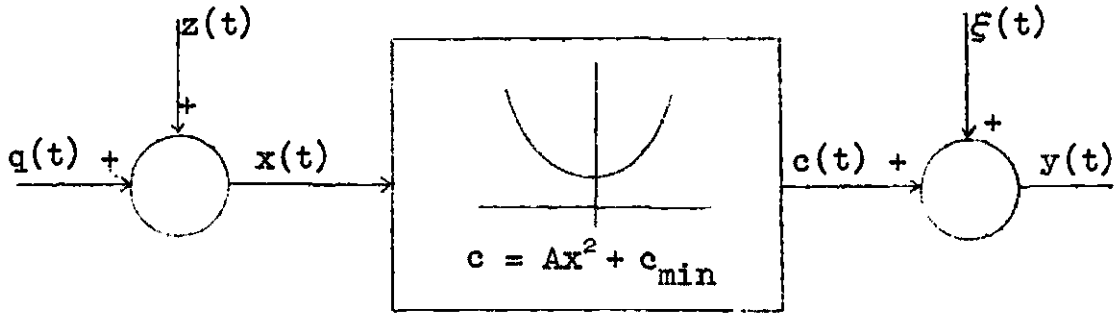

Fig. 1.3 Plant with measurement noise

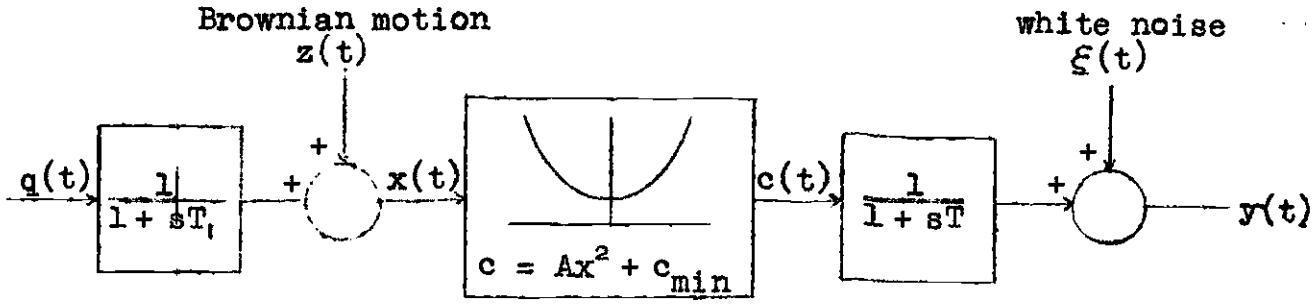

Fig. 1.4 Plant with noise and lags

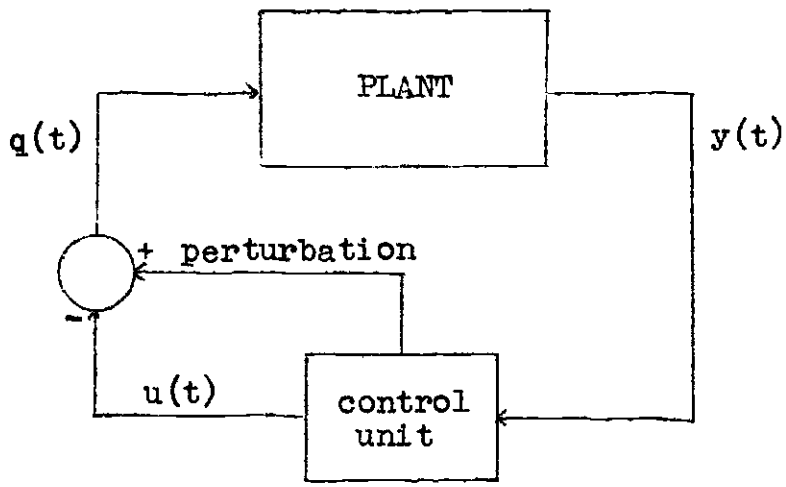

Fig. 1.5 General representation of 'linearised' perturbation system

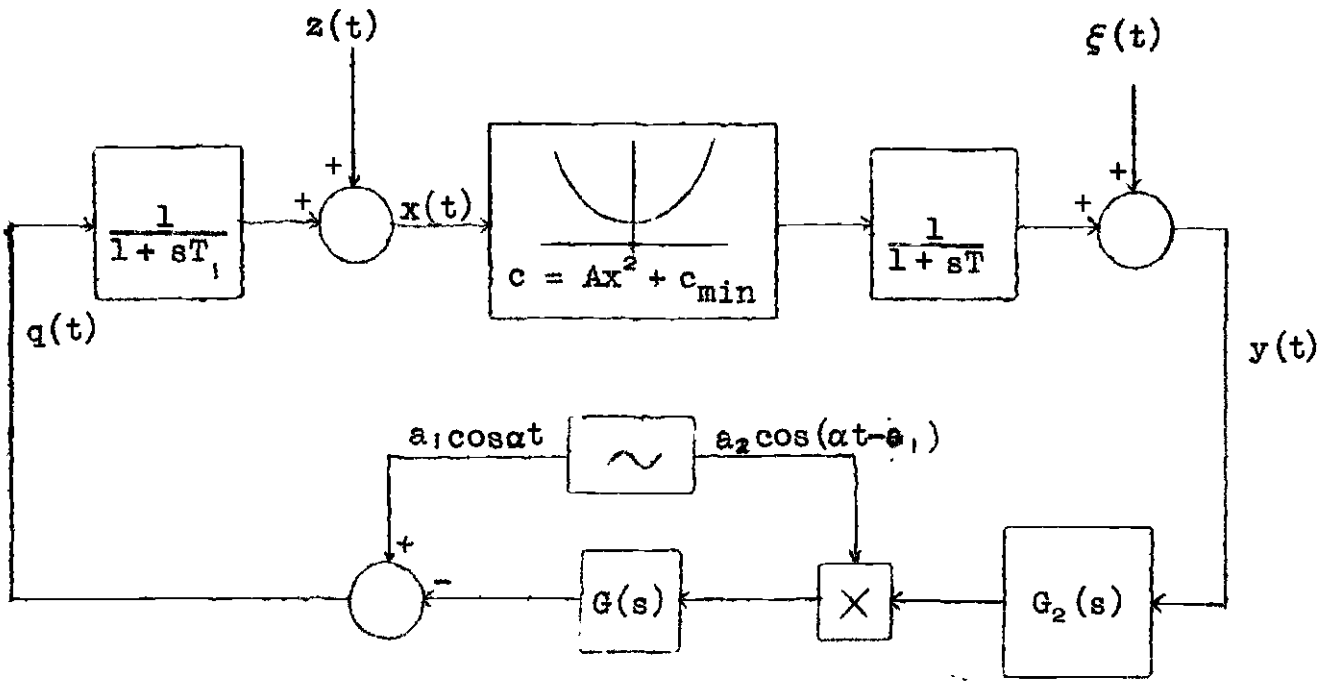

Fig. 2.1 General sinusoidal perturbation system

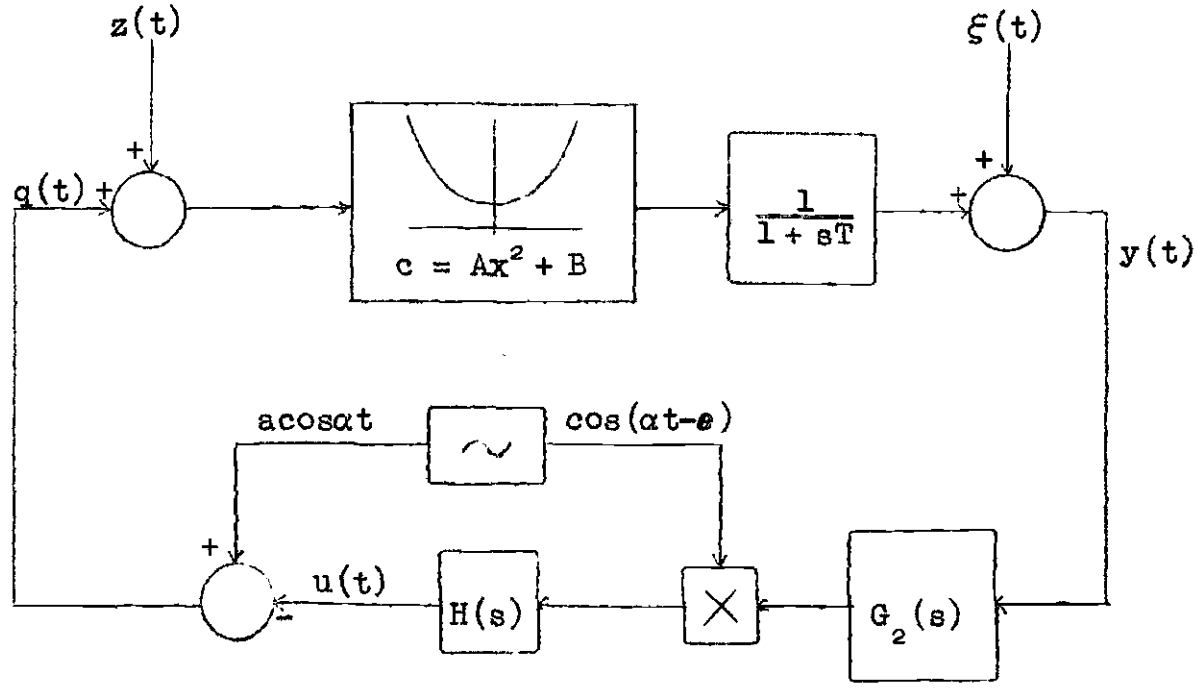

Fig. 2.2 System for equivalent circuit derivation

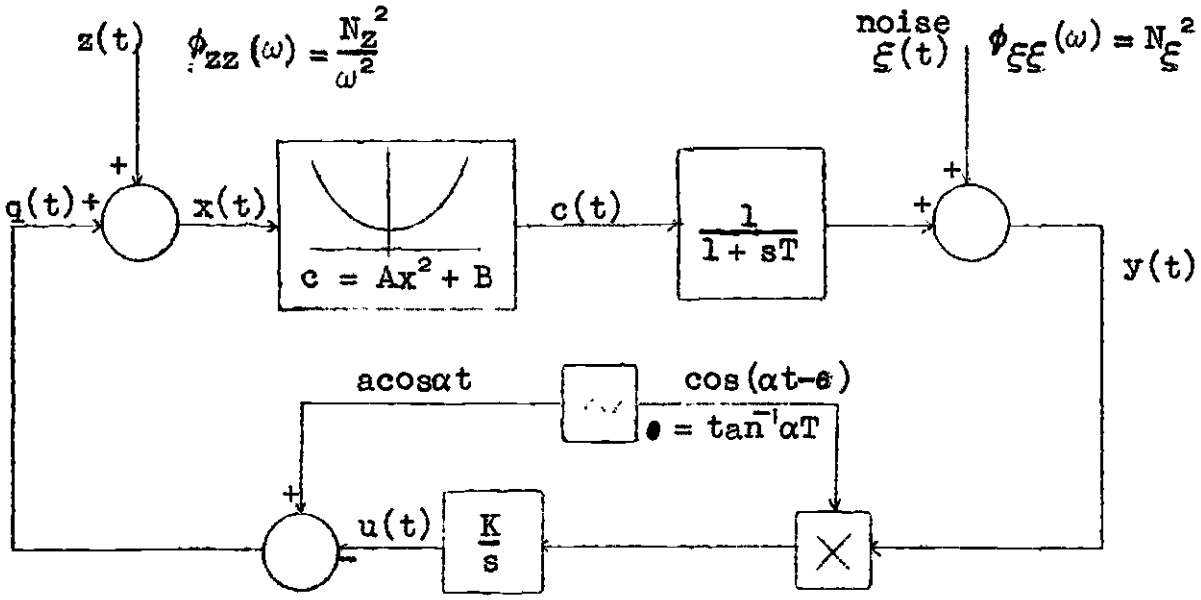

Fig. 2.3 System for design procedure

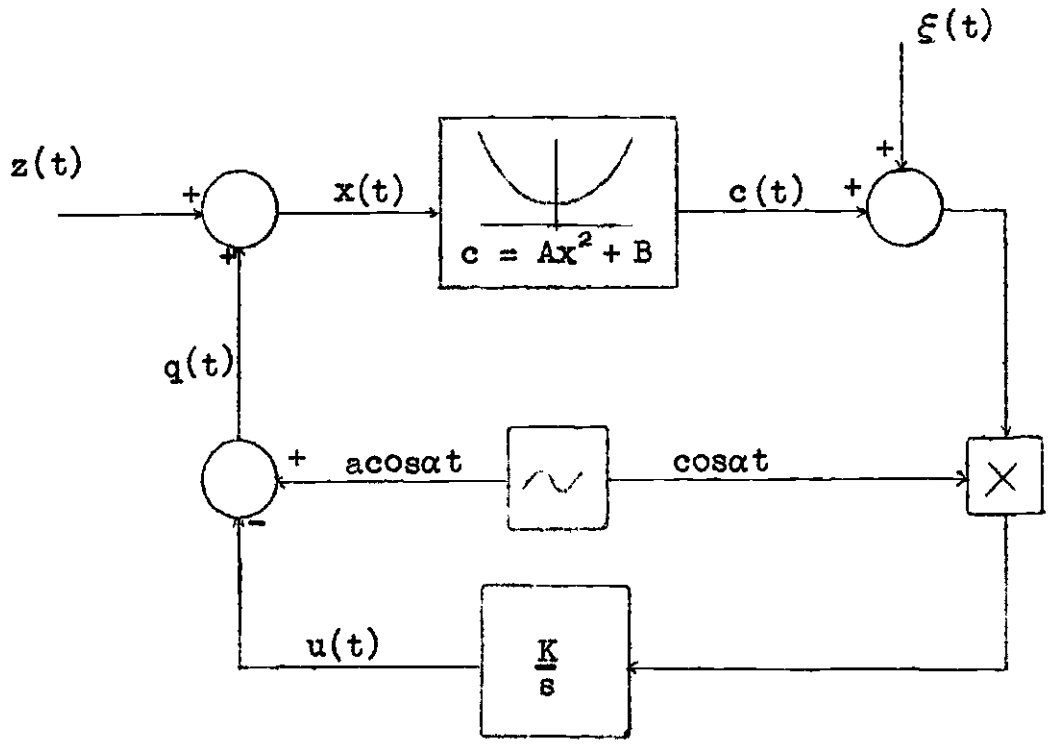

Fig. 2.4 Sinusoidal perturbation system with no lags

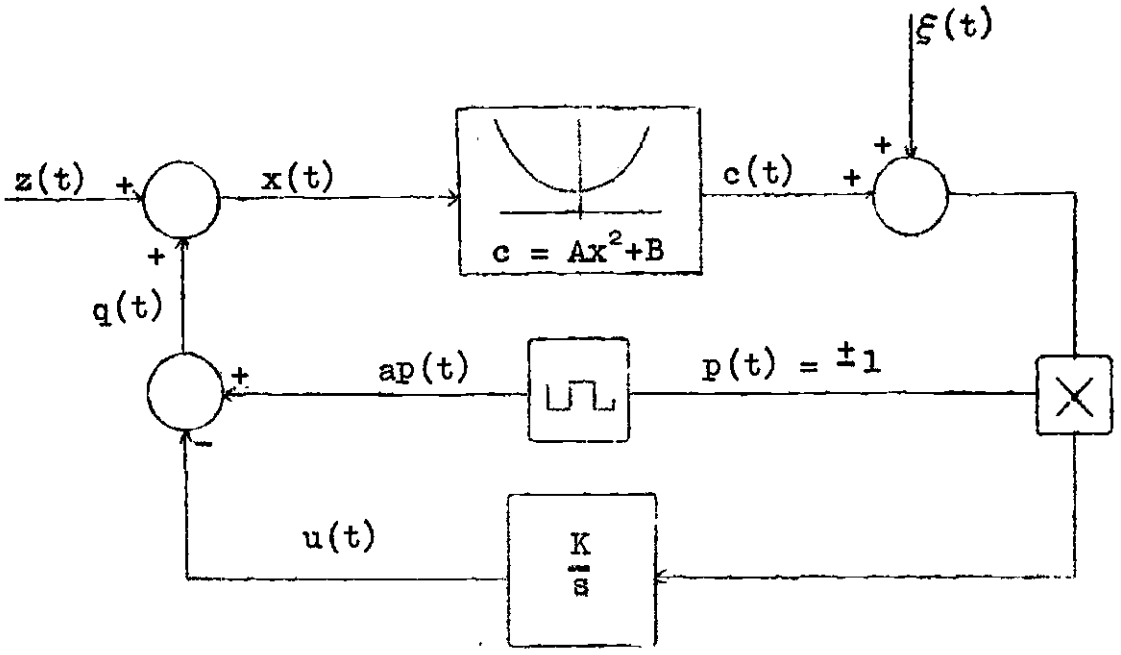

Fig. 2.5 Square wave perturbation system with no lags

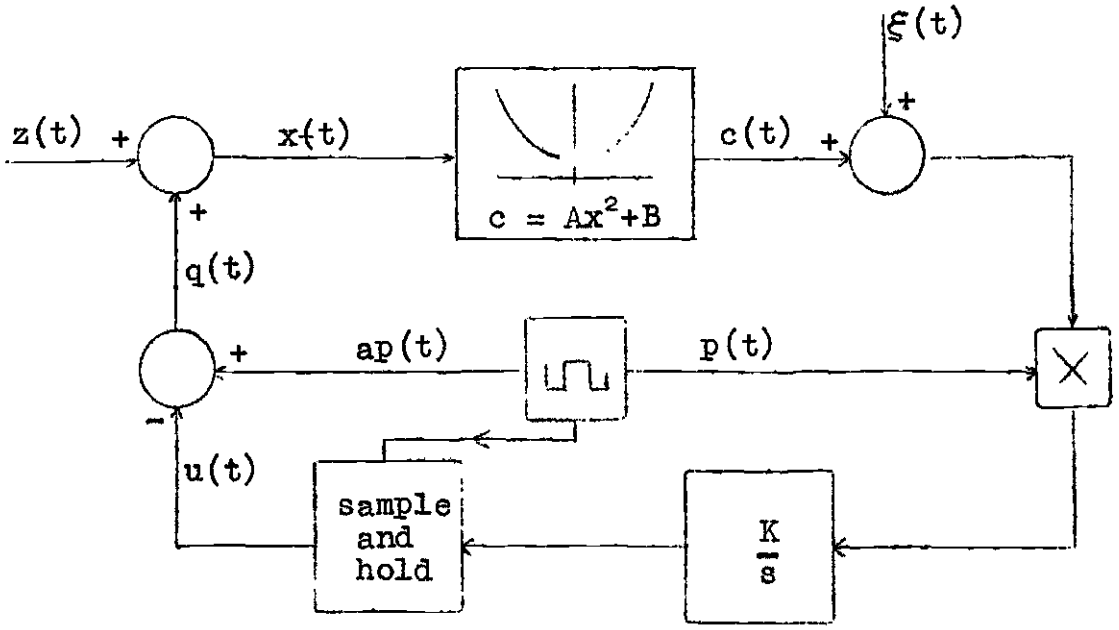

Fig. 2.6 Square wave perturbation system with sample and hold unit in the controller

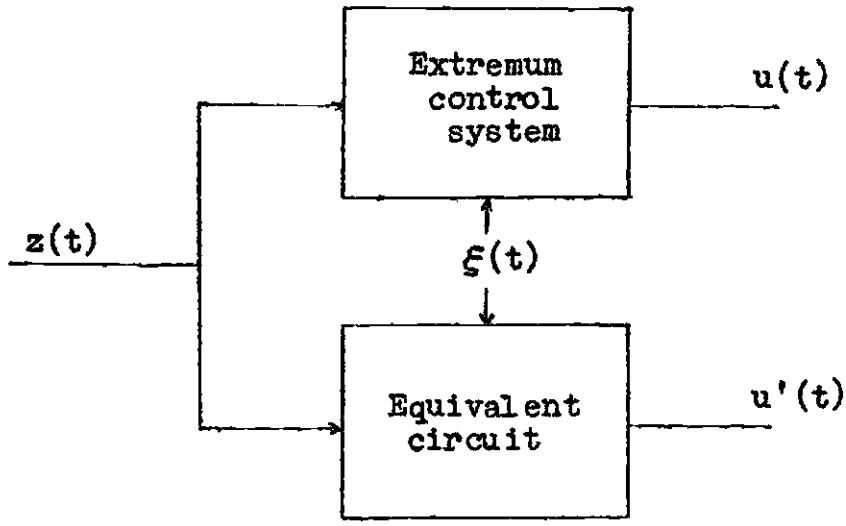

Fig. 3.1 Purpose of equivalent circuit

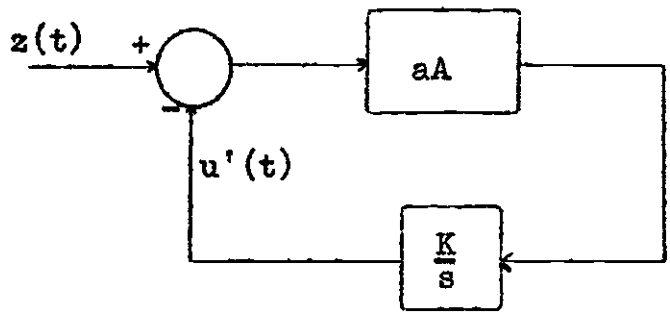

Fig. 3.2 Equivalent circuit for simplified system

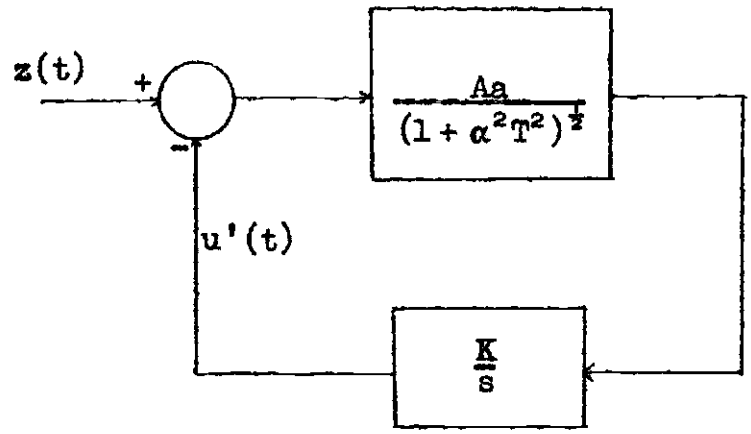

Fig. 3.3 Equivalent circuit for system with lag

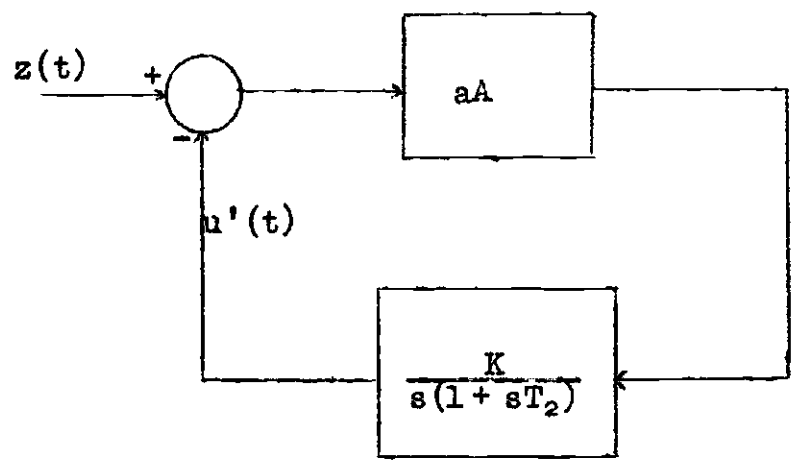

Fig. 3.4 Equivalent circuit for system with band-pass filter

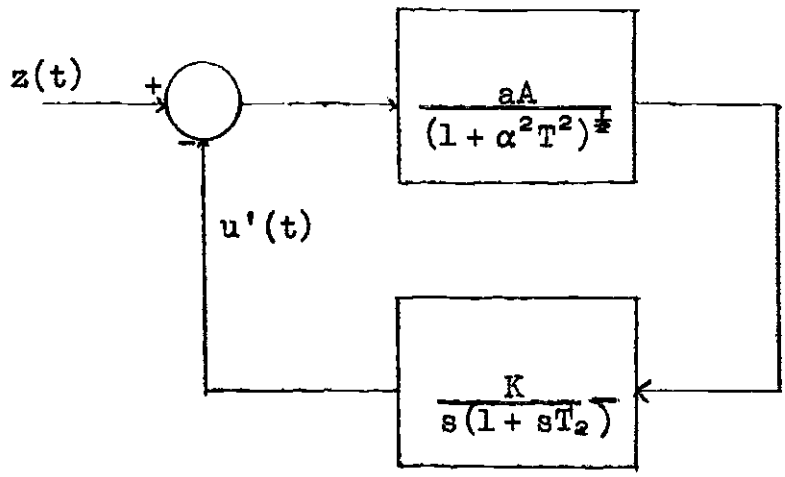

Fig. 3.5 Equivalent circuit for system with measurement lag and band-pass filter

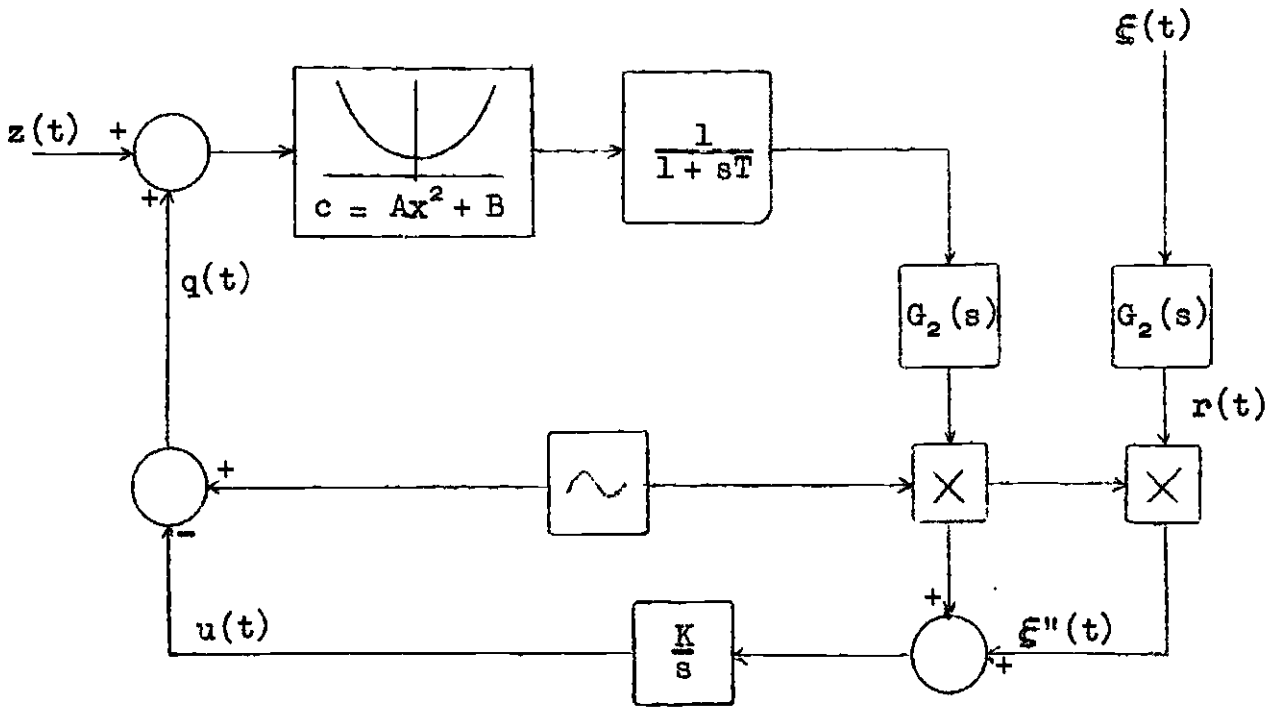

Fig. 3.6 System with equivalent noise ξ"(t) added at integrator input

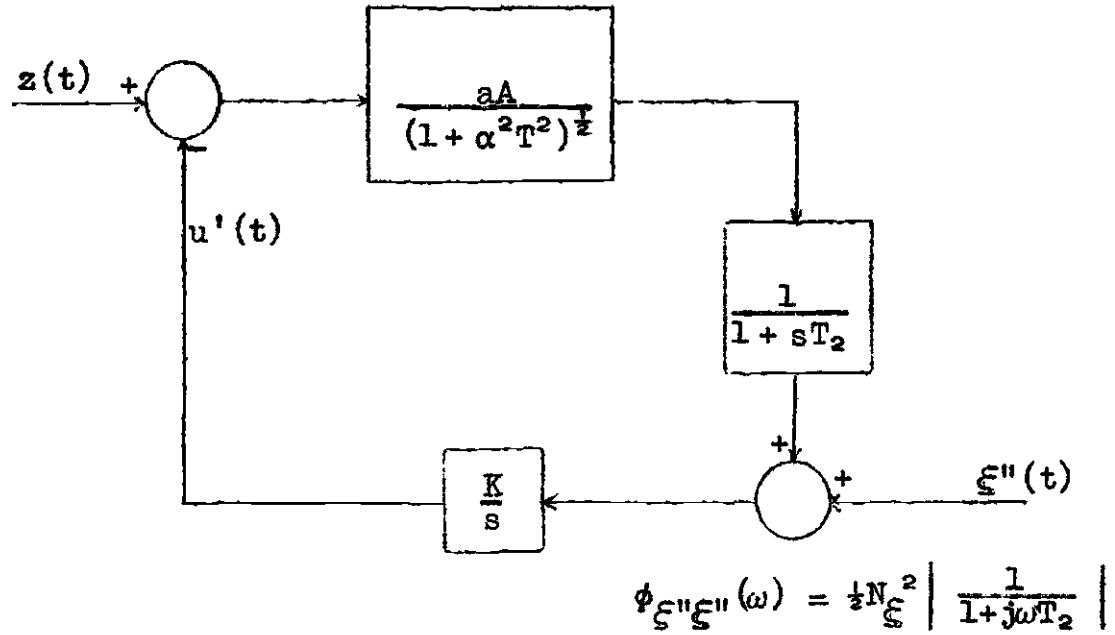

Fig. 3.7 Equivalent circuit with equivalent noise $\xi''(t)$ added at controller integrator input

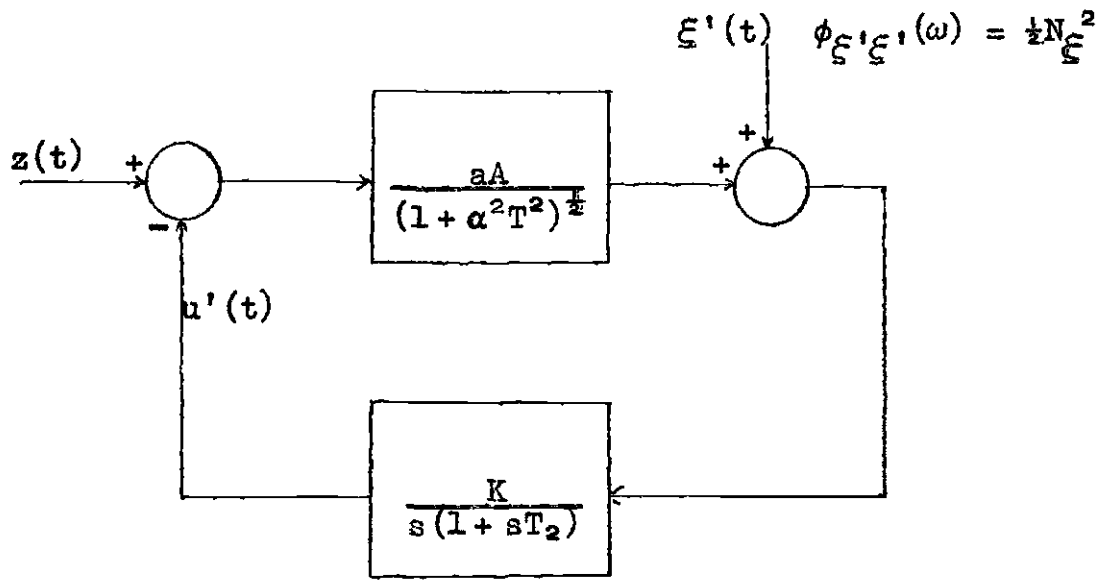

Fig. 3.8 Equivalent circuit with equivalent noise $\xi'(t)$

Fig. 3.9 Transient response of basic system

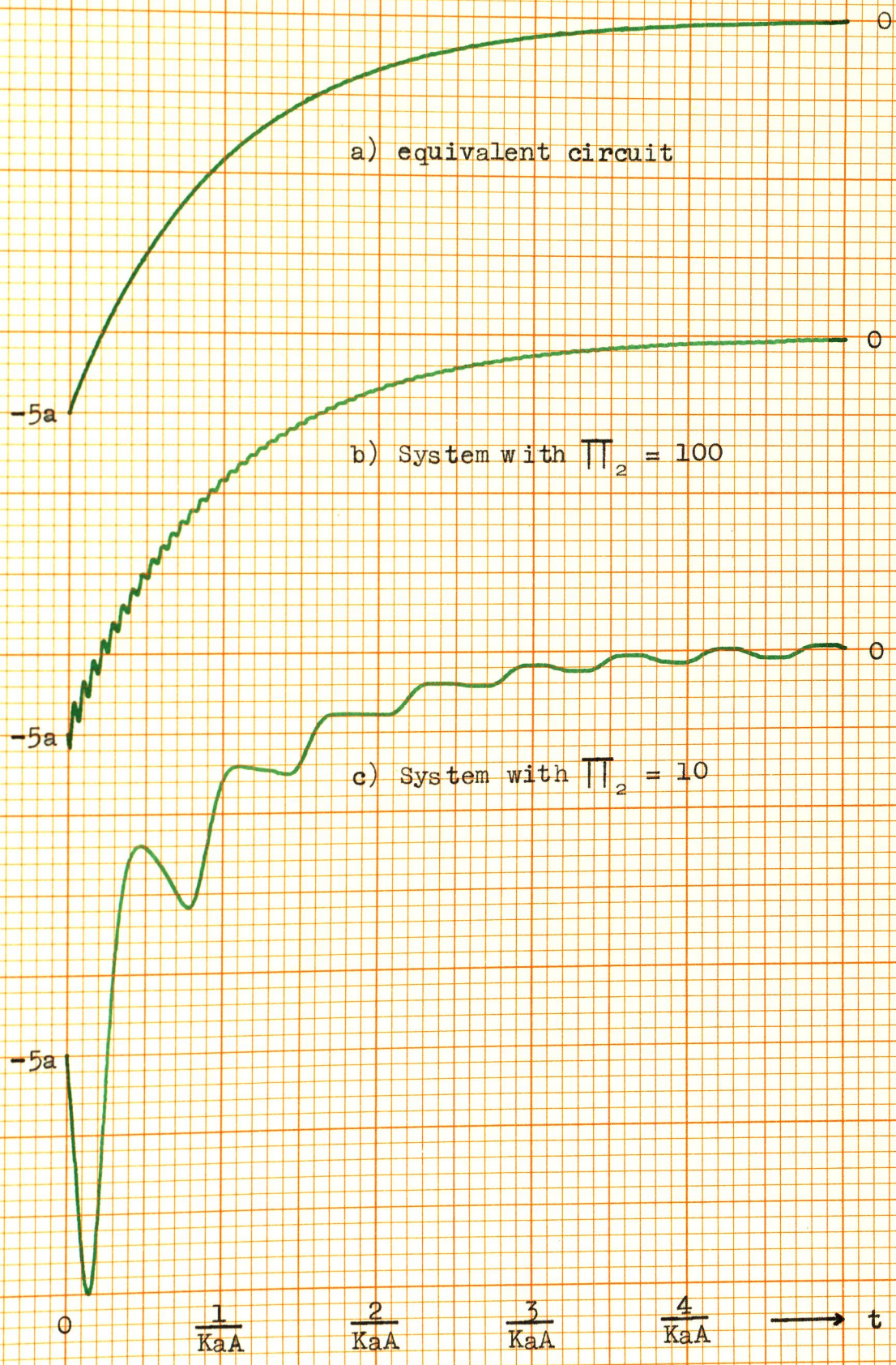

Fig. 3.10 Transient response of system with measurement lag

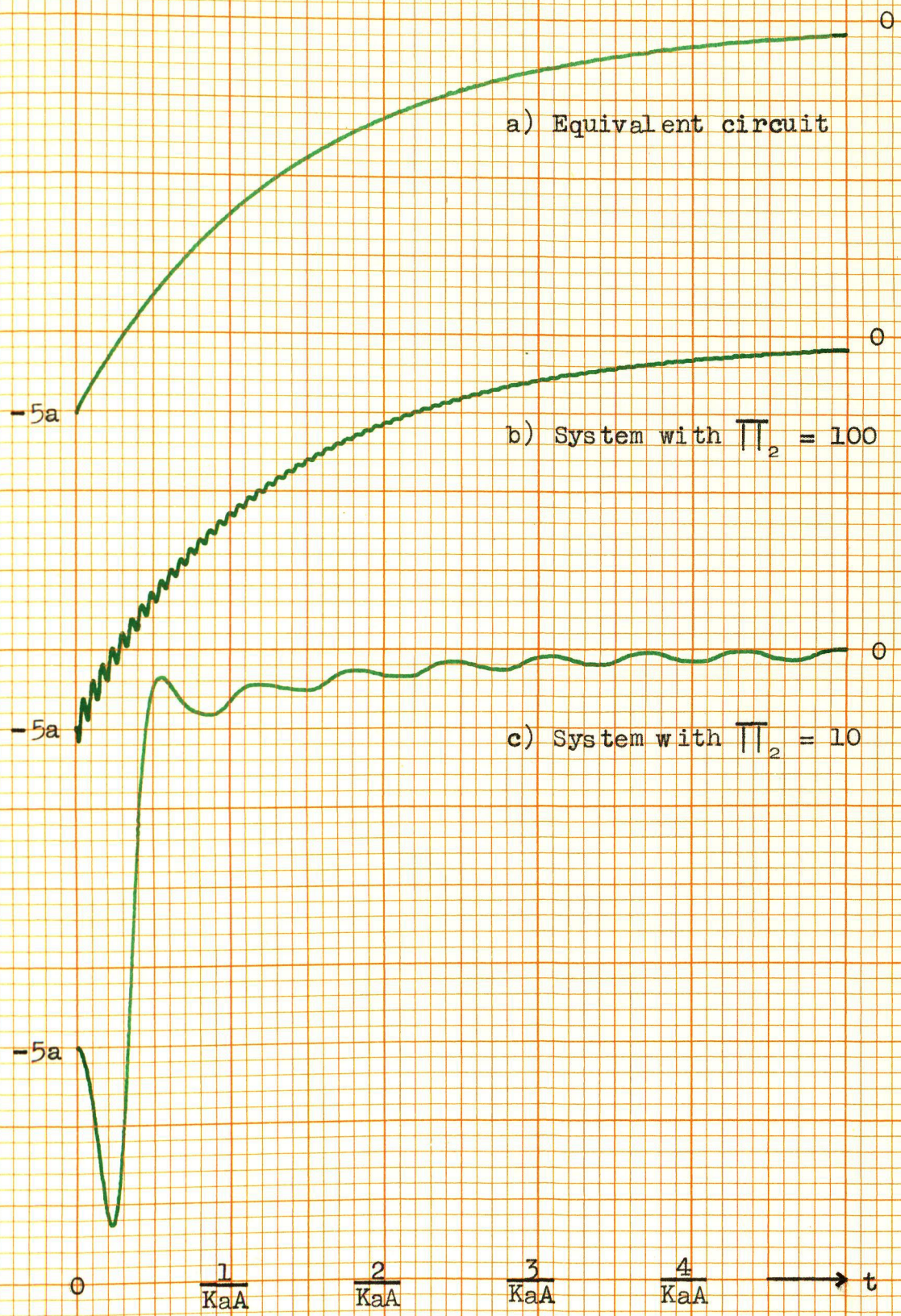

Fig. 3.11 Transient response of system with band-pass filter

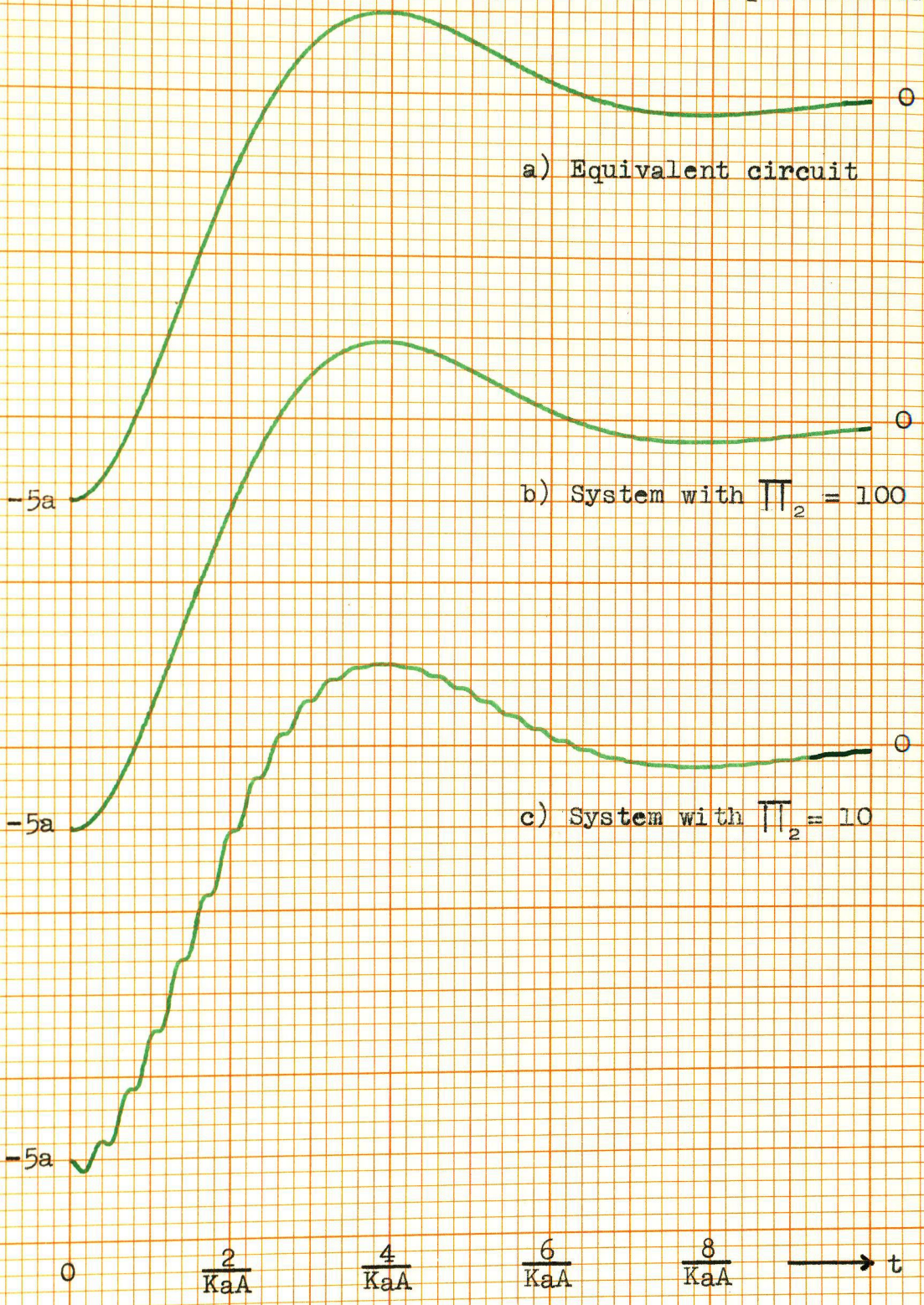

Fig. 3.12 Transient response of system with measurement lag and band-pass filter

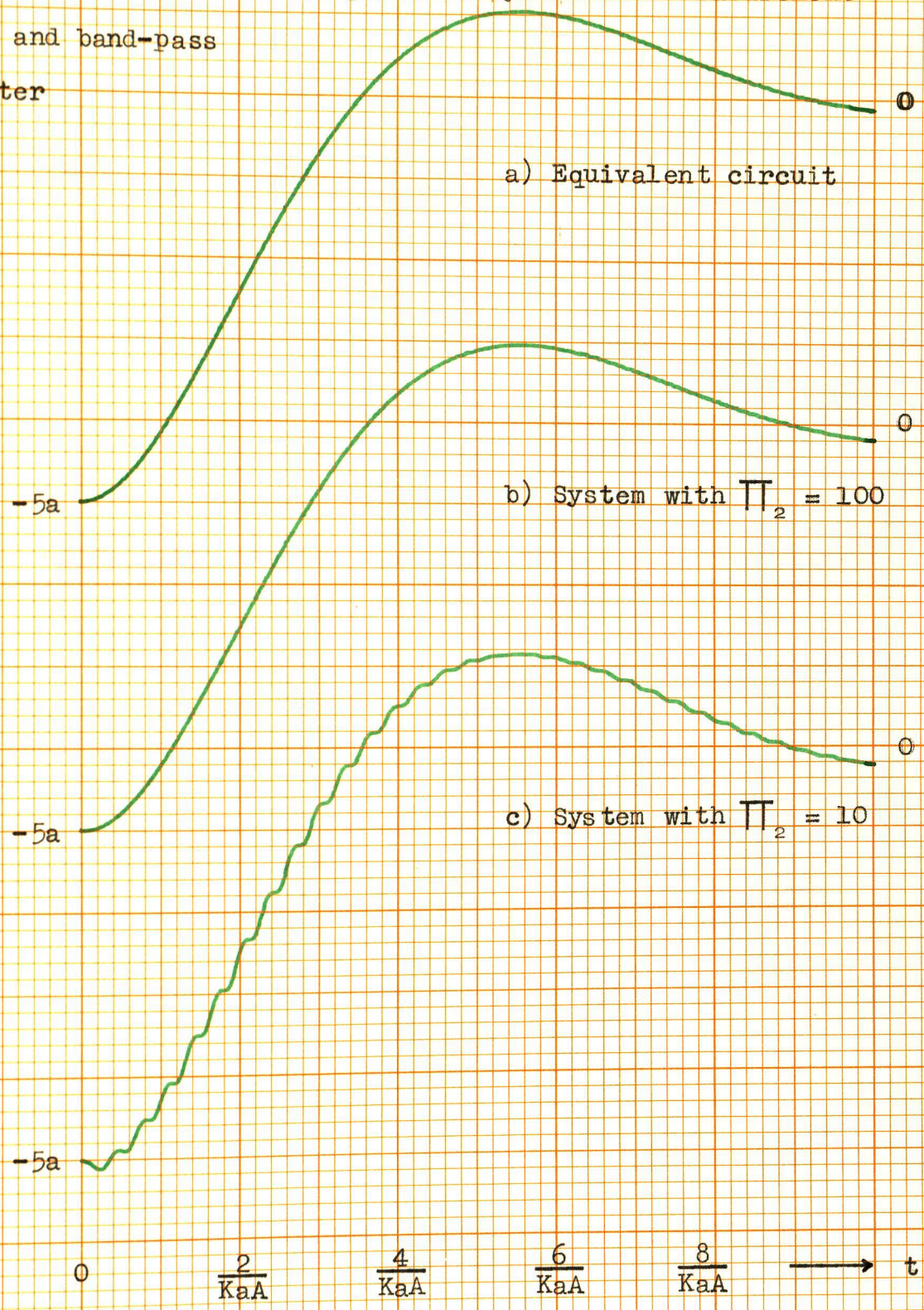

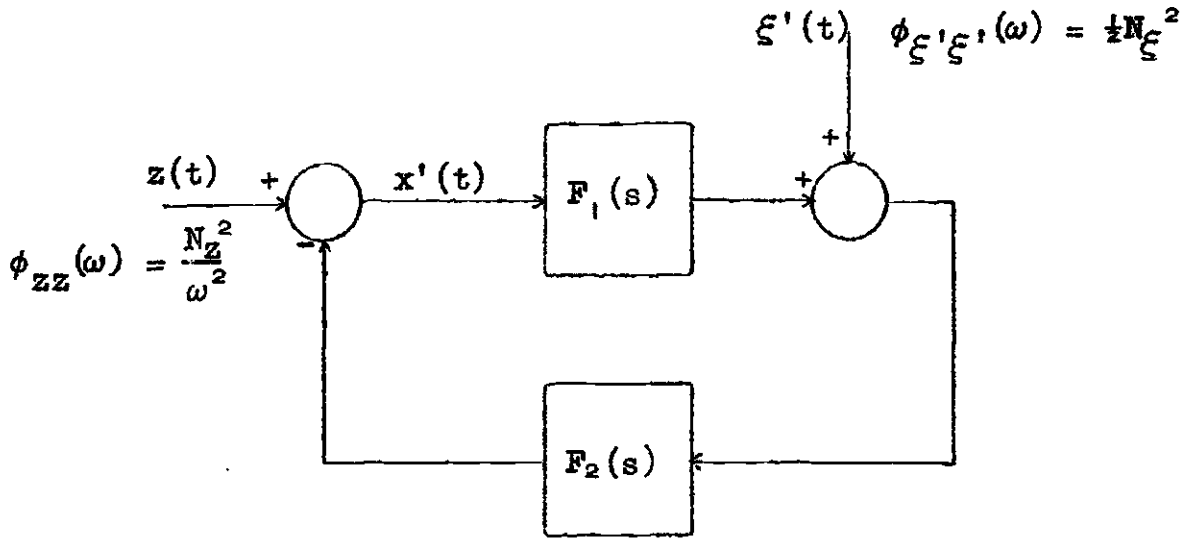

Fig. 3.13 Generalised form of equivalent circuits

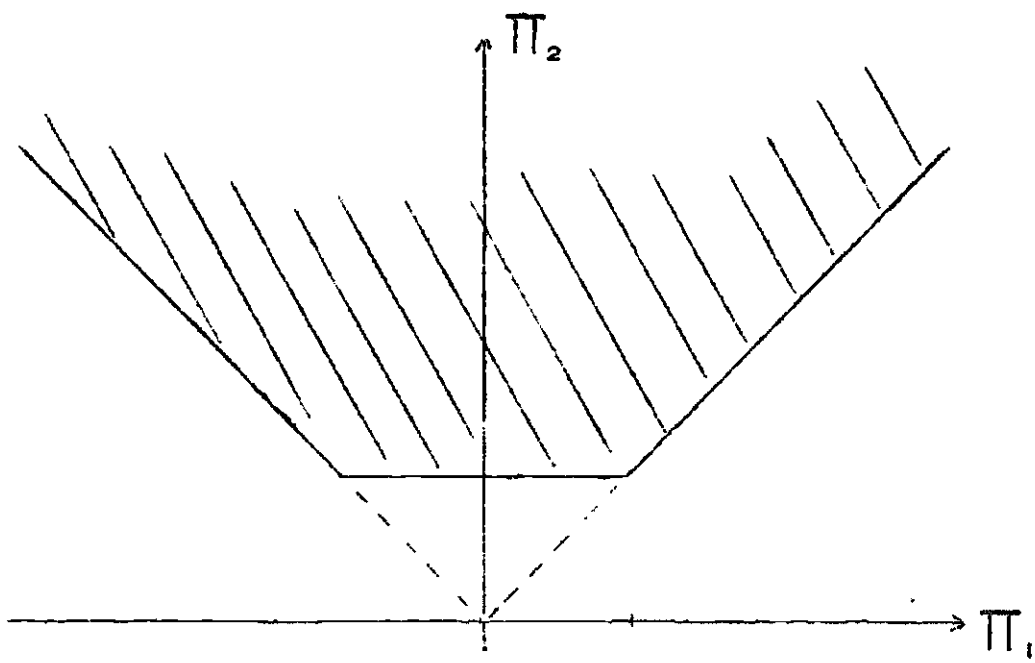

Fig. 4.1 Theoretical region of validity of equivalent circuit

Fig. 4.2

$Y(\Pi_1, \Pi_2)$ with Disturbances Only

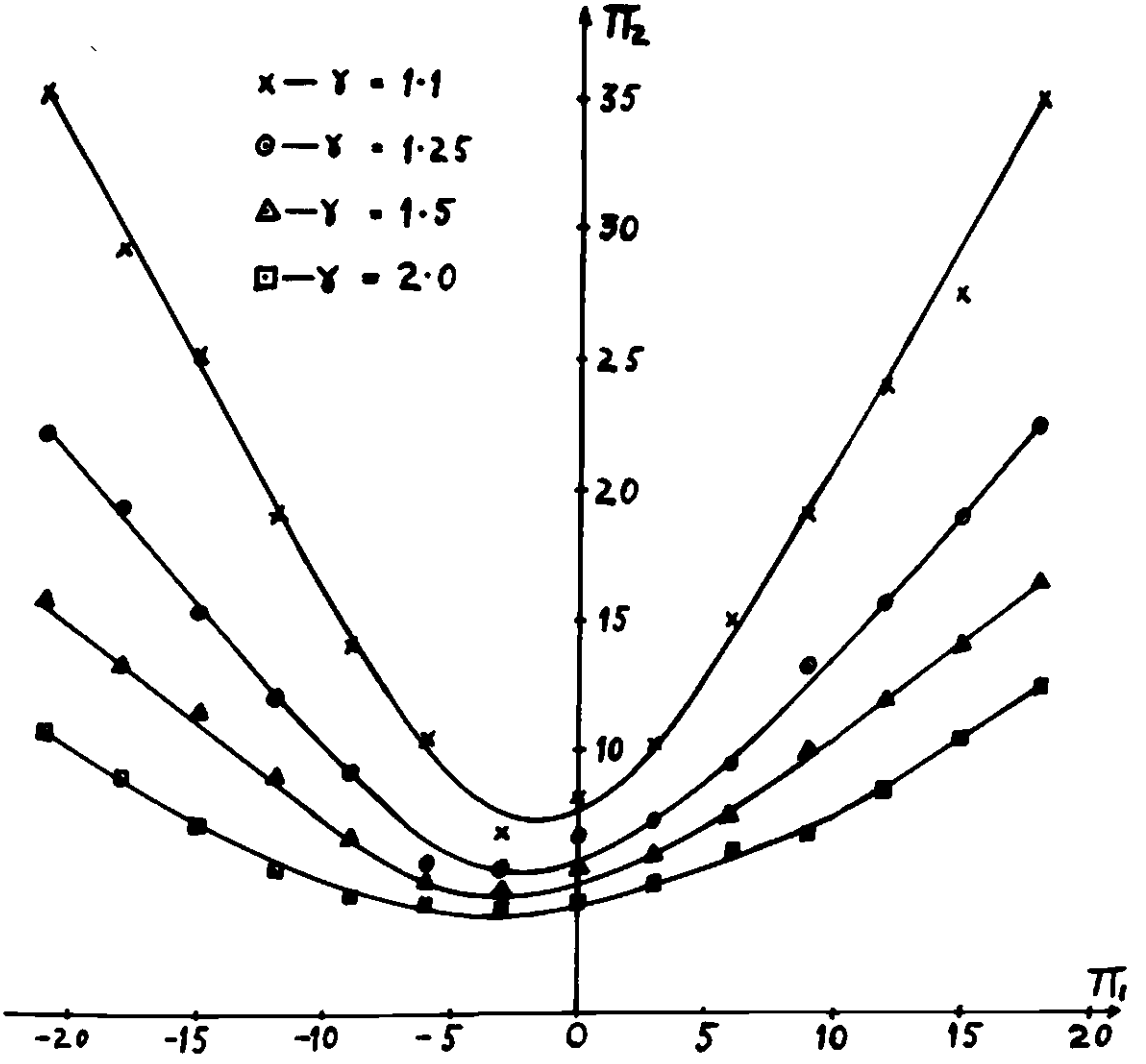

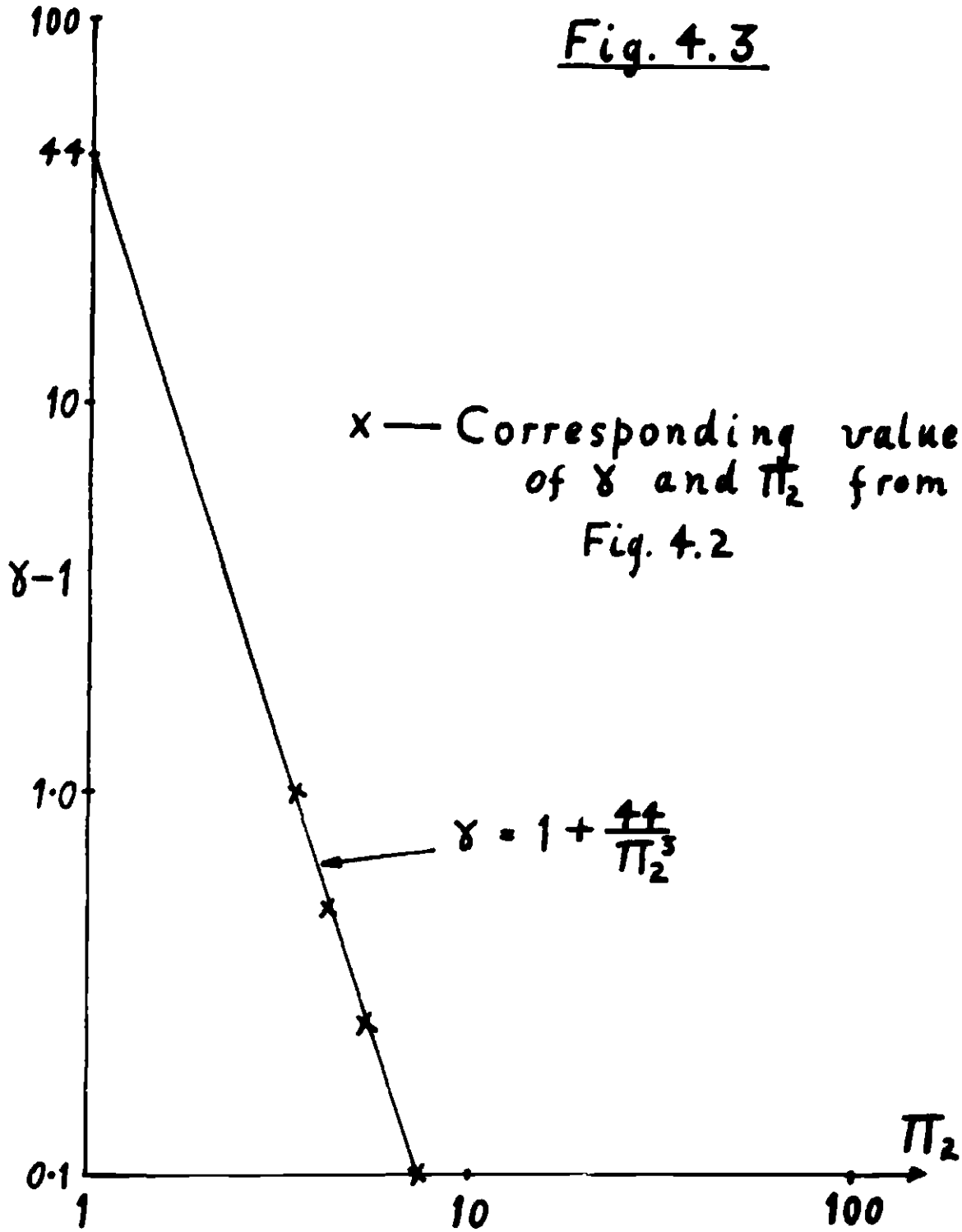
100
44
10
γ-1
1·0
0·1
1
10
100
Π_2
x — Corresponding values of γ and Π_2 from Fig. 4.2
$\gamma = 1 + \frac{44}{\Pi_2^3}$

Fig. 4.3

Fig. 4.4

$\gamma(\Pi_1, \Pi_2)$ with Noise Only

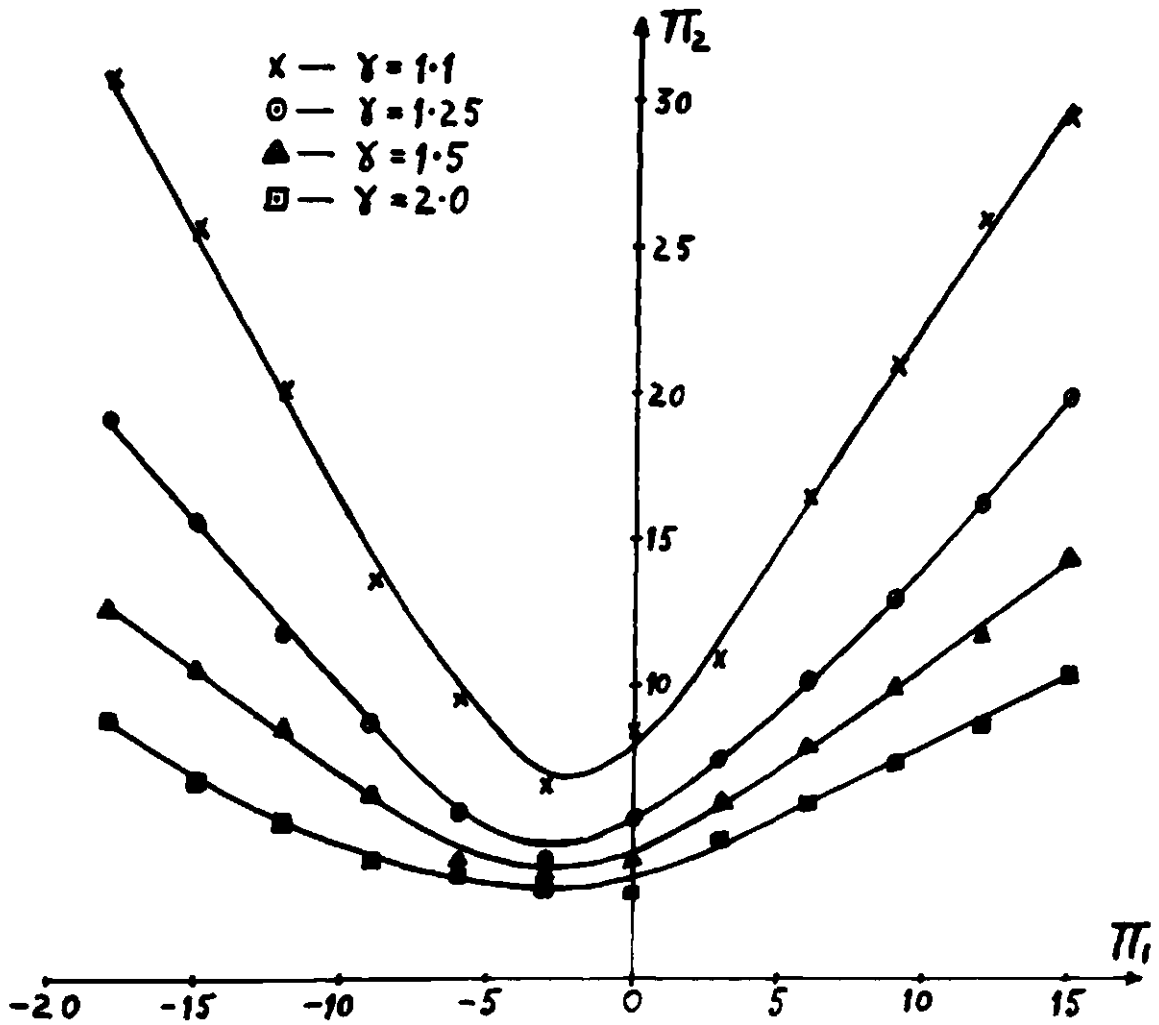

Fig. 4.5 Evolution of $\frac{u}{a}$ and $\frac{y}{Aa^2}$

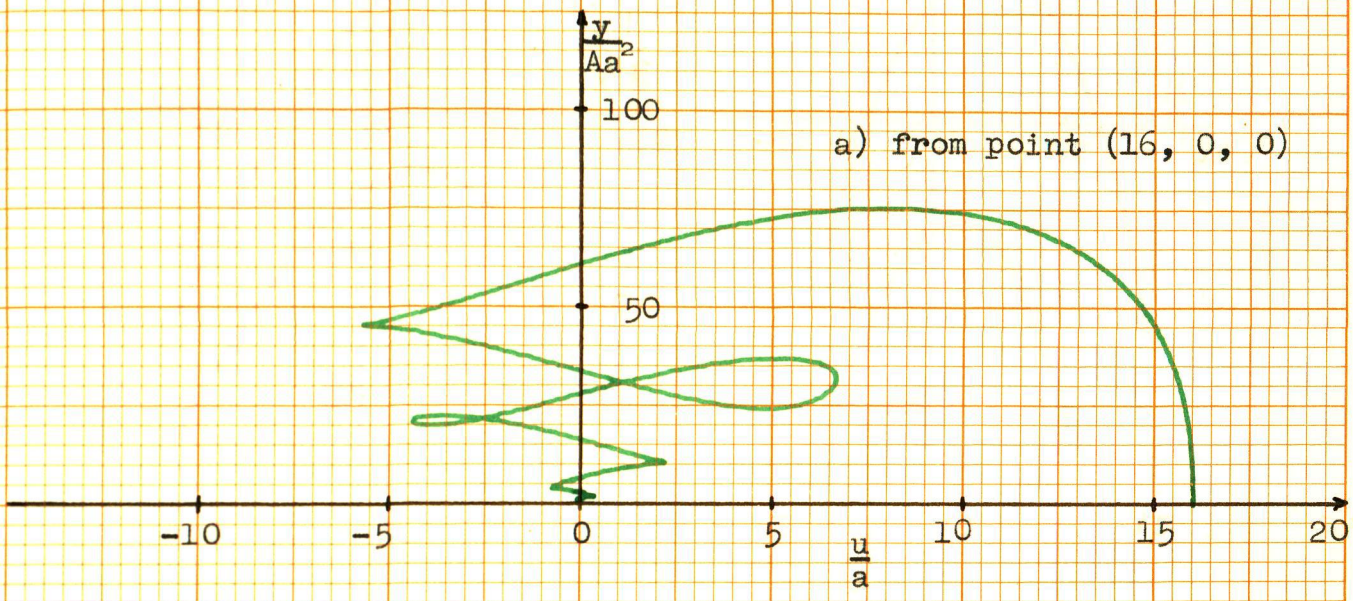

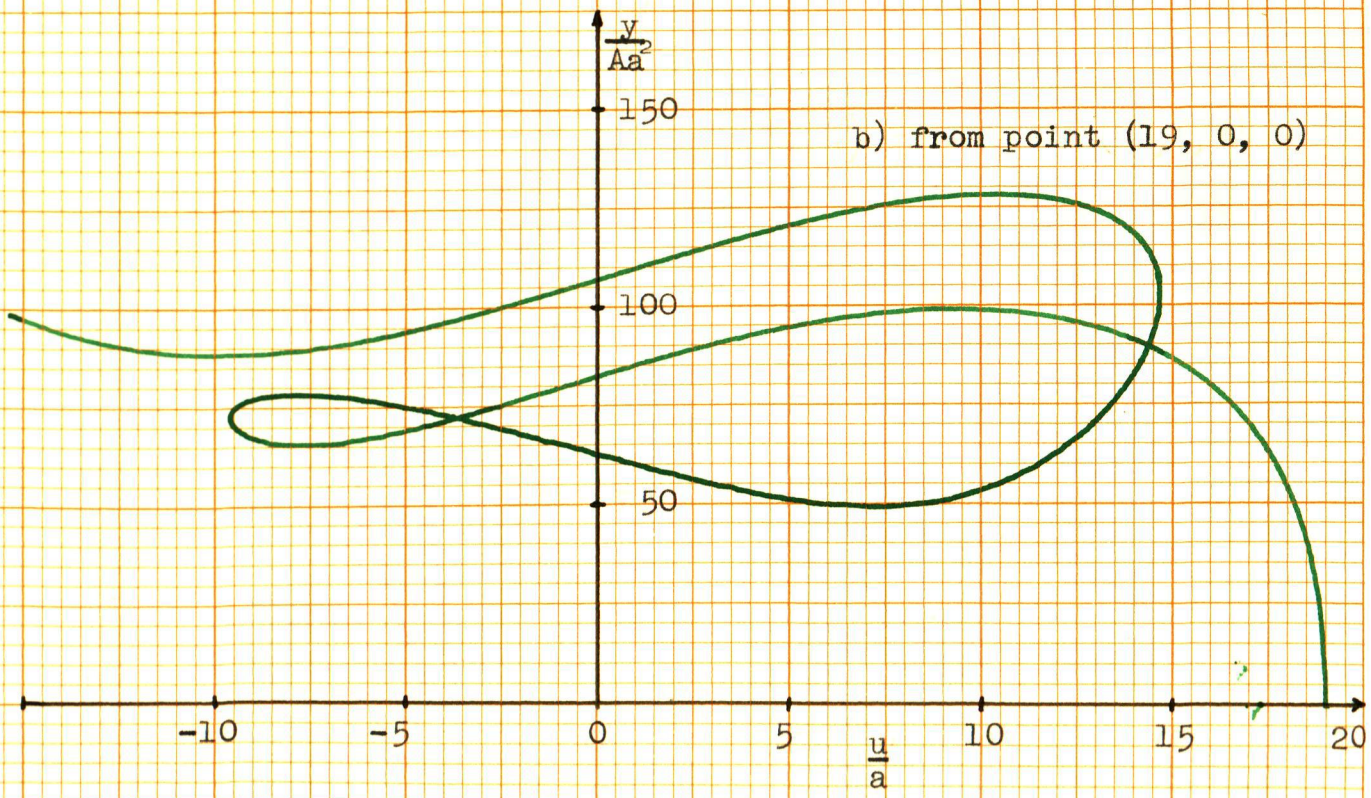

Fig. 4.6 Sections Through Stability Boundary

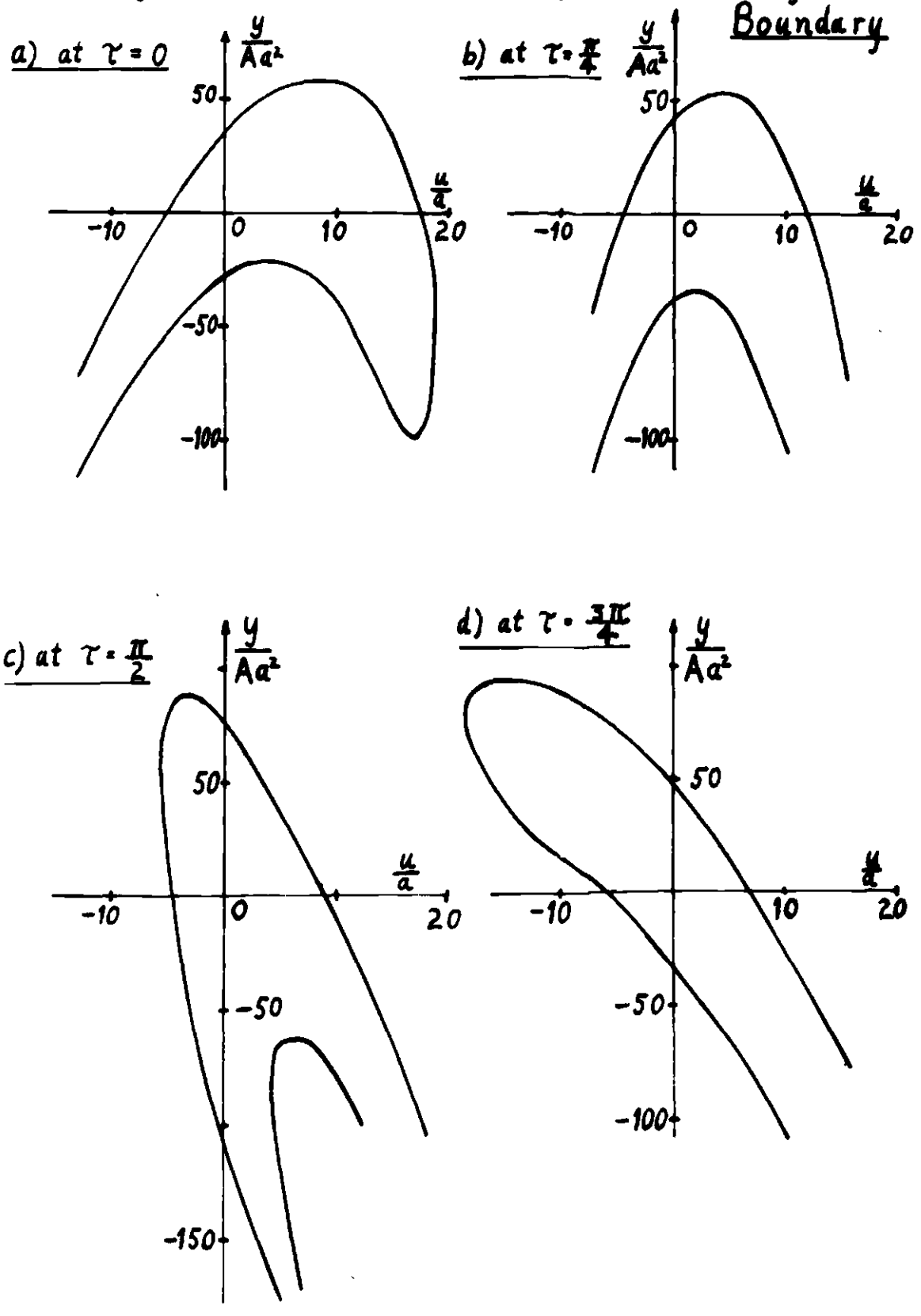

Fig. 5.1a

Π_e v. Π_p For Complete System

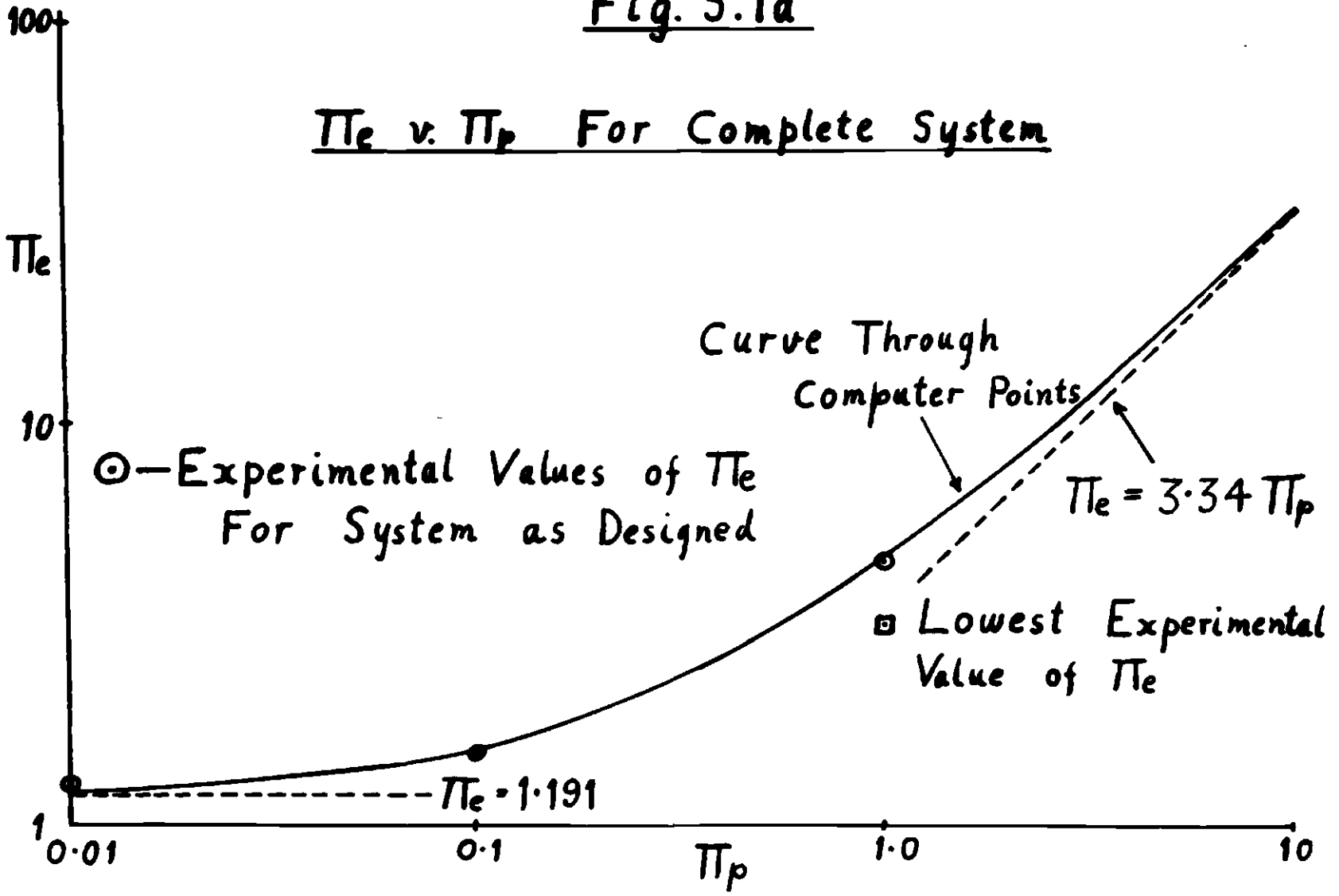

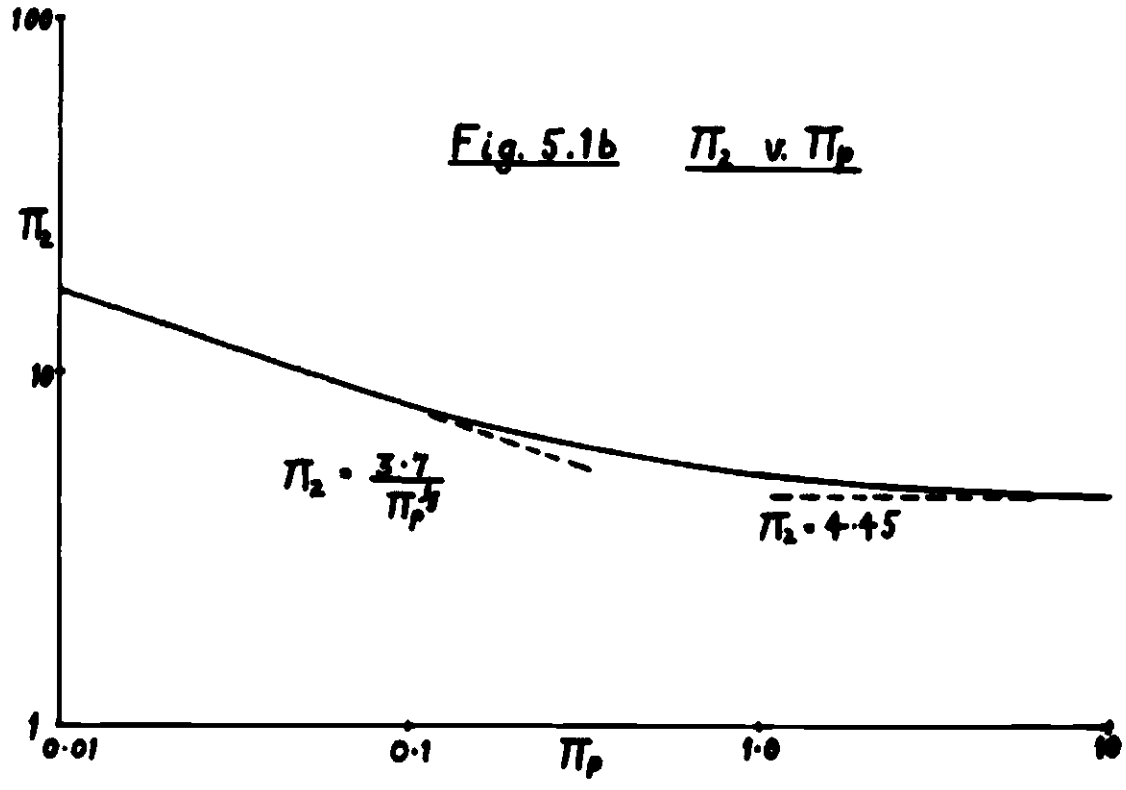

Fig. 5.1b Π_2 v. Π_p

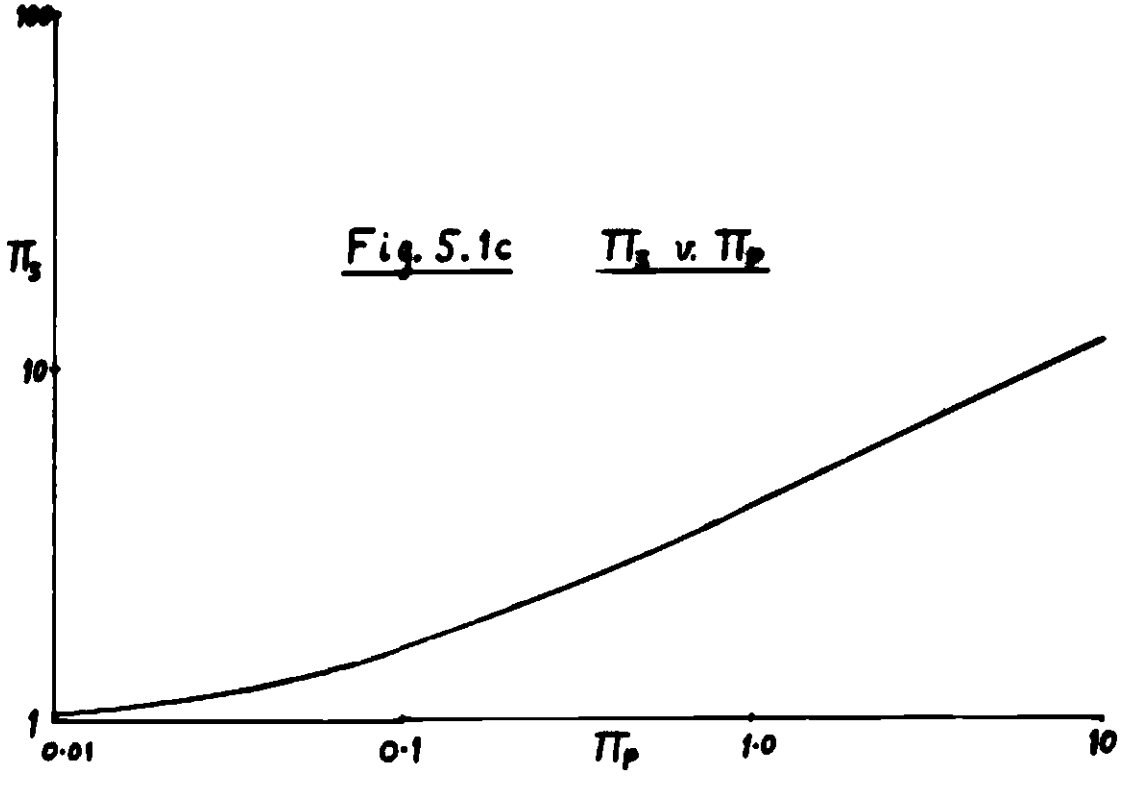

Fig. 5.1c Π_3 v. Π_p

Fig 5.1d Π_t v. Π_p

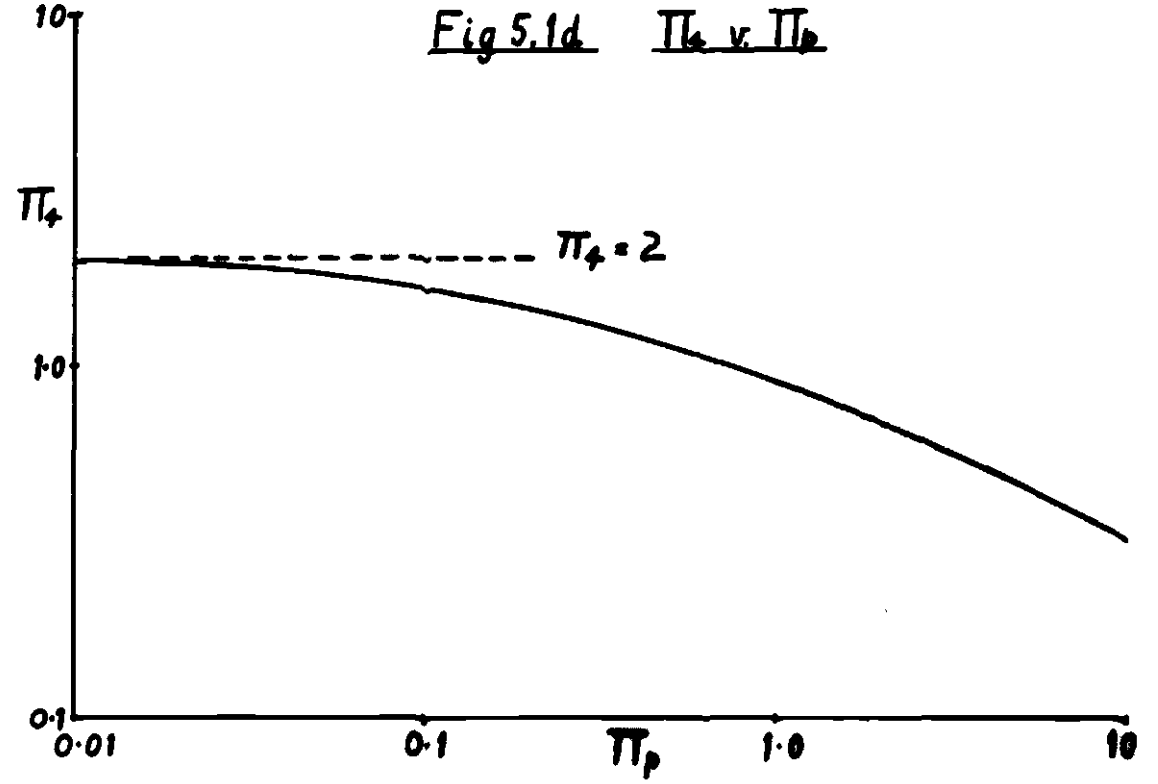

Fig. 5.1e $\propto T$ v. Π_p

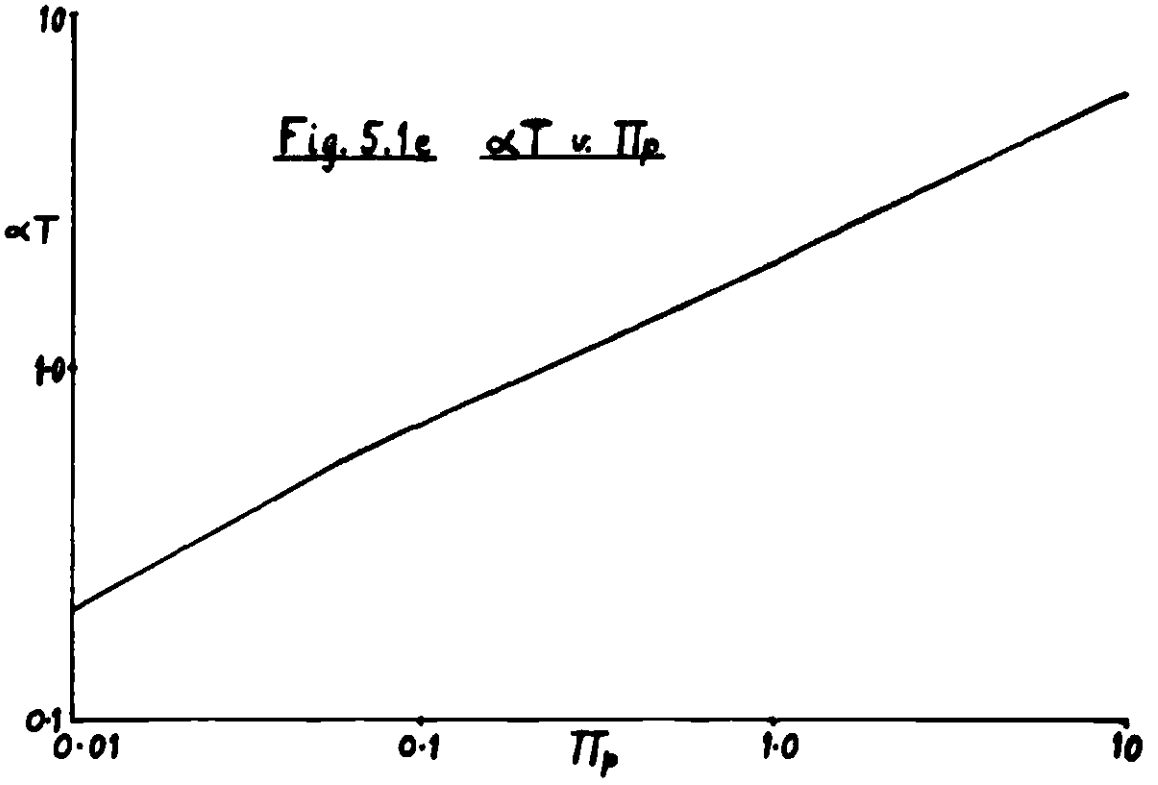

Fig.5.1f γ v. Π_p

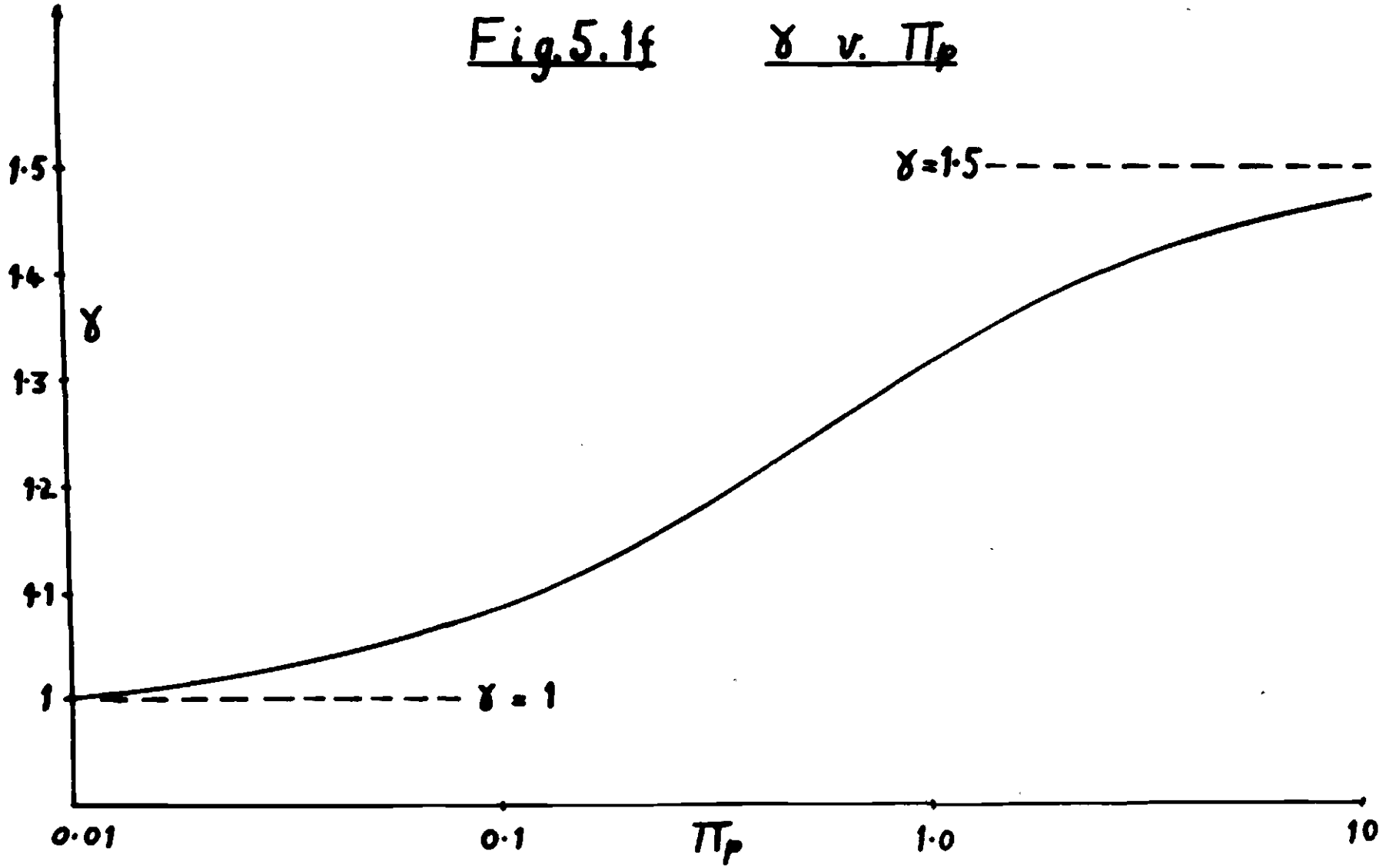

Fig. 7.1

Π_e v. Π_α Sine Wave Perturbation

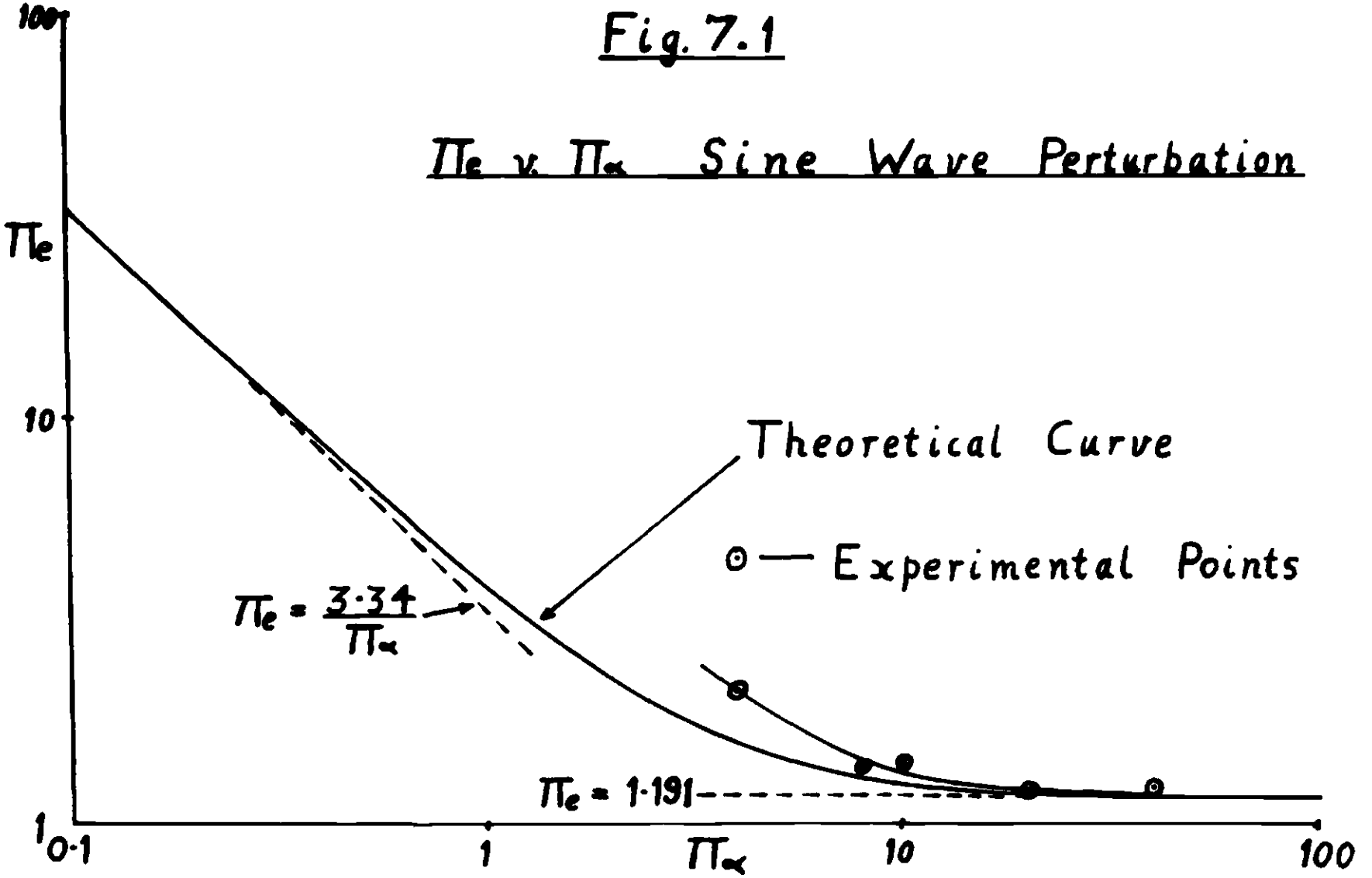

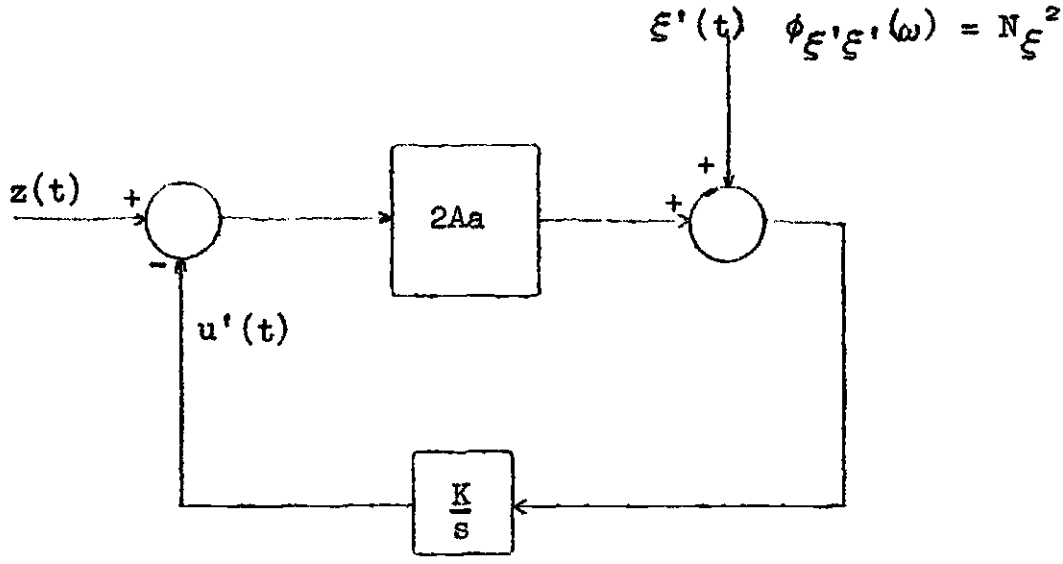

Fig. 7.2 Equivalent circuit for system with square wave perturbation

Fig. 7.3

$\gamma(\pi_1, \pi_2)$ Square Wave Perturbation

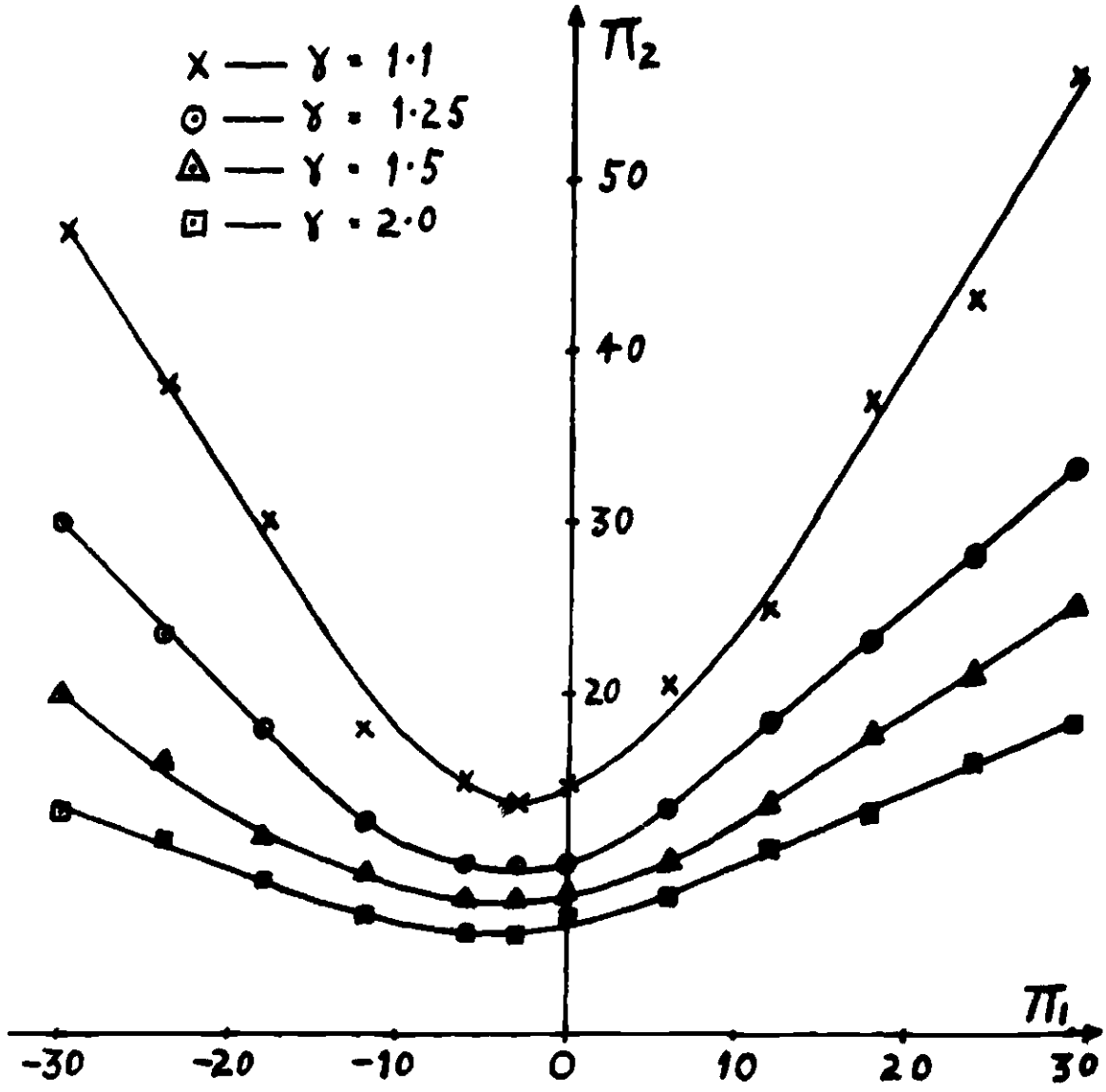

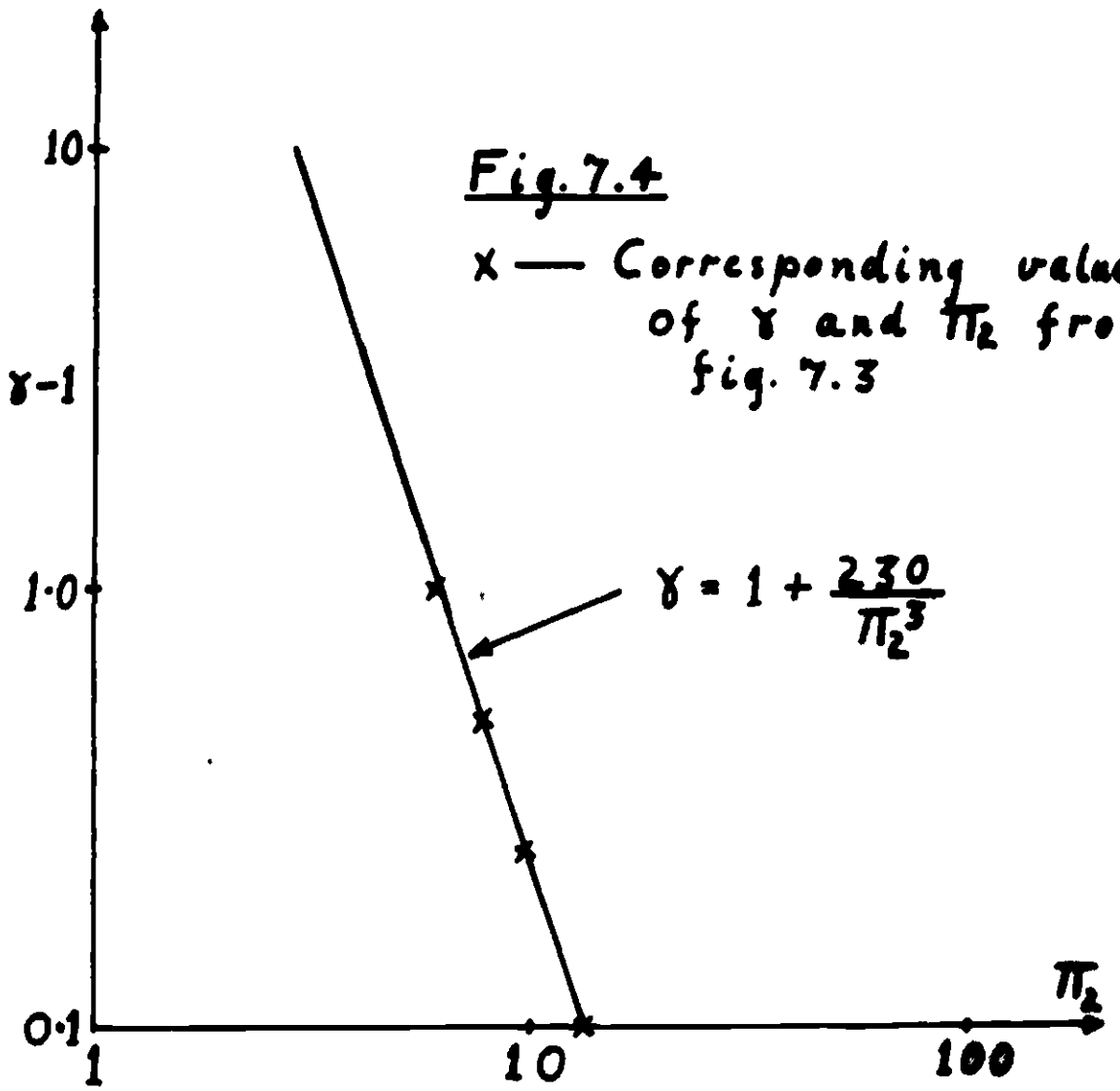

Fig. 7.4

× — Corresponding values of γ and π_2 from fig. 7.3

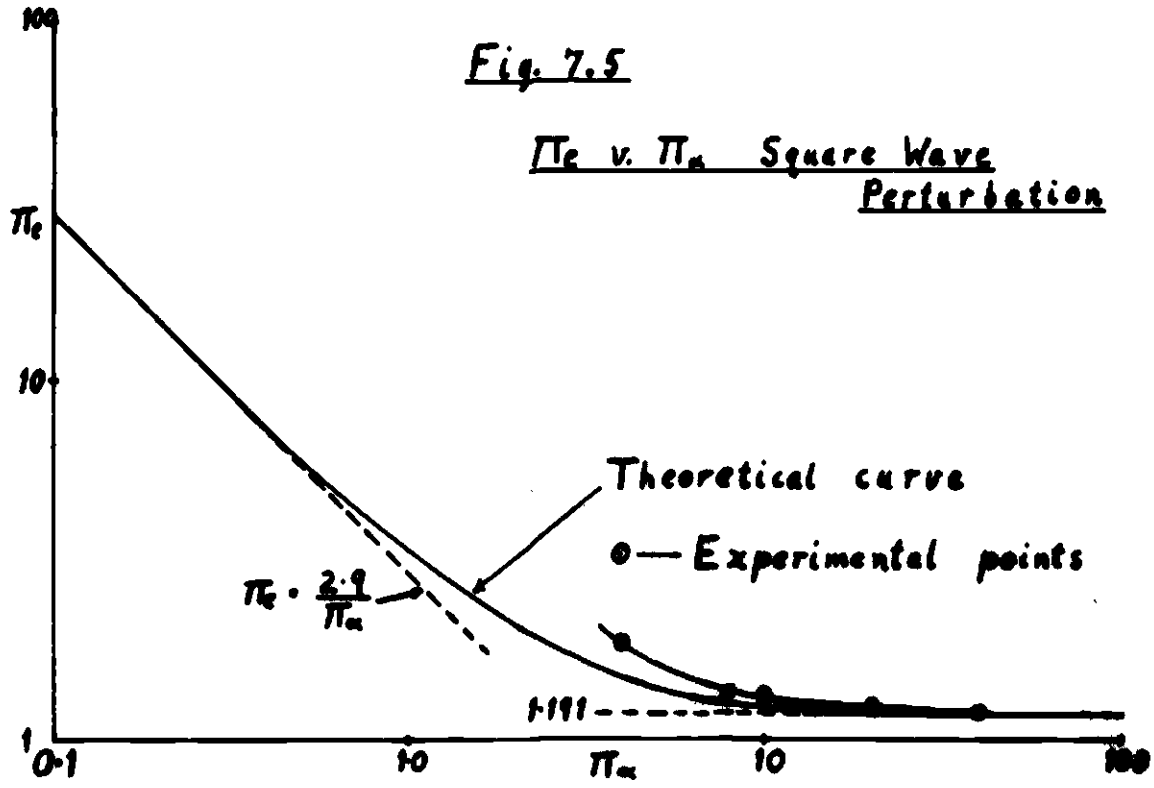

Fig. 7.5

Π_e v. Π_α Square Wave Perturbation

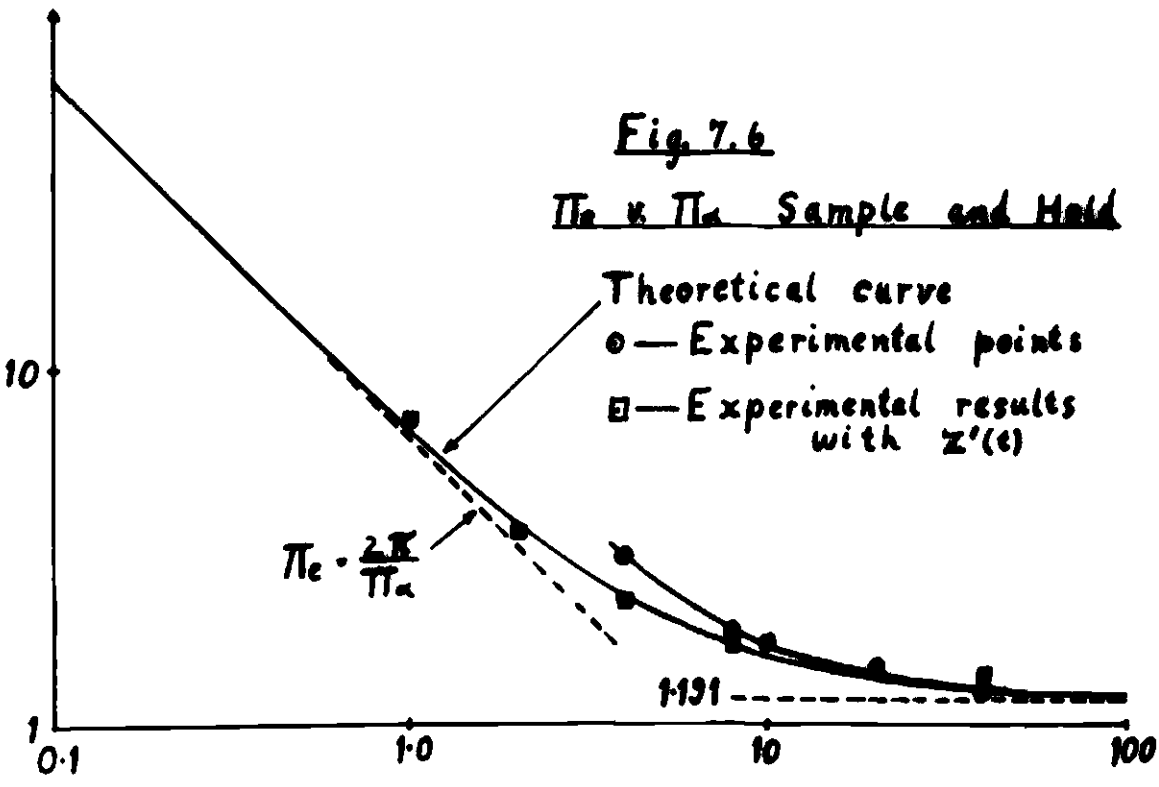

Fig. 7.6

Π_e v. Π_α Sample and Hold

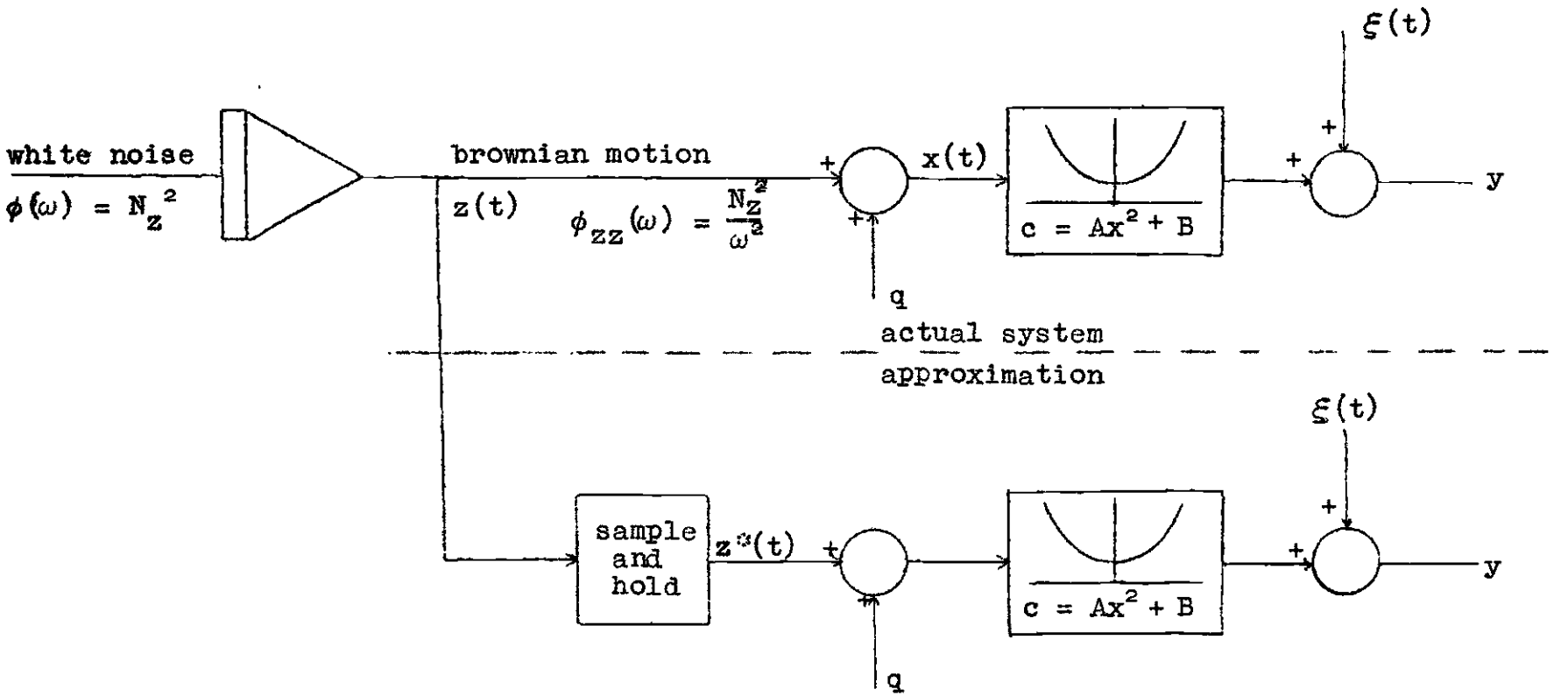

Fig. 7.7 Approximation of z(t) by $z^*(t)$

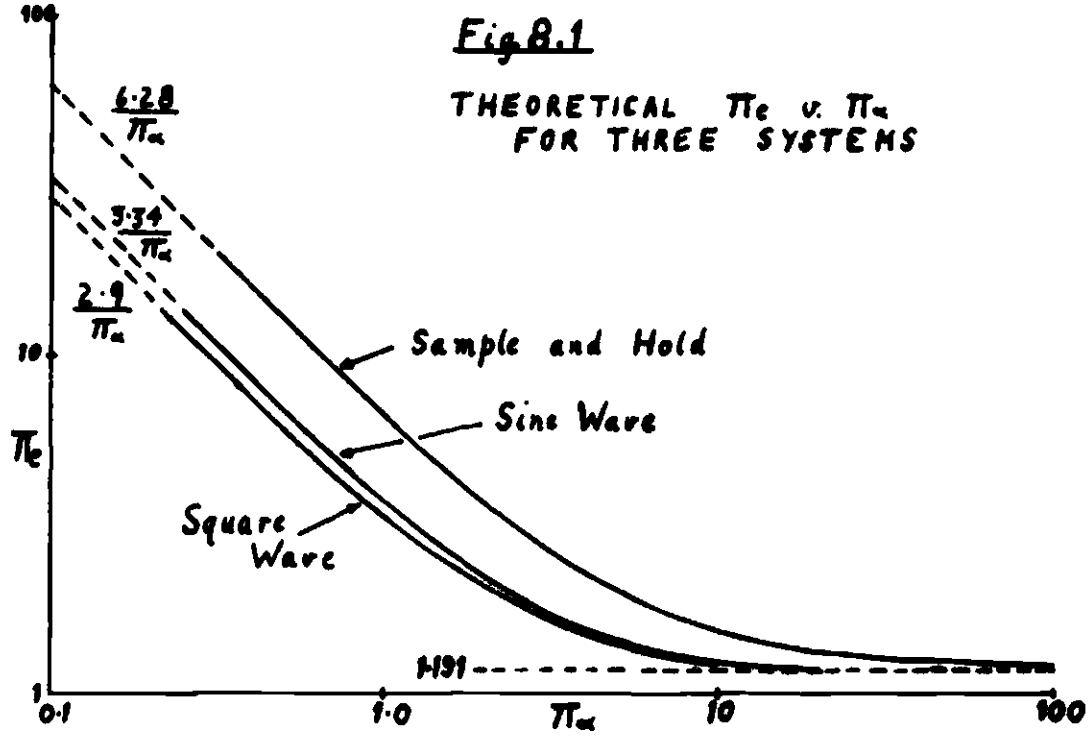
Fig. 8.1
THEORETICAL π_e v. π_α
FOR THREE SYSTEMS
100
10
1
π_e
$\frac{6.28}{\pi_\alpha}$
$\frac{3.34}{\pi_\alpha}$
$\frac{2.9}{\pi_\alpha}$
Sample and Hold
Sine Wave
Square Wave
1·191
0·1
1·0
π_α
10
100

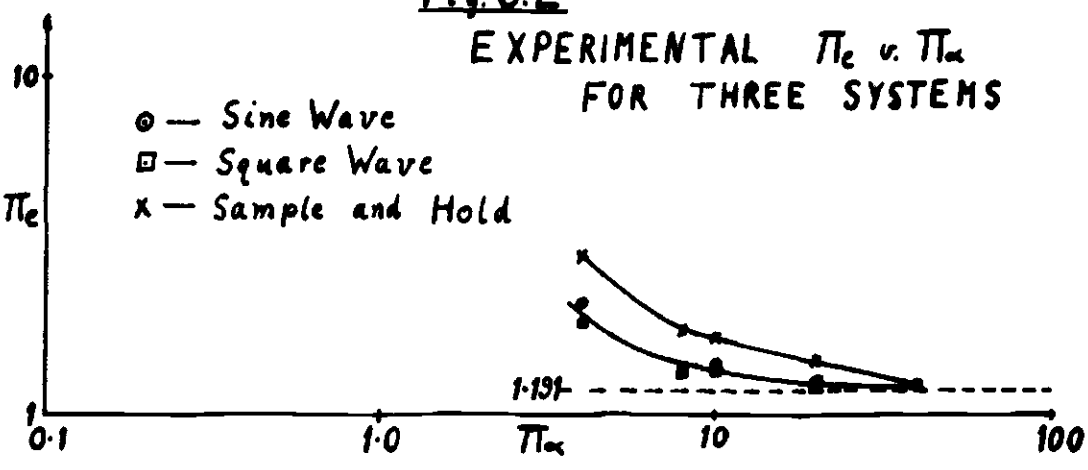
Fig. 8.2
EXPERIMENTAL π_e v. π_α
FOR THREE SYSTEMS
10
1
π_e
⊙ — Sine Wave
⊡ — Square Wave
x — Sample and Hold
1·191
0·1
1·0
π_α
10
100

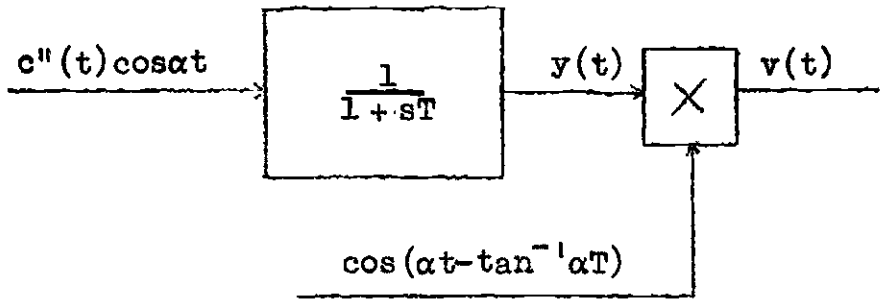

Fig. A1.1 Demodulation of low pass filtered signal

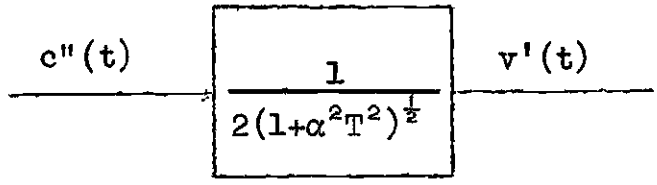

Fig. A1.2 Equivalent circuit for fig. A1.1

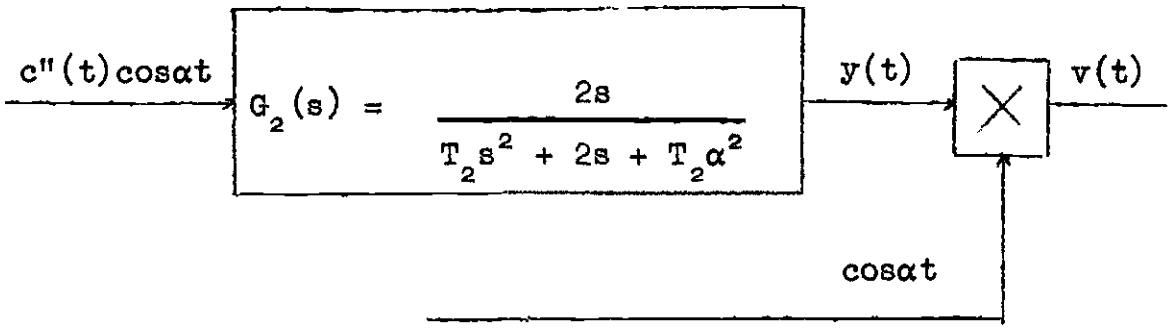

Fig. A2.1 Demodulation of band-pass filtered signal

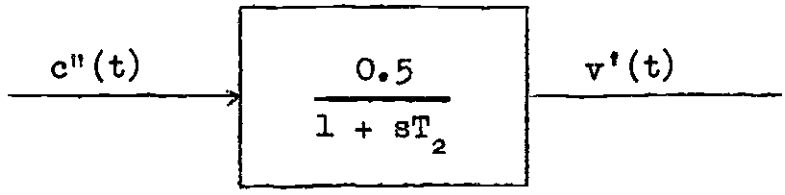

Fig. A2.2 Equivalent circuit for fig. A2.1

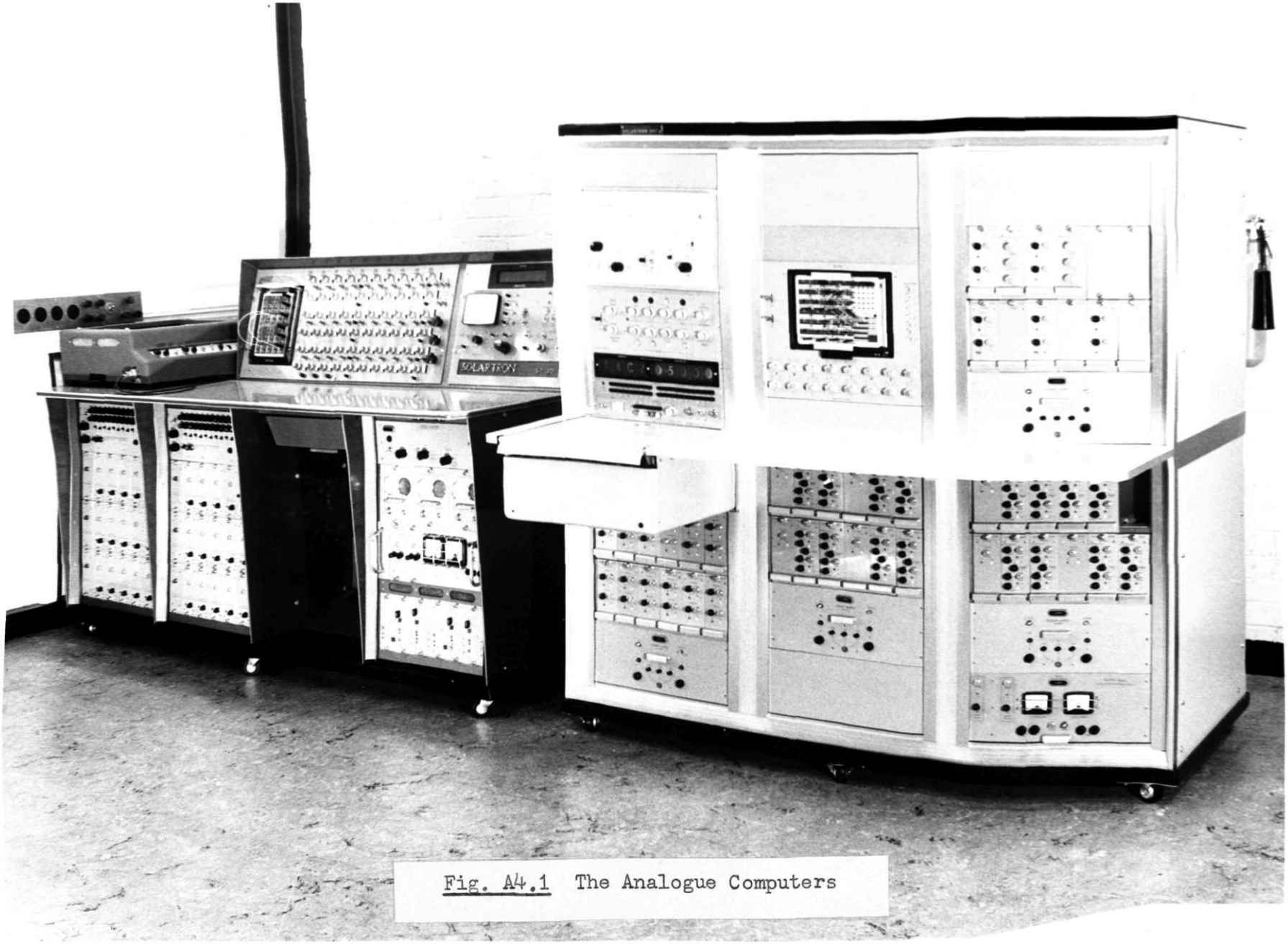

Fig. A4.1 The Analogue Computers

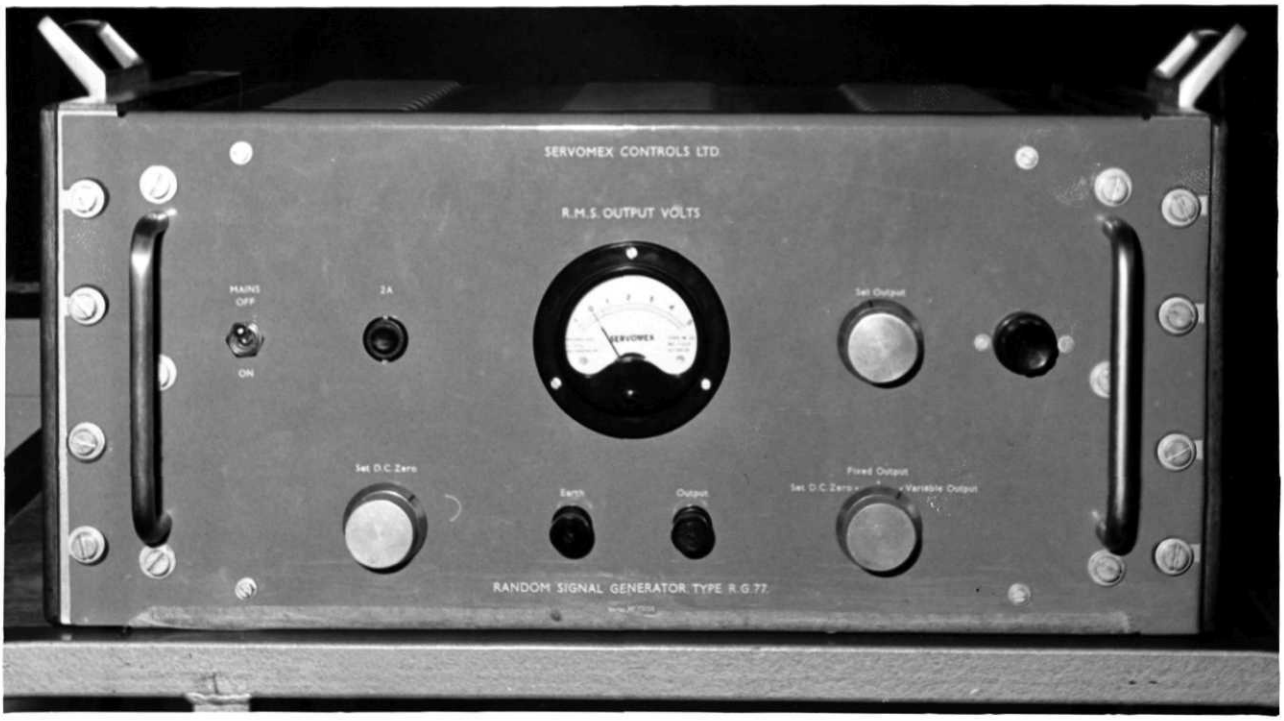

Fig. A4.2 Disturbance Noise Generator

Fig. A4.3

Measurement Noise Generator

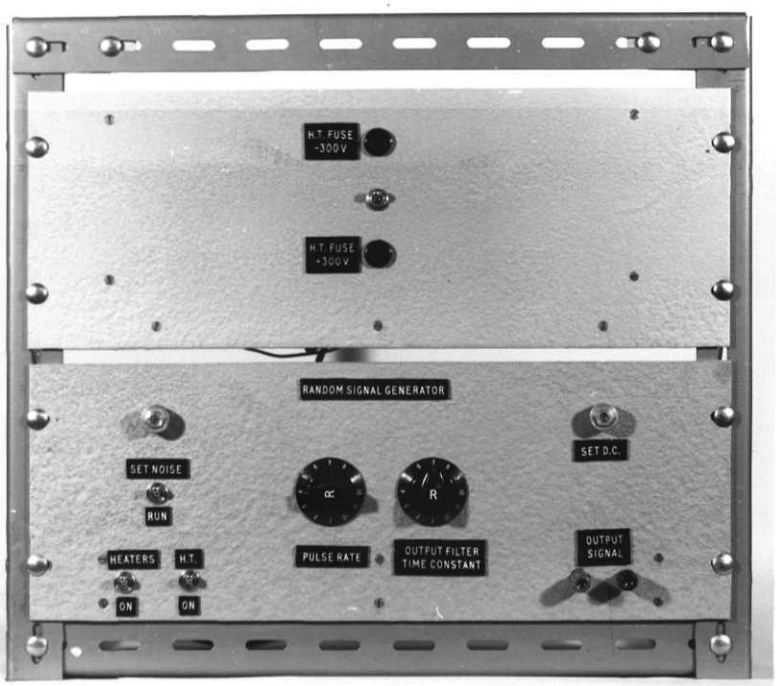

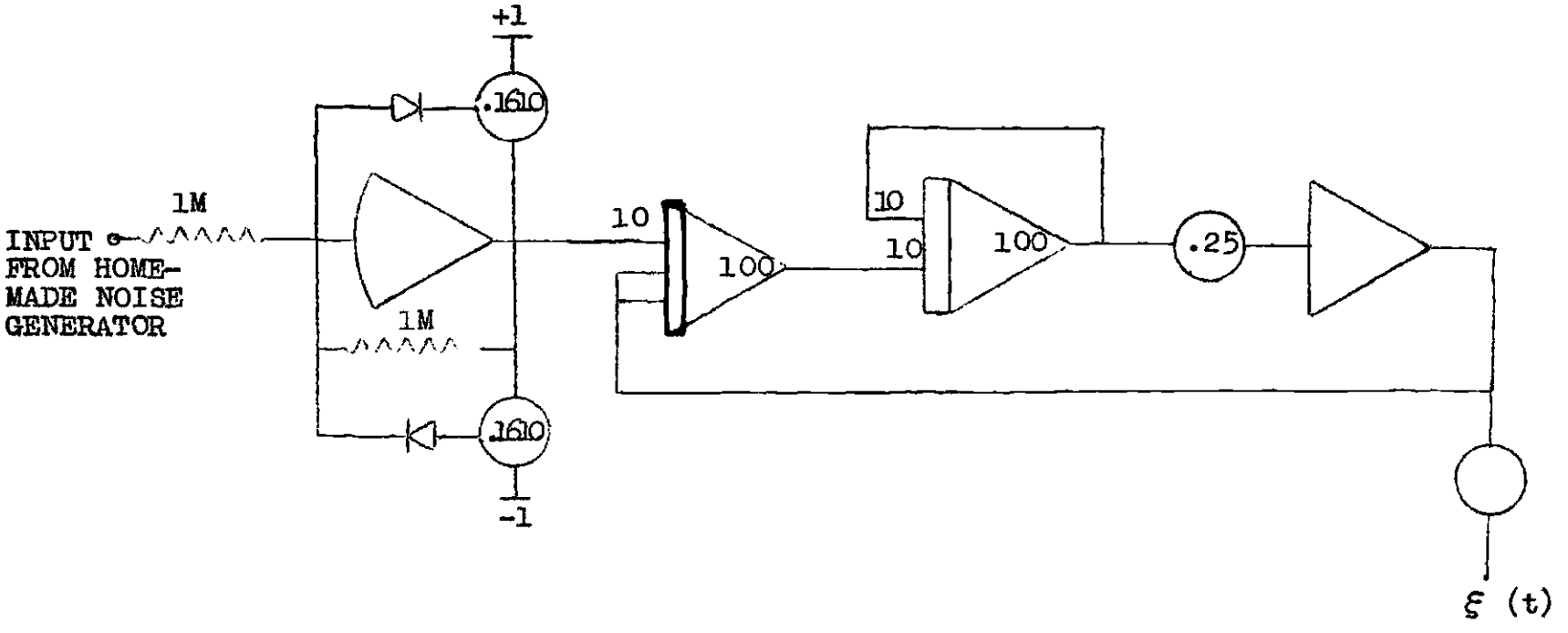

Fig. A4.4 Computer diagram for production of $\xi(t)$

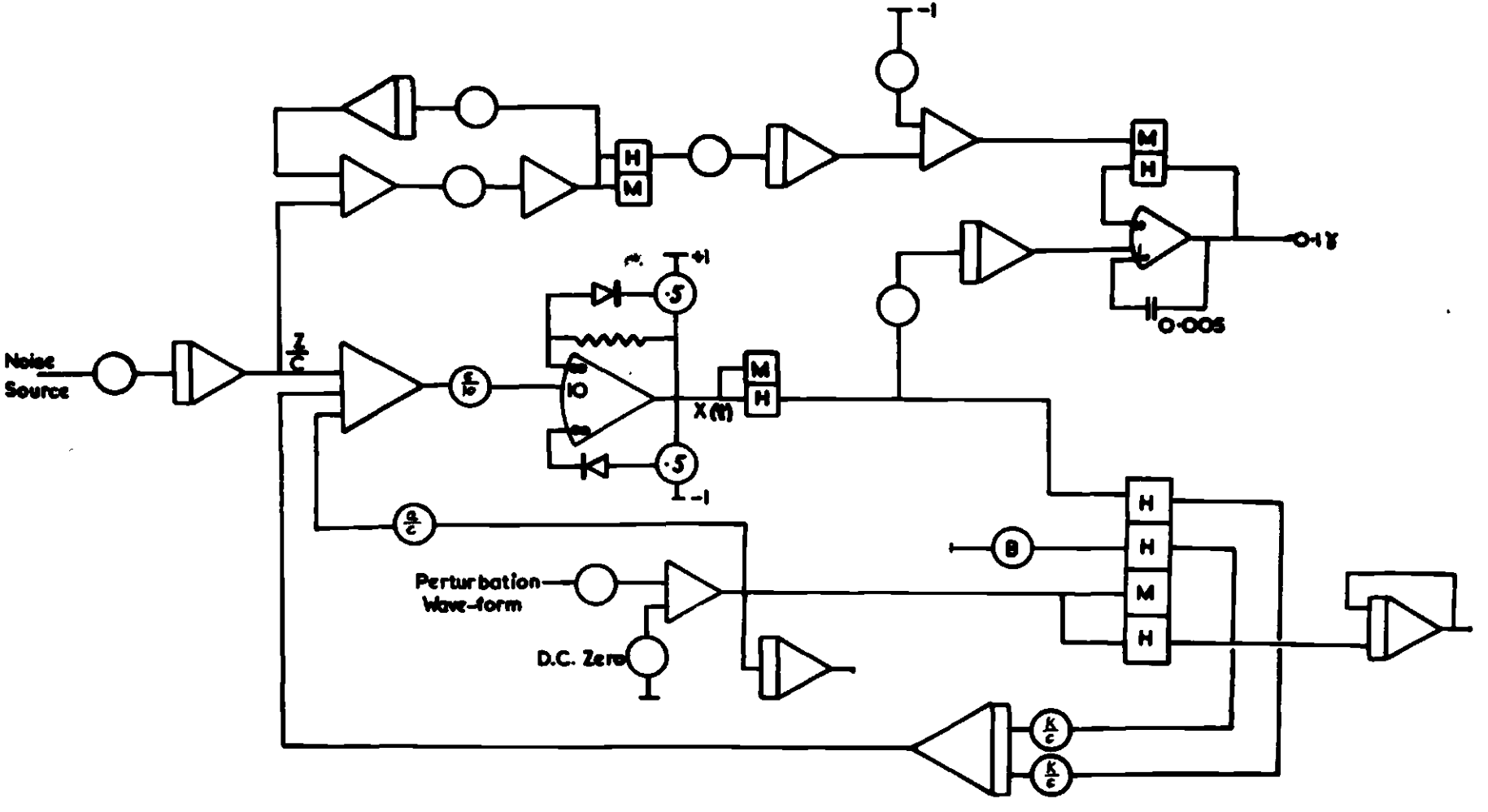

FIG. A4.5 Simulation With Disturbances Only

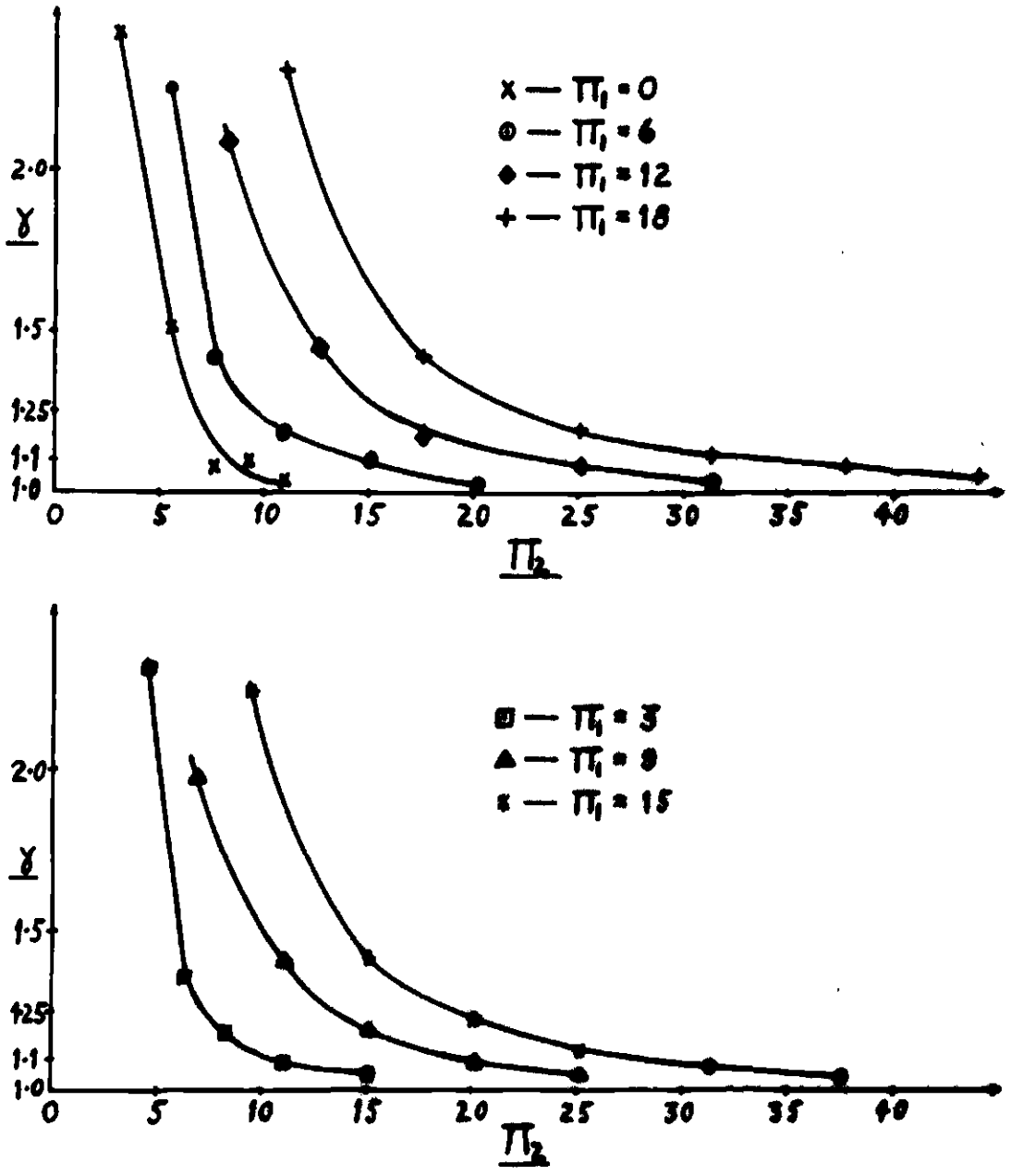

Fig. A4.6a $\gamma(\pi_1, \pi_2)$ with Disturbances Only

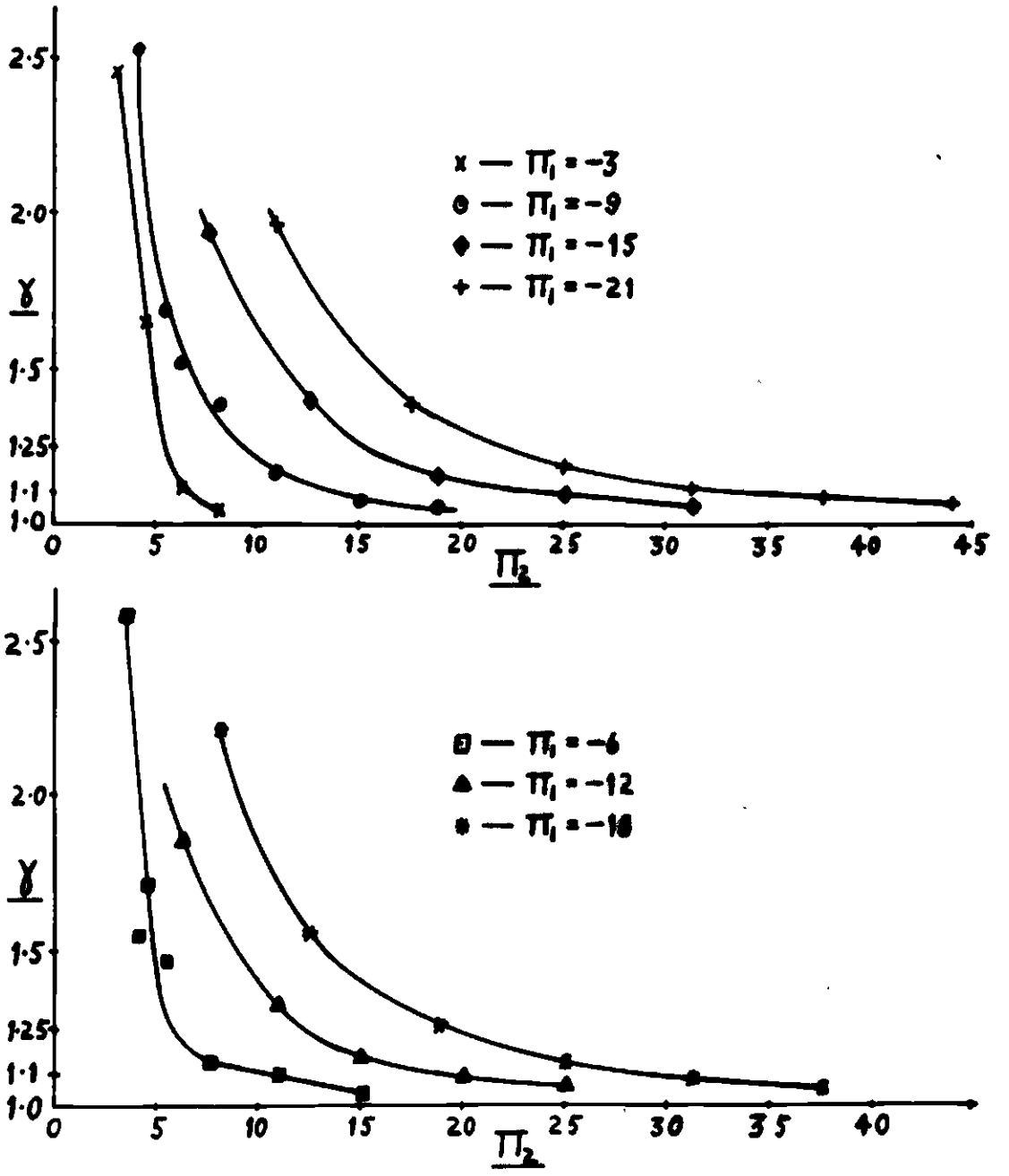

Fig. A4.6b $\gamma(\Pi_1, \Pi_2)$ with Disturbances Only

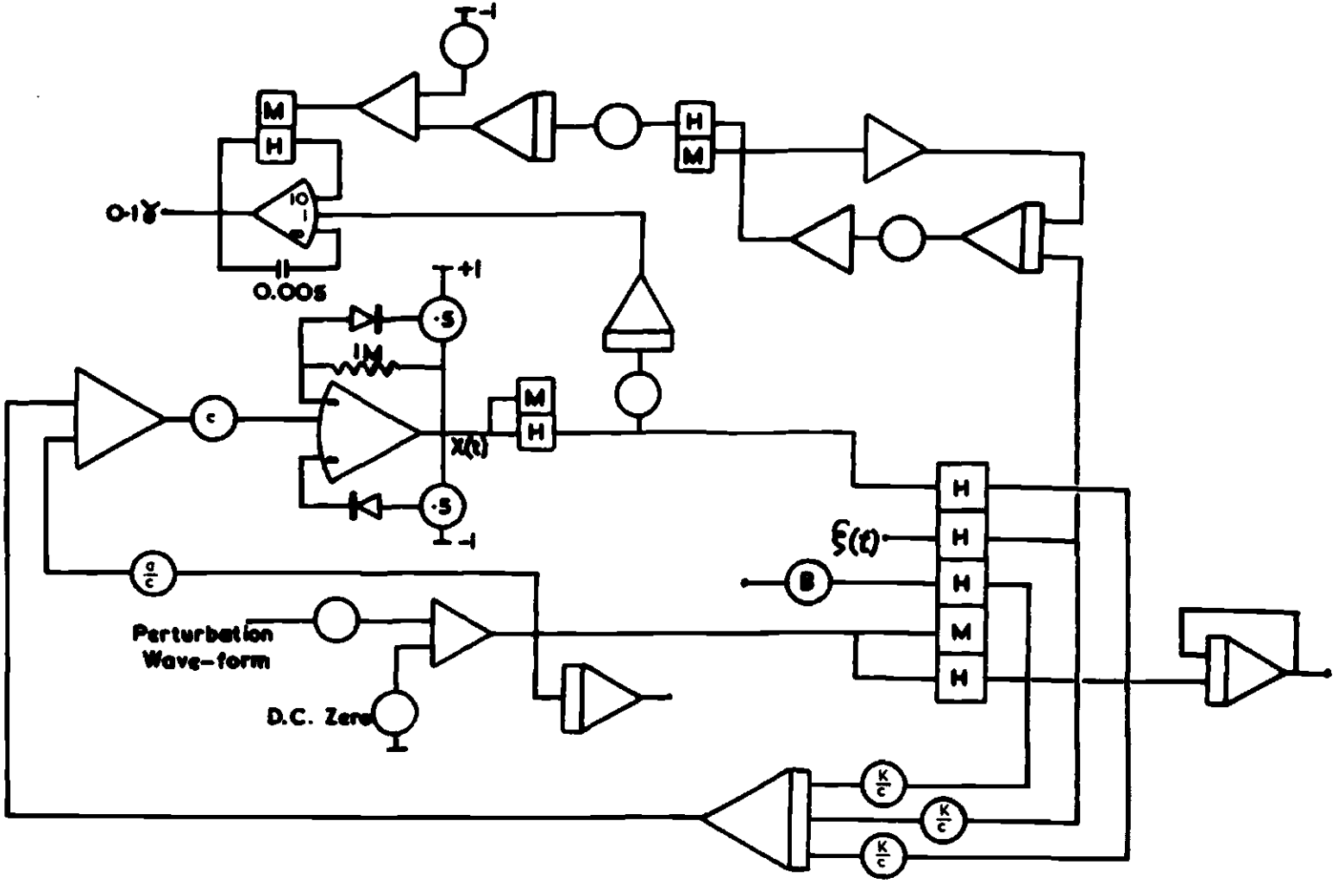

Fig. A4.7 Simulation With Noise Only

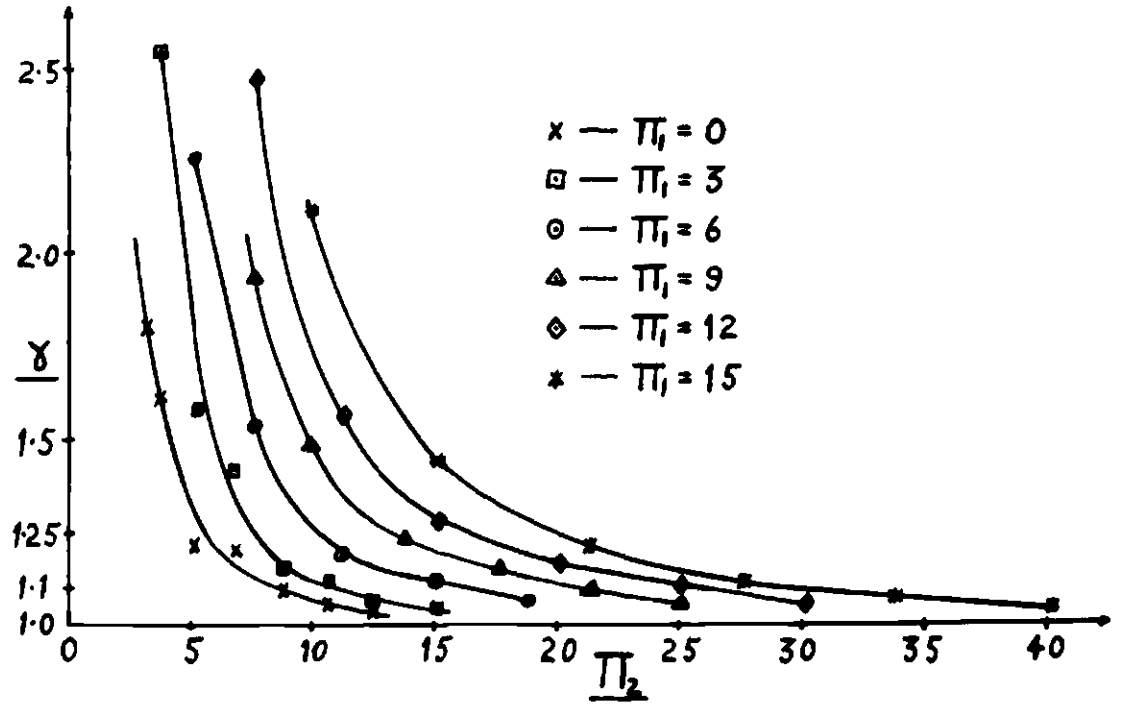

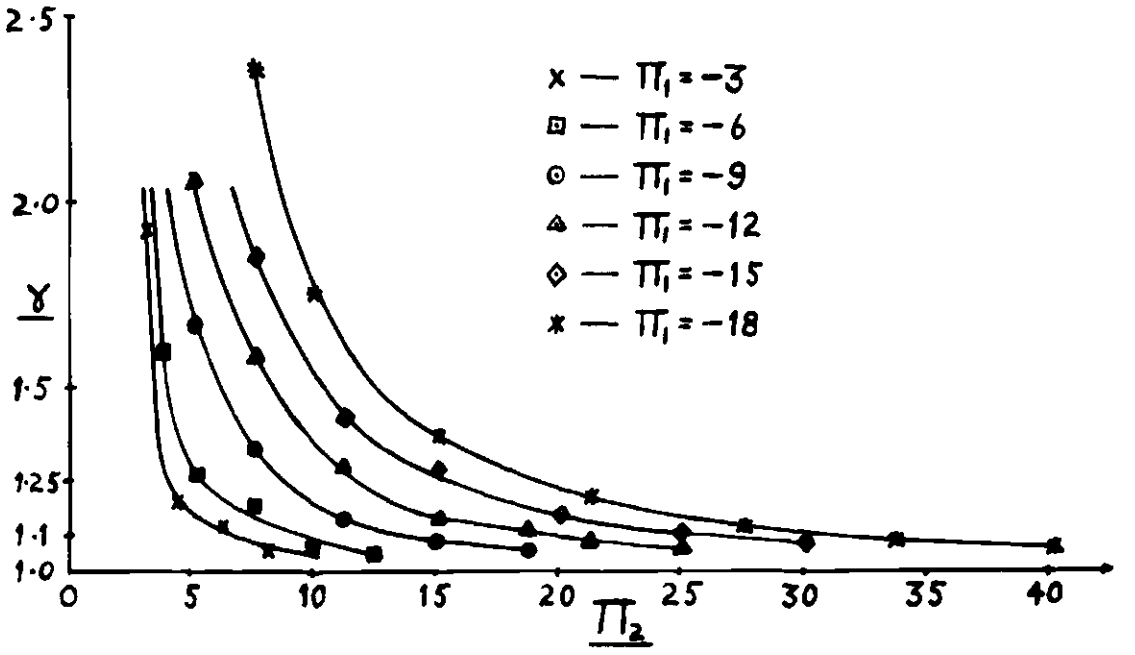

Fig. A4.8 $\gamma(\Pi_1, \Pi_2)$ with Noise Only

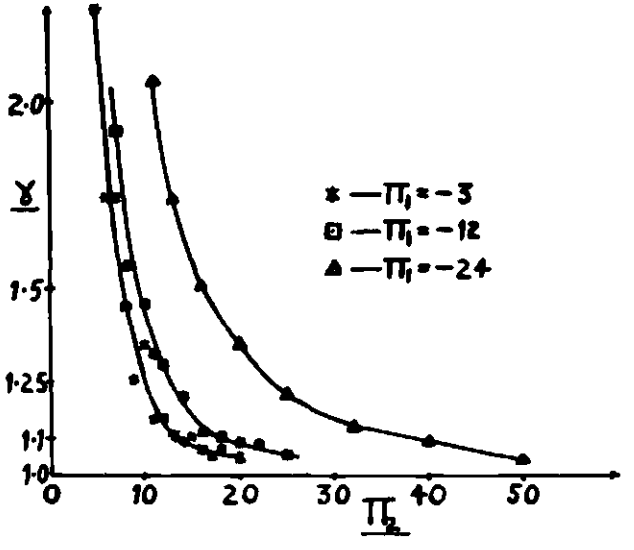

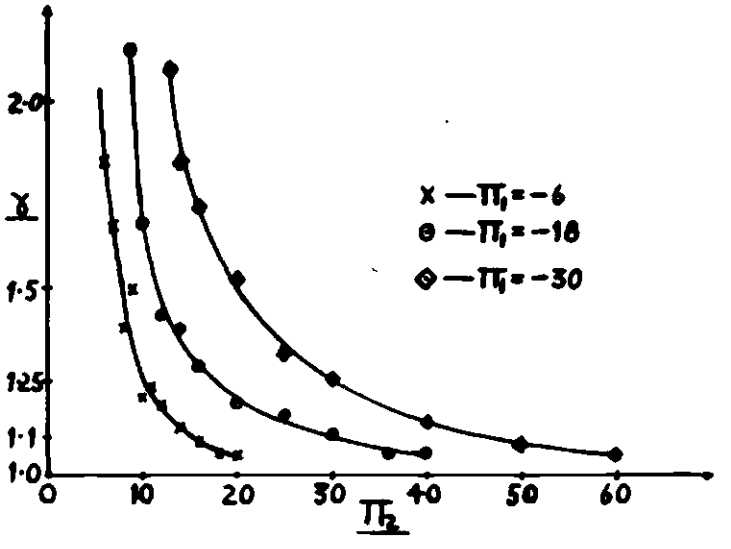

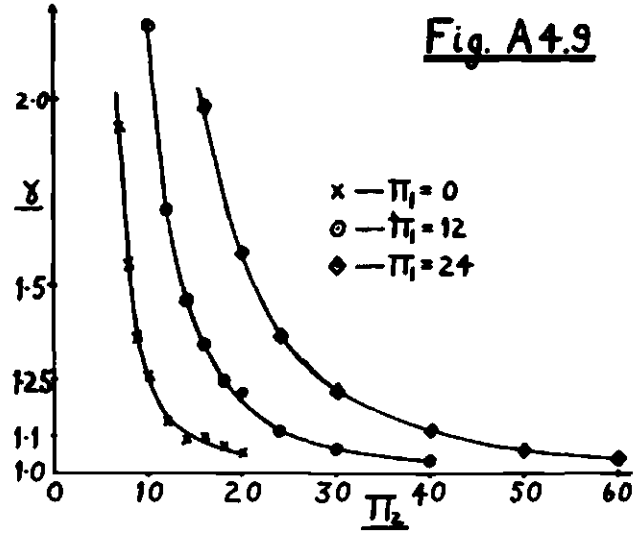

Fig. A4.9 $\gamma(\Pi_1, \Pi_2)$ with Square Wave Perturbation

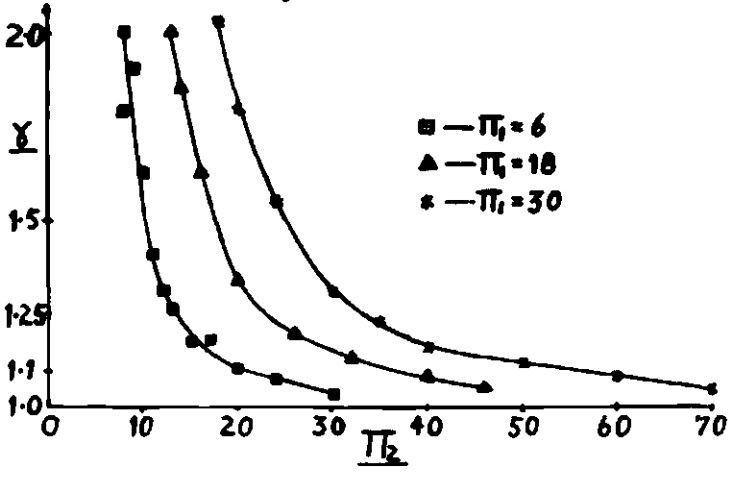

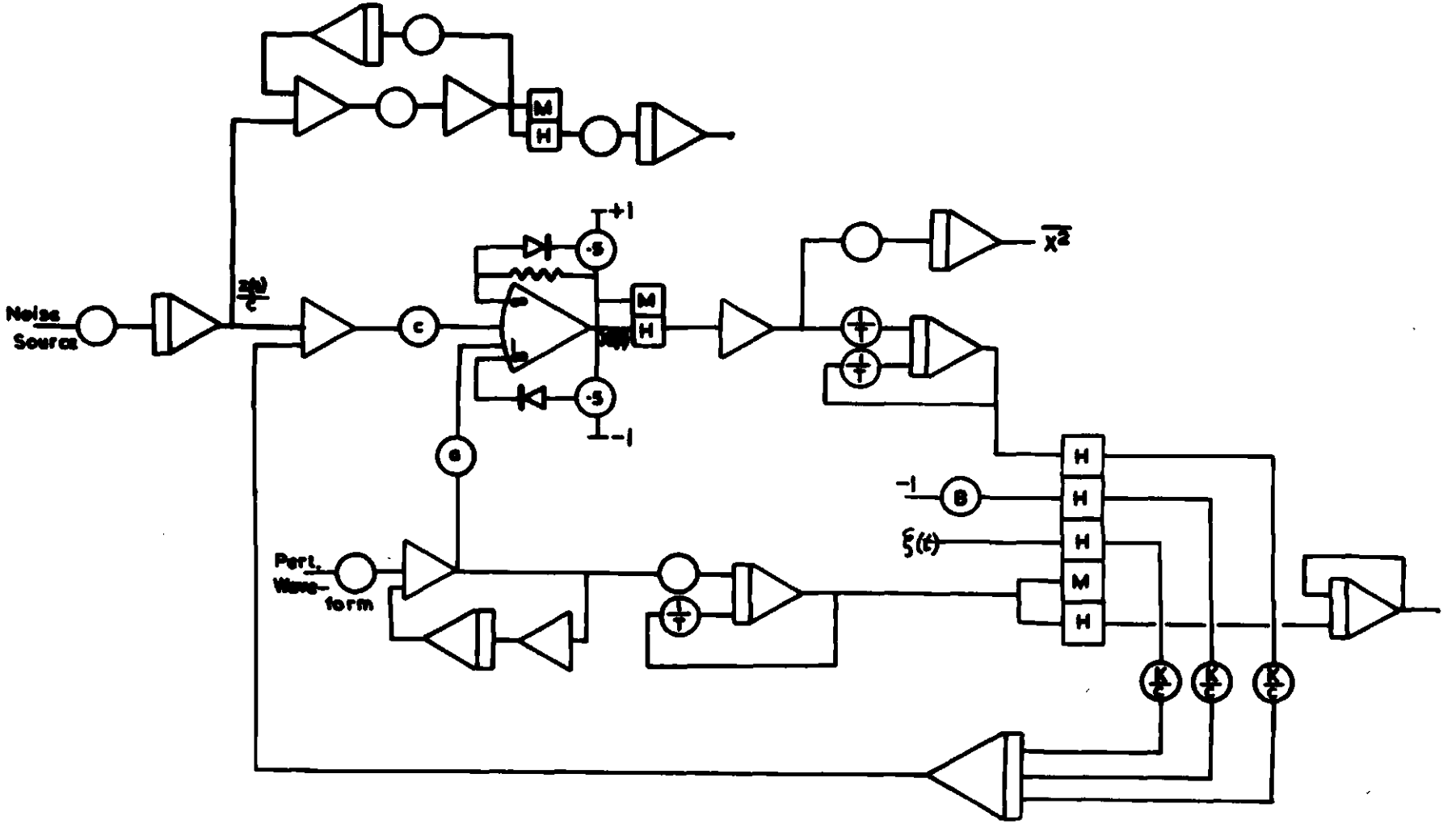

Fig. A4.10 Simulation Of Complete System

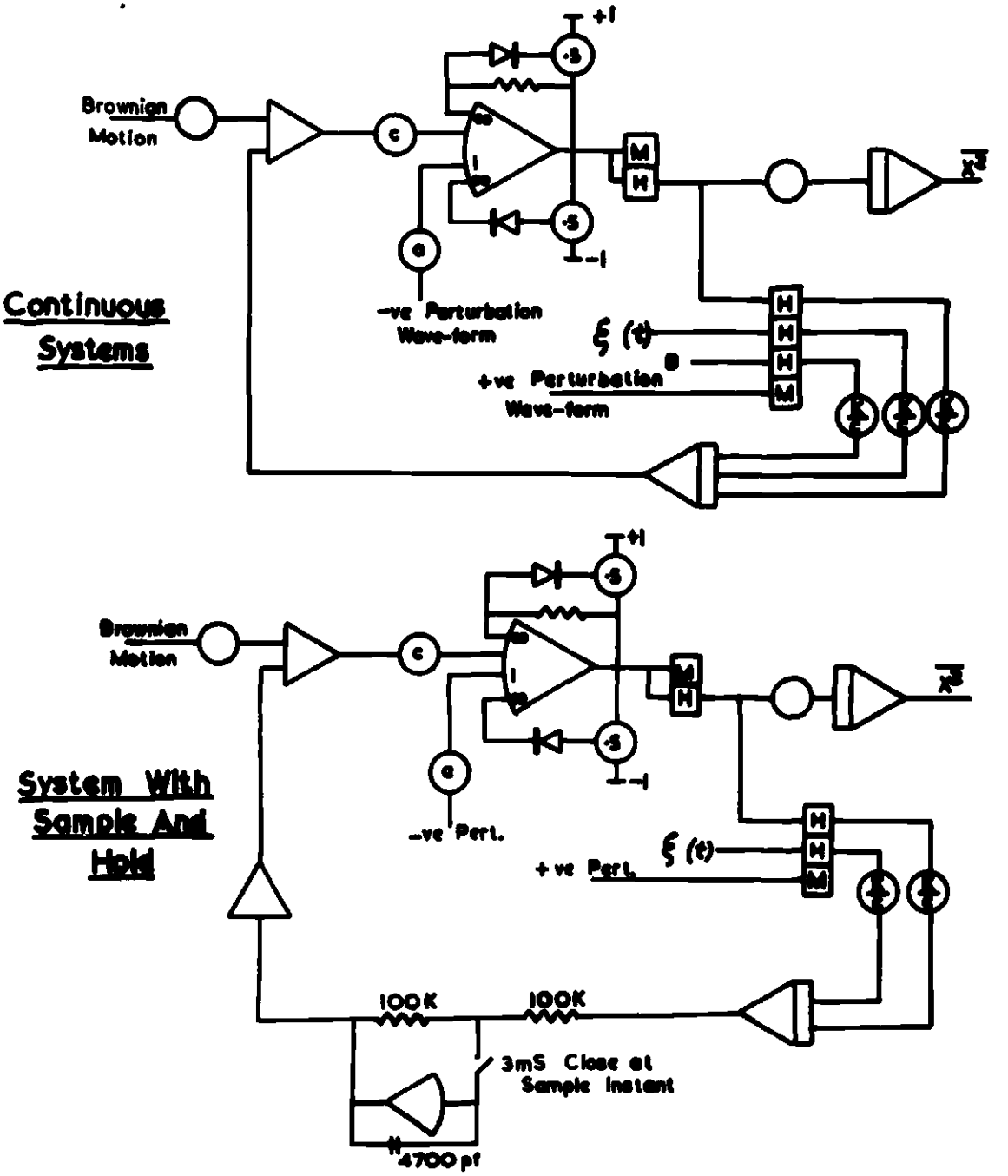

Fig. A4.11 Simulation of Three Systems